THE

LONDON, EDINBURGH, AND DUBLIN

PHILOSOPHICAL MAGAZINE

AND

JOURNAL OF SCIENCE.

[SEVENTH SERIES.]

SEPTEMBER 1933.

XLIII. *The Clock Problem in Relativity.* (Second Paper.)

By J. W. CAMPBELL, *Ph.D.**

1. *Introduction.*

IN this paper the clock problem is treated under the following circumstances: of two observers, A and B, A remains at rest in a Galilean frame of reference, while B moves relative to A with varying speed along a radial straight line. This is the case which was discussed in general principle by Einstein†, and later treated in mathematical detail by Kopff ‡, by using a fictitious gravitational potential. The problem is here treated by another method, viz., that of moving axes. It is true that this method does not, like the former, admit of the general extension to motion in actual gravitational fields, as I showed in my first paper §, but it nevertheless gives an insight into some features of the phenomenon which are not exhibited by using the fictitious gravitational potential. Moreover, the former method is limited to

* Communicated by the Author.

† A. Einstein, "Dialog über Einwände gegen die Relativitätstheorie," *Die Naturwissenschaften*, vi. p. 697 *et seq.* (1918).

‡ A. Kopff, 'The Mathematical Theory of Relativity,' p. 124 *et seq.*

§ J. W. Campbell, "The Clock Problem in Relativity," Phil. Mag. (7) xv. p. 48 (Jan. 1933).

velocities which are not too large, while the present method is applicable to velocities of any magnitude.

2. *The Fundamental Equations.*

Let $O.xyzt$ be a rectangular coordinate system of axes for A, and let $O'.x'y'z't'$ be a rectangular system for B, A and B being at O and O′ respectively. Let the x-axes of the two systems coincide, and suppose that O′ has, as observed from O, a velocity u relative to O, the u not necessarily being constant. Also, the system $O.xyzt$ is, at O, Galilean or inertial in the following sense:—

(1) O is not in the vicinity of ponderable matter.
(2) All undisturbed particles observed from O and not in the neighbourhood of other matter follow straight-line paths in the frame $O.xyzt$, and this regardless of their distance from O.

Now consider an intermediate system $O''.x''y''z''t''$ which instantaneously coincides with $O'.x'y'z't'$ at the instant considered, but for which the velocity relative to O is not changing. We shall assume that O′ never comes into the vicinity of ponderable matter, and then O″ will also be at rest in a Galilean frame of reference.

Then $O.xyzt$ and $O''.x''y''z''t''$ are connected by the well-known Lorentz transformations.

$$\left.\begin{aligned} &dx''=\beta(dx-u\,dt),\ dy''=dy,\ dz''=dz,\\ &dt''=\beta(dt-u\,dx/c^2),\ \beta=(1-u^2/c^2)^{-1/2},\end{aligned}\right\},\quad . \quad (1)$$

where c is the velocity of light.

Let us now put

$$x=x_1,\ x'=x_1',\ x''=x_1'',\ ct=ix_4,\ ct'=ix_4',\ ct''=ix_4'',\ . \quad (2)$$

where $i=\sqrt{-1}$.

Then from (1) and (2) we obtain

$$\left.\begin{aligned} dx_1''&=dx_1\cos\psi-dx_4\sin\psi,\\ dx_4''&=dx_1\sin\psi+dx_4\cos\psi,\end{aligned}\right\},\ .\ .\ .\ (3)$$

where

$$\tan\psi=iu/c. \quad . \quad . \quad . \quad . \quad . \quad . \quad . \quad (4)$$

Hence, as is also well known, we can represent geometrically the transformation (1) by inclined x_1x_4 axes

as shown in fig. 1, where Q is the point of O.*xyzt* which coincides with O″ at the instant considered.

This suggests a means of obtaining the transformation connecting O.*xyzt* and O′.*x′y′z′t′*. For if u is varying then the $x_1'x_4'$ axes are turning relative to the $x_1''x_4''$ axes, as indicated in fig. 2.

Now if $(x_1', 0)$ and $(x_1'', 0)$ denote a given event at the instant when the axes coincide, then $x_1'=x_1''$. Also if $(x_1'+dx_1', dx_4')$ and $(x_1''+dx_1'', dx_4'')$ denote a neighbouring

Fig. 1.

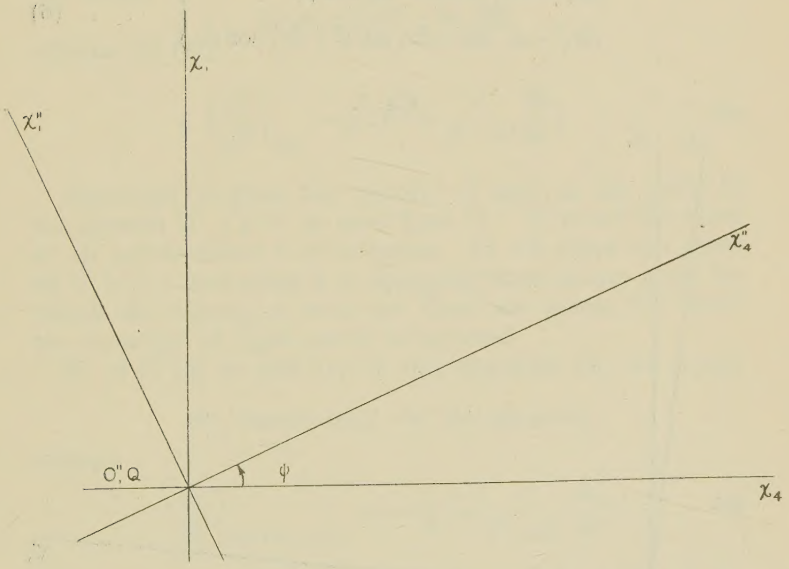

event at a subsequent instant when the axes have become inclined at angle $d\psi$, then

$$x_1''+dx_1''=(x_1'+dx_1')\cos(d\psi)+dx_4'\sin(d\psi),$$
$$dx_4''=-(x_1'+dx_1')\sin(d\psi)+dx_4'\cos(d\psi).$$

Therefore, retaining only first order infinitesimals, and remembering that $x_1'=x_1''$, we have

$$\left.\begin{aligned} dx_1''&=dx_1',\\ dx_4''&=dx_4'-x_1'\,d\psi. \end{aligned}\right\} \quad . \quad . \quad . \quad . \quad . \quad (5)$$

Moreover, the event $(x_1', 0)$ is an event which is contemporaneous with O′ in the extended time sense, and likewise $(x_1'', 0)$ is an event which is contemporaneous with O″ in the same sense. Hence, equations (5) define the way in which variations of the extended times and positions at any given place are related for observers moving with O′ and O″.

The combination of (3) and (5) gives the fundamental relations connecting the systems of O and O′, and these relations, therefore, are :

$$\left.\begin{aligned} dx_1' &= dx_1 \cos\psi - dx_4 \sin\psi, \\ dx_4' - x_1'\, d\psi &= dx_1 \sin\psi + dx_4 \cos\psi. \end{aligned}\right\} \quad . \quad . \quad (6)$$

Fig. 2.

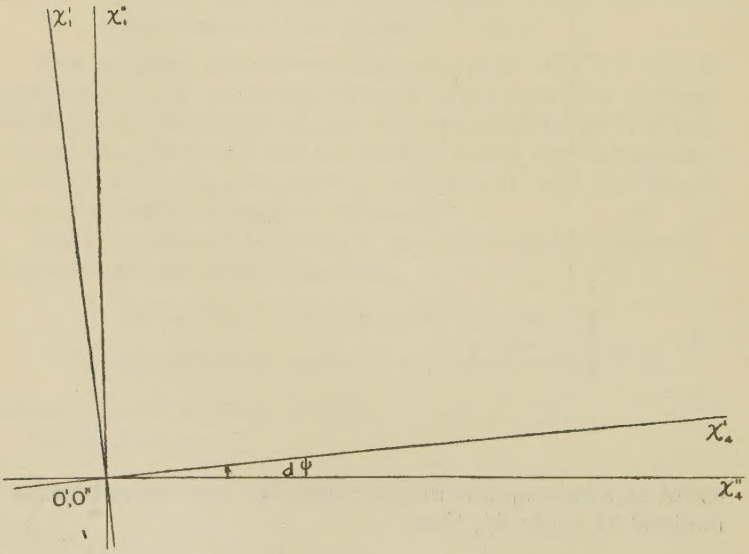

3. *Consequences of Equations* (6).

(*a*) By squaring and adding (6) we obtain

$$(dx_1')^2 + (dx_4' - x_1'\, d\psi)^2 = (dx_1)^2 + (dx_4)^2,$$

and each side of this equation is the "$-ds^2$" for the point under consideration. Therefore, equating the sides separately to zero gives the velocity of light as seen in the two systems.

From

$$(dx_1)^2+(dx_4)^2=0,$$

we obtain,

$$\frac{dx}{dt}=\pm c. \quad . \quad . \quad . \quad . \quad . \quad . \quad (7)$$

This is the velocity of light in the Galilean system, and it is seen that it is the same at all points.

From

$$(dx_1')^2+(dx_4'-x_1'\,d\psi)^2=0,$$

we obtain

$$dx'=\pm(c\,dt'-ix'\,d\psi),$$

whence by (4),

$$\left(\frac{dx'}{dt'}\right)_{\text{light}}=\pm c\left(1+\frac{x'}{c^2-u^2}\frac{du}{dt'}\right). \quad . \quad . \quad . \quad (8)$$

Equation (8) gives the velocity of light at any point in the system $O'.x'y'z't'$ as seen from O'. It is not the same at all points unless u is constant. In all cases the value at O' is $\pm c$, but when u is changing there is one point for which the velocity is zero and there are points for which the direction of light-travel is reversed.

(*b*) If in (6) we put $dx_1=0$ and eliminate dx_4, we obtain

$$dx_1'\cos\psi+(dx_4'-x_1'\,d\psi)\sin\psi=0,$$

whence

$$\left(\frac{dx'}{dt'}\right)_{\text{point fixed re O}}=-u\left(1+\frac{x'}{c^2-u^2}\frac{du}{dt'}\right) \quad . \quad . \quad (9)$$

Equation (9) gives the velocity, as seen from O', of any point which is fixed in the system of O. It follows that such velocities are not all equal unless u is constant. Here again, however, it should be noticed that, no matter how u is changing, points which are at rest in the Galilean system and which are in the vicinity of O' will be observed to have a velocity $-u$.

(*c*) If we put $x_1'=0$ and $dx_1'=0$, we are fixing our attention on O'. Equations (6) then become

$$0=dx_1\cos\psi-dx_4\sin\psi,$$

$$dx_4'=dx_1\sin\psi+dx_4\cos\psi.$$

Therefore

$$\cos\psi\, dx_4' = dx_4, \quad . \quad . \quad . \quad . \quad . \quad . \quad (10)$$

or

$$dt' = \sqrt{1-u^2/c^2}\, dt. \quad . \quad . \quad . \quad . \quad . \quad . \quad (11)$$

Equation (11) gives the rate of a clock at O′ in terms of the rate of a clock at O, and as compared from O.

(*d*) If we put $dx_1=0$ in (6), we are fixing our attention on any point which is fixed in the Galilean system, and for it we have

$$dx_1' = -dx_4 \sin\psi,$$

$$dx_4' - x_1'\, d\psi = \quad dx_4 \cos\psi,$$

whence

$$dx_4 = (dx_4' - x_1'\, d\psi)\cos\psi - dx_1' \sin\psi, \quad . \quad . \quad (12)$$

or, by (2), (4), and (9),

$$dt = \left(1 + \frac{x'}{c^2-u^2}\frac{du}{dt'}\right)\sqrt{1-u^2/c^2}\, dt'. \quad . \quad . \quad (13)$$

Equation (13) gives the rate of any clock in the Galilean system as seen from O′. Concerning it a few things may be noted.

When u is constant it reduces to the reverse of (11) as it should do, for in that case both systems are Galilean. Also, even when u is changing it reduces to the reverse of (11) at O′. Hence, locally, the rate of clocks at rest in the inertial system is, to B, dependent on his velocity and not on his acceleration. For clocks not in his vicinity this is not so, however.

Again, equation (12), from which equation (13) is obtained, may be written in the form

$$dx_4 = dx_4' \cos\psi - d(x_1' \sin\psi),$$

and this equation differs from (10) only by the presence of the exact differential term $d(x_1' \sin\psi)$. Hence, the definite integrals of equations (11) and (13) will agree provided that the term $x_1' \sin\psi$ vanishes between the limits. It is readily seen that this fact agrees identically with a similar result obtained in my first paper.

4. *The Triple Timing at Each Point.*

For both the observers A and B there are at every point three time-rates involved. These are given by the following three clocks :—

(*a*) The fictitious extended time clock of the observer.

(*b*) A natural ideal clock which is at the point and which is at rest relative to the observer.

(*c*) A natural ideal clock which is at the point and which is at rest in the other system.

With A considered as observer, clock (*a*) has the rate dt, clock (*b*) has the rate dt, and clock (*c*) the rate dt''.

With B considered as observer, however, clock (*a*) has the rate dt', clock (*b*) the rate dt'', and clock (*c*) the rate dt.

That the clock at rest relative to B has the rate dt'' is seen from (6). For, by that equation,

$$-ds^2=(dx_1')^2+(dx_4'-x_1'\,d\psi)^2.$$

Hence the rate of an ideal clock at rest relative to B is

$$\frac{i}{c}(dx_4'-x_1'd\psi)=\Big(1+\frac{x'}{c^2-u^2}\frac{du}{dt'}\Big)dt'=dt''.$$

For the observer A his fictitious extended time clock and the natural ideal clock at rest relative to him at the point run synchronously, but for B this is not so when the u is changing. During acceleration the system of natural ideal clocks at rest relative to B will vary in rate relative to the extended time clocks. The corresponding intervals by these clocks will differ by the amount

$$\int_{u_1}^{u_2}\frac{x'\,du}{c^2-u^2},$$

and it is readily seen that this quantity vanishes when, and only when, $u_1=u_2$.

It is also evident, since the actual clock-rate at a point at rest relative to B is dt'', and since this is also the rate in a Galilean system moving with velocity u relative to A, that the relative rates of two ideal clocks at a given point and at rest relative to A and B respectively, is independent of B's acceleration. This is the generalization of

a relation which has previously been pointed out between the ideal clocks of A and B in the vicinity of B.

5. *The Distribution of Light-Signals.*

Let us now consider what happens to a distribution of light-signals relative to O′ when an acceleration takes place.

From equation (8) we have that at the point $(x', 0, 0)$ the velocity of light is

$$\frac{dx'}{dt'} = \pm c\left(1 + \frac{x'}{c^2 - u^2}\frac{du}{dt'}\right),$$

and therefore at the point $(x' + \Delta x', 0, 0)$ the velocity is

$$\frac{d}{dt'}(x' + \Delta x') = \pm c\left(1 + \frac{x' + \Delta x'}{c^2 - u^2}\frac{du}{dt'}\right).$$

Therefore

$$\frac{d}{dt'}(\Delta x') = \pm c\frac{\Delta x'}{c^2 - u^2}\frac{du}{dt'},$$

Hence

$$\frac{d(\Delta x')}{\Delta x'} = \pm c\frac{du}{c^2 - u^2},$$

and

$$\log(\Delta x') = \pm\tfrac{1}{2}\log\frac{c+u}{c-u} + \log k,$$

or

$$\Delta x' = k\frac{c \pm u}{\sqrt{c^2 - u^2}}, \quad \ldots \quad (14)$$

where k is a constant.

Suppose, then, that before u begins to change, a train of light-signals from A is reaching B, and that as seen by B these signals are arriving as equally spaced, the spaces being

$$k(c+u)/\sqrt{c^2 - u^2}.$$

In this case these signals would be travelling relative to B with a positive velocity, and equation (14) means that if an acceleration takes place, no matter what its value, the signals will continue to reach B from A as if equally spaced along the train, the spaces continuing to be

$$k(c+u)/\sqrt{c^2 - u^2}.$$

Or, again, suppose that before u begins to change, a train of light-signals from some point P, fixed in the Galilean system but on the side of O′ remote from O, is reaching B as if spaced at the intervals

$$k(c-u)/\sqrt{c^2-u^2}.$$

Such signals would be reaching B with a negative velocity, and equation (14) means that, no matter how u changes, these signals will continue to reach B as if they constituted a train equally spaced at the intervals

$$k(c-u)/\sqrt{c^2-u^2}.$$

Now suppose that A, as seen by B, is at the point $(x', 0, 0)$. Then the flight of time of A relative to the flight of time of B, and as seen by B, is given by (13).

Moreover, by (8) and (9), signals coming from A will start, as seen by B, with a velocity relative to A of

$$(c+u)\left\{1+\frac{x'}{c^2-u^2}\frac{du}{dt'}\right\}.$$

Therefore, if signals are sent out from both A and B with a frequency n according to the sender's clock, then, according to B, the signals will leave A at space intervals of

$$l=(c+u)\left\{1+\frac{x'}{c^2-u^2}\frac{du}{dt'}\right\}dt'\div n\,dt,$$

and by (13) this equation becomes

$$l=\frac{c(c+u)}{n\sqrt{c^2-u^2}} \quad \ldots\ldots\ldots \quad (15)$$

Hence, by (14), no matter how u changes, signals from A will always reach B as if they were distributed between O and O′ at intervals given by (15). The spacing of the signals all the way along the line will always immediately adjust itself so as to satisfy (15).

The situation is, however, quite different for A. If two signals leave B at a space interval of l_1, they will remain at this interval until they reach A, no matter how the velocity of B may change after their departure from B and before their arrival at A, and they will reach A at a time interval of l_1/c. The separation of two signals travelling from A to B is at all times a function of B's

velocity, whereas the separation of two light-signals travelling from B to A is constant once they have both left B.

6. *A Numerical Example.*

It has already been shown that no matter how u changes while B makes an excursion from A and returns, there is agreement between the ratios of $\int n\,dt$ and $\int n\,dt'$ when compared by either A or B. Nevertheless a special numerical example may be of interest.

Suppose B leaves A by impulsively attaining a velocity $u=a$, that he moves with this constant velocity for a time $t_1/2$ according to A, that he then impulsively reverses his velocity and returns to A at the constant rate $u=-a$, making an impulsive stop at the end.

During the outward journey the signals from B will be at space intervals of

$$(c+a)\,dt \div n\,dt',$$

which by (11) is

$$\frac{c(c+a)}{n\sqrt{c^2-a^2}}.$$

The signals will reach A with the speed c and hence they will arrive with frequency

$$n\sqrt{c^2-a^2}/(c+a).$$

Moreover, this frequency of arrival will be maintained until the signal, which left B at the time of the reversal, has reached A, after which time the frequency of the arrival will be

$$n\sqrt{c^2-a^2}/(c-a).$$

Hence it is clear that the total number of signals received by A during the excursion of B will be

$$\frac{n\sqrt{c^2-a^2}}{c+a}\left(1+\frac{a}{c}\right)\frac{t_1}{2}+\frac{n\sqrt{c^2-a^2}}{c-a}\left(1-\frac{a}{2}\right)\frac{t_1}{2}$$

$$=n\sqrt{c^2-a^2}\,t_1/c.$$

That is, the ratio of the total number of signals

received by A from B to the number of signals sent out by A during the excursion is

$$\sqrt{c^2-a^2}/c.$$

To see the matter from the standpoint of B, however, if the total time according to him was t_1', then the frequency of arrival of signals from A would be

$$n\sqrt{c^2-a^2}/(c+a)$$

for the first half of t_1', and immediately on reversal it would become

$$n\sqrt{c^2-a^2}/(c-a).$$

Hence the total number of signals received by B from A would be

$$\left\{\frac{n\sqrt{c^2-a^2}}{c+a}+\frac{n\sqrt{c^2-a^2}}{c-a}\right\}\frac{t_1'}{2}=\frac{nct_1'}{\sqrt{c^2-a^2}}.$$

Therefore the ratio of the total number of signals received by B from A to the number of signals sent out by B during the excursion would be

$$c/\sqrt{c^2-a^2}.$$

Hence A and B would agree on the ratio of the flows of their respective times during a separation.

Suppose, in particular, that a were $\sqrt{3}.c/2$, and that t_1 were 80 years. Then

$$\sqrt{c^2-a^2}/(c+a)$$

would be 1/3·732, and

$$\sqrt{c^2-a^2}/(c-a)$$

would be 1/·268. Also, $(1+a/c)\,t_1/2$ would be approximately 75 years, and $(1-a/c)\,t_1/2$ would be approximately 5 years.

Suppose, also, that A and B, when they separated, were each 10 years old. Then until A reached the age of 85 he would observe B to live a very slow life. The intervals between B's meals would be nearly four times as great as the intervals between his own, and all B's other actions would appear slowed down accordingly. When A reached

the age of 85 he would see B to be but 30, and then B would appear to become exceedingly active. Instead of his life being four times as slow and leisurely it would be about four times as fast as A's, and the result would be that in the next 5 years A would observe B to age by 20 years. That is, when B returned to A, A would himself be 90 and B would be but 50.

From B's point of view, however, the appearances during separation would be different. For the first 20 years he was away, by his own time, he would observe A to live a very leisurely life, a life at a rate nearly four times as slow as his own. When he had reached the age of 30 he would observe A to be but 15. Then he would see A begin to live a hectically fast life, and in the following 20 years he would see A advance from a boy of 15 to an old man of 90. He would return after the excursion to find himself 50 years old and A 90.

Thus, though the intervening appearances are different, the final appearance is the same to both A and B.

7. *Remarks.*

(*a*) Appearances to B are not affected by his own past history in the matter of velocity. For since the distribution of light-signals reaching him from A is a function of his velocity only, there are no after-effects of acceleration. Hence, if B joined company with any other observer along the way the distribution of light-signals reaching them would be the same no matter what their individual past records of motion.

(*b*) Suppose B had several successive accelerations, back and forth. Then, by equation (13), in the case of some of the accelerations, signals would be returning to A which had already left; or, in other words, relative to the extended time of B the time of A would be flowing backwards. This is only as projected in the extended time of B, however, for, no matter what the acceleration, the signals from A would always approach B with the velocity c. There is variation in the frequency with which signals reach B, but they always continue to arrive, and every one of them arrives at the same velocity. That is, there is no implication that the flow of time of A is *observed* by B to be reversed.

(*c*) Acceleration is a matter of relationship to the rest of the universe. It is true that when the relative velocity

of two observers changes, either may say that the other is accelerated relative to him. But acceleration in that sense alone cannot be made a basis for any conclusions about either observer. In the problem here discussed it was B that was accelerated and not A. When the acceleration took place, the distribution of light-signals from B, as observed by A, was not modified until the signal leaving B at the time of the acceleration reached A. If B were 100 light-years distant from A, the effect of a change of the relative velocity would not be apparent to A until 100 years later. On the other hand, the distribution of the light-signals reaching B from A immediately adapts itself to the changed velocity. That is, the attendant effects of the change of relative velocity are immediately evident to B, while they are not evident to A until a signal reaches him from B. *Something happened*, and it happened *to B*.

(*d*) It follows from the definition given for an inertial system that if A's system is inertial, then every system moving relative to A with a constant velocity is inertial. Also, if B is accelerated relative to one inertial system he is accelerated relative to every inertial system. However, on account of the way in which velocities are compounded, the magnitude of the acceleration will not be the same relative to all systems. That is, the existence of acceleration is an absolute thing, but its magnitude is not. On the other hand, any one inertial system may be used as a standard of reference, for differences in magnitude of acceleration will not introduce contradictions because checks by reunions are impossible.

8. *Summary of the Problem.*

The time difference between the clocks of A and B over a period from separation to return is, of course, an invariant. For measurement of time is essentially a counting, and so it matters not who makes the two counts. The easiest counts to calculate are those of A direct. To get the counts from the standpoint of B two methods have been used. In my first paper, already referred to, a fictitious potential of uniform gradient was applied over the whole universe to eliminate B's acceleration. Then a comparison of the counts of the clocks of A and B was made, although in making the comparison

the counts were taken by using A's coordinate system. This was legitimate, for, as just pointed out, when a comparison of times over a period from separation to return is wanted, it matters not who makes the counts. It was convenient to use A's system in order to compare the result with that obtained when no fictitious gravitational potential was imposed. In the present paper, on the other hand, the comparison of time durations as they appear to B has been made by using B's own coordinate system, and while it has not the generality of application of the former method, it nevertheless gives a more vivid picture of the workings in the special case treated.

A discussion of the clock problem has been given by Lange * in which he criticizes various treatments which have been given. In particular, Lange is much concerned about the effect of the acceleration on the phenomenon, when viewed by A as well as when viewed by B. He challenges the use of equation (11) for obtaining the time difference, for periods when u is not constant. Objection to such use, however, seems to me to be without foundation. For suppose $O.xyzt$ and $O'.x'y'z't'$ are two inertial systems, and suppose that a given object has the position (x, y, z, t) in the former and (x', y', z', t') in the latter. Then for this object the line element is given by

$$ds^2=c^2dt^2-dx^2-dy^2-dz^2=c^2dt'^2-dx'^2-dy'^2-dz'^2.$$

The proper-time element for this object is ds/c, no matter how it moves. This element is, therefore,

$$\sqrt{1-v^2/c^2}\,dt,$$

where

$$v^2=(dx^2+dy^2+dz^2)/dt^2,$$

irrespective of how v varies. In particular the object may be at O', and then with our previous notation the proper-time element is

$$\sqrt{1-u^2/c^2}\,dt.$$

Equation (11) is therefore always valid for comparing the times of A and B when viewed by A, an acceleration of B having no effect.

* Luise Lange, "The Clock Paradox in the Theory of Relativity," Amer. Math. Monthly, xxxiv. p. 22 (Jan. 1927).

When viewed by B, Lange pictures the time of A as jumping forward during the period of acceleration. This is true relative to B's extended time only, and not as *observed* by B. The extra signals emitted by A do not come out as a concentrated quantity to be later picked up by B in bulk, so to speak. As far as B is concerned the observations are always regular and not spasmodic. Their frequency of arrival is a function of B's velocity alone; at no time is it a function of his acceleration. Nevertheless, the effect of the acceleration on what B observes is fully allowed for by the adjustment of the frequency of arrival in this way.

There is, however, a point worth noting regarding the acceleration. It is not permissible to have the acceleration of B produced by a fictitious gravitational potential. Any potential difference introduced between A and B would modify the relative motions of their clocks. Also, it is not potential but potential gradient that determines acceleration, and so a quite arbitrary effect on the slowing of B's clock relative to A's would be introduced by using a gravitational field to accelerate B. It might be thought that, this being the case, a potential of zero value at the point of turning but of suitable gradient might be introduced. This cannot be admitted, however, for the turning does not take place at a point but over an interval, and if the potential is zero at one point in the interval it is different from zero at other points. Moreover, the shorter the interval the higher the gradient that would be necessary, and so the greater the potential difference introduced at the other points of the interval. Hence, it is improbable that a gravitational field could in any way be devised that would produce the given acceleration of B and at the same time have a negligible effect on the slowing of B's clock.

There is, besides, an intuitive reason why a gravitational potential cannot be used in this way. Gravitational potential as an agent producing acceleration is unique in character. It is the only agent whereby no relative acceleration is involved among the particles within an infinitesimal region. To picture, therefore, an acceleration produced in some other way as being produced by a gravitational potential instead, would be to *substitute* for one condition, a condition which is physically different. On the other hand, the *addition* over the whole universe

of a gravitational field of uniform gradient would not make conditions physically different anywhere for it would not introduce any relative accelerations. The use of such a fictitious field to reduce any desired observer to a point of view of rest is therefore justifiable.

University of Alberta.
April 1933.

XLIV. *The Determination of the Interelectrode Times of Transit of Electrons in Triode Valves with Positive Grid Potentials.* *By* J. S. McPetrie, *B.Sc., A.M.I.E.E.* (*The National Physical Laboratory*) *.

Summary.

The performance of electrical circuits incorporating three-electrode valves is affected seriously at very high frequencies by the times of transit of the electrons between the various electrodes. It is shown in the following paper how these times may be determined for any valve with a positive potential on the grid and any potential on the anode. It is also shown how the velocity of emission of the electrons from the cathode may be taken into account.

Introduction.

The times of transit of the electrons between the electrodes of a triode are controlling factors in the performance of valve circuits at very high frequencies. The frequency of the electronic oscillations obtained when the grid is maintained at a relatively high positive, and the anode at a low potential with respect to the filament is also intimately bound up with the electronic times of transit. In both cases it is advantageous to know these times, and it is shown below how they may be determined for any cylindrical electrode valve having a positive potential on the grid and any positive or negative potential on the anode.

* Communicated by R. L. Smith-Rose, Esq.

Scheibe [1] has given the analysis for the cylindrical electrode triode, but his results are applicable only when the potential of the grid is positive and the anode negative with respect to the filament. In the following paper the analysis is extended so as to include the case when the anode is also positive. The analysis may also be made to take account of the velocity of emission of the electrons from the filament.

Scheibe's Analysis.

Scheibe's result for the time of transit of an electron from the filament to grid of a valve is given by

$$t=\frac{2r_g}{\sqrt{\frac{2e\mathrm{V}_g}{m}}}\times f\left(\sqrt{\log_e\frac{r_g}{r_f}}\right), \quad . \quad . \quad . \quad (1)$$

in which r_g and r_f are the radii of grid and filament respectively, and V_g is the potential of the grid with respect to the filament.

The similar equation giving the time from the grid to the position in the grid-anode space at which the electron velocity is zero (the anode is negative with respect to the filament) is

$$t=\frac{2r_g}{\sqrt{\frac{2e\mathrm{V}_g}{m}}}\times g\left(\sqrt{\frac{\mathrm{V}_g}{\mathrm{V}_g-\mathrm{V}_a}\log_e\frac{r_a}{r_g}}\right), \quad . \quad . \quad (2)$$

in which r_a is the radius of the anode and V_a is its potential with respect to the filament.

In these equations the functions $f(x)$ and $g(x)$ have the form

$$f(x)=xe^{-x^2}\int_0^x e^{u^2}\,du \quad . \quad . \quad . \quad . \quad . \quad (3)$$

and

$$g(x)=xe^{x^2}\int_0^x e^{-u^2}\,du. \quad . \quad . \quad . \quad . \quad . \quad (4)$$

The values of $f(x)$ and $g(x)$ for different values of x are shown graphically in figs. 1 and 2.

Extension of Scheibe's Analysis to include Positive Values of Anode Potential

Let a and b (fig. 3) represent two coaxial cylinders of radius r_1 and r_2, and let the potentials of the two cylinders be V_a and V_b, zero potential being that for

Fig. 1.

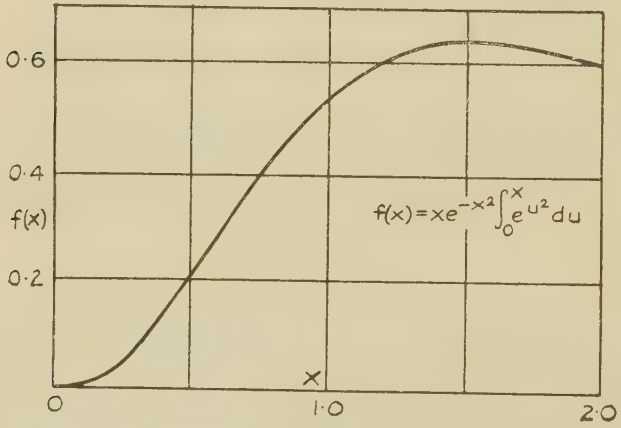

Fig. 2.

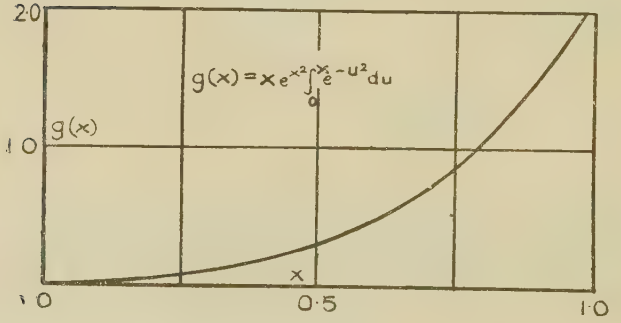

which the velocity of the electrons passing between the two cylinders would be zero.

The potential at any point between a and b, and distant r from the axis of the cylinders, is

$$V_r = \frac{(V_b - V_a)\log_e \frac{r}{r_1}}{\log \frac{r_2}{r_1}} + V_a.$$

From the definition of potential the velocity v_r of the electrons at this point is

$$v_r = \sqrt{\frac{2e}{m}V_r},$$

so that

$$v_r = \sqrt{\frac{2e}{m}\left\{\frac{(V_b - V_a)\log_e \frac{r}{r_1}}{\log_e \frac{r_2}{r_1}} + V_a\right\}}^{\frac{1}{2}}.$$

Fig. 3.

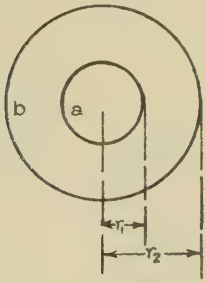

The time of transit of the electrons from electrode "*a*" to electrode "*b*" is given by

$$t_{ab} = \int_{r_1}^{r_2} \frac{dr}{v_r}$$

$$= \frac{1}{\sqrt{\frac{2e}{m}}} \int_{r_1}^{r_2} \frac{dr}{\left\{\frac{(V_b - V_a)\log_e \frac{r}{r_1}}{\log_e \frac{r_2}{r_1}} + V_a\right\}^{\frac{1}{2}}}. \quad . \quad (5)$$

After some reduction this equation gives the time of transit from *a* to *b* as

$$t_{ab} = \frac{2r_1}{\sqrt{\frac{2eV_a}{m}}}\left[\frac{r_2}{r_1}\sqrt{\frac{V_a}{V_b}}f(x_1) - f(x_2)\right], \quad . \quad (6)$$

in which $f(x)$ has the form given in rel. (3) and

$$x_1 = \sqrt{\frac{V_b}{V_b - V_a}} \log \frac{r_2}{r_1}$$

and

$$x_2 = \sqrt{\frac{V_a}{V_b - V_a}} \log_e \frac{r_2}{r_1}.$$

Time of Transit from Filament to Grid of Triode for Zero Velocity of Emission.

Let a and b represent the filament and grid of the triode of radius r_g and r_f respectively, the grid being at a potential V_g above that of the filament. In this case V_a is zero and V_b is V_g. It will be seen that x_1 and x_2 in rel. (6) become $\sqrt{\log_e \frac{r_2}{r_1}}$ and zero respectively. As $f(0)$ is zero, rel. (6) reduces in this case to

$$t = \frac{2r}{\sqrt{\frac{2eV_g}{m}}} f\left(\sqrt{\log_e \frac{r_g}{r_f}}\right),$$

which is identical with that found by Scheibe and given in rel. (1). The value of $f\left(\sqrt{\log_e \frac{r_g}{r_f}}\right)$ for different values of $\frac{r_g}{r_f}$ is shown graphically in fig. 4.

Time of Transit from Filament to Grid of Triode when Velocity of Emission is not Zero.

Suppose the velocity of emission is v, and that

$$V_0 = \frac{mv^2}{2e}.$$

In this case, if the potential difference between a and b is maintained equal to $V_b - V_a$, then the potentials of V_a and V_b are equal to V_0 and $V_b + V_0$. Using the same symbols as in the previous paragraph, rel. (6) then reduces to

$$t = \frac{2r_g}{\sqrt{\frac{2e}{m}(V_g + V_0)}} \left[f(x_1) - \frac{r_f}{r_g} \sqrt{\frac{V_g + V_0}{V_0}} f(x_2) \right], \quad (7)$$

in which

$$x_1 = \sqrt{\frac{V_g + V_0}{V_g}} \log_e \frac{r_g}{r_f}$$

and

$$x_2 = \sqrt{\frac{V_0}{V_g}} \log_e \frac{r_g}{r_f}.$$

A result similar to that given in rel. (7) has been found previously by Kapzov and Gevosdower, but they did not

Fig. 4.

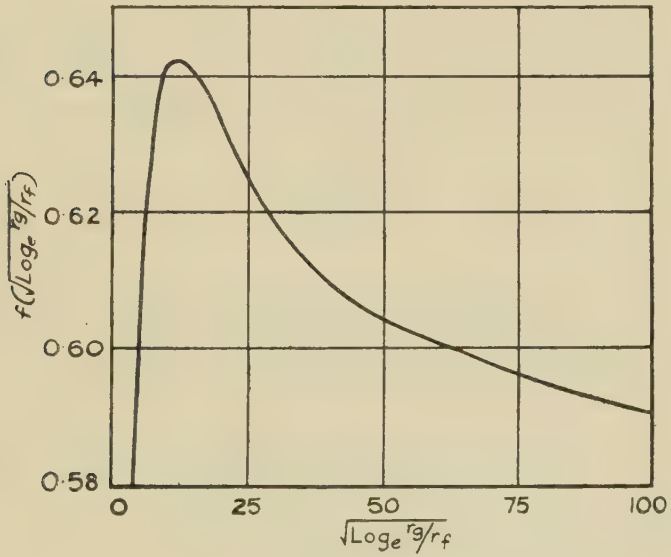

give rel. (6) from which the results given in the next section may be deduced.

Time of Transit in Grid-Anode Space when the Emission Velocity is Zero.

Let a and b represent the grid and anode of the valve of radius r_g and r_a respectively. In the case of the grid-filament space the grid was considered as having a higher potential than that of the filament, that is V_b in rel. (6) was greater than V_a. In the grid-anode space now under consideration, however, the potential of the anode may

be less than that of the grid, or even negative. It can be shown that the term involving $f(x_1)$ in rel. (6) becomes zero when V_a is greater than V_b. The result that $f(x_1)$ becomes zero takes account of the fact that when the anode has a negative potential the electrons do not traverse the whole path between a and b, and the limits of the integral in rel. (5) have to be modified accordingly.

When $V_b < V_a$ rel. (6) then reduces to

$$t = \frac{-2r_1}{\sqrt{\frac{2eV_a}{m}}}[f(x_2)],$$

or using the symbols appropriate for the grid-anode space in which r_g and r_a are the radii and V_g and V_a the potentials of the grid and anode respectively.

$$t = \frac{-2r_g}{\sqrt{\frac{2eV_g}{m}}}[f(x_2)], \quad . \quad . \quad . \quad . \quad . \quad (8)$$

in which

$$x_2 = \sqrt{\frac{V_g}{V_a - V_g}} \log_e \frac{r_a}{r_g}.$$

But $V_a < V_g$ so that x_2 is imaginary.

Let $x_2 = ix$. Then

$$x = \sqrt{\frac{V_g}{V_g - V_a}} \log_e \frac{r_a}{r_g}. \quad . \quad . \quad . \quad . \quad . \quad (9)$$

It can readily be shown that

$$f(ix) = -g(x),$$

so that rel. (8) reduces to

$$t = \frac{2r_g}{\sqrt{\frac{2eV_g}{m}}} g(x), \quad . \quad . \quad . \quad . \quad . \quad (10)$$

in which the value of x is given by rel. (9).

Rel. (10) is exactly that found by Scheibe, and given earlier in this paper as rel. (2). Scheibe's analysis, however, applies only to the case in which the anode has a negative potential. The analysis given above shows

that rel. (10) is valid for all values of anode potential less than the grid potential.

When the anode potential is greater than the grid potential, rel. (6) must be used complete and gives

$$t = \frac{2r_g}{\sqrt{\frac{2eV_g}{m}}}\left[\frac{r_a}{r_g}\sqrt{\frac{V_a}{V_g}}f(x_1)-f(x_2)\right], \quad . \quad . \quad (11)$$

in which

$$x_1 = \sqrt{\frac{V_a}{V_a-V_g}}\log_e\frac{r_a}{r_g} \quad \text{and} \quad x_2 = \sqrt{\frac{V_g}{V_a-V_g}}\log_e\frac{r_a}{r_g}.$$

Let the time for the grid-anode space for any value of the anode potential be given by

$$t = \frac{2r_g}{\sqrt{\frac{2eV_g}{m}}}F(x),$$

then fig. 5 shows graphically the variation of $F(x)$ with the ratio of anode to grid potentials for various typical values of the ratio of anode to grid radii. Scheibe's analysis gives the values of $F(x)$ for negative values of V_a/V_g.

Time of Transit in Grid-Anode Space when the Velocity of Emission is not Zero.

If the velocity of emission of electrons from the filament corresponds to a potential V_0 the results given in the above section are valid if V_g+V_0 and V_a+V_0 are substituted for V_g and V_a respectively. Rel. (10), for the case in which $V_a<V_g$, then becomes

$$t = \frac{2r_g}{\sqrt{\frac{2e(V_g+V_0)}{m}}}g(x_3), \quad . \quad . \quad . \quad . \quad (12)$$

in which from rel. (9),

$$x_3 = \sqrt{\frac{V_g+V_0}{V_g-V_a}}\log_e\frac{r_a}{r_g}.$$

Similarly, rel. (11) for the case in which $V_a > V_g$, gives

$$t = \frac{2r_g}{\sqrt{\frac{2e(V_g+V_0)}{m}}} \left[\frac{r_a}{r_g} \sqrt{\frac{V_a+V_0}{V_g+V_0}} f(x_4) - f(x_5) \right], \quad (13)$$

Fig. 5.

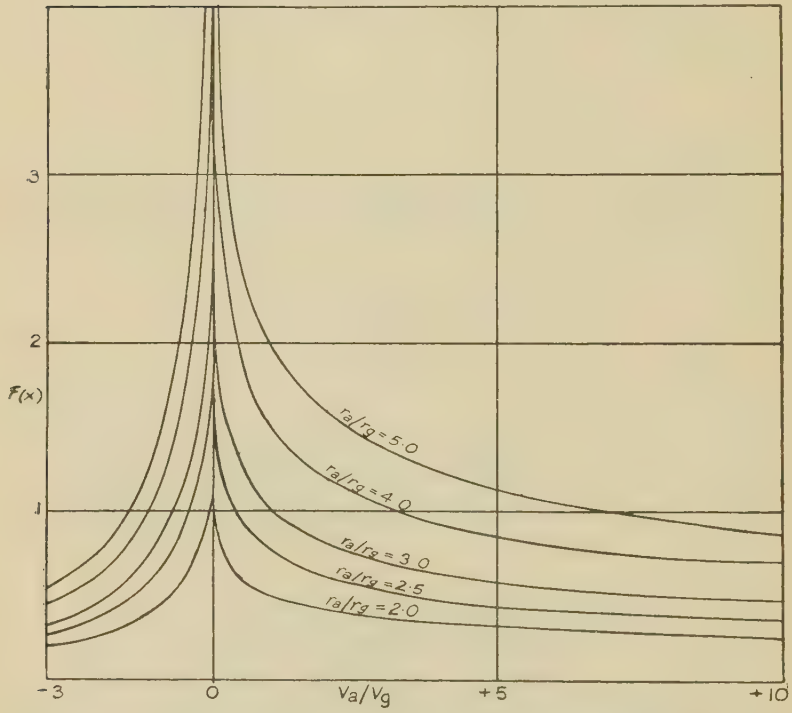

Graph from which the electron transit times in grid-anode space can be determined for different electrode dimensions and potentials.

in which

$$x_4 = \sqrt{\frac{V_a+V_0}{V_a-V_g}} \log_e \frac{r_a}{r_g} \quad \text{and} \quad x_5 = \sqrt{\frac{V_g+V_0}{V_a-V_g}} \log_e \frac{r_a}{r}.$$

Conclusions.

The interelectrode transit times of the electrons in triodes with positive grid potentials can be determined from the analysis given in the above paper. Previously,

workers have considered only the case in which the anode has a negative potential with respect to the filament. The analysis given above is extended in order to give the results for any anode potential, positive or negative. It is also shown how the velocity of emission of the electrons from the filament may be taken into account.

The effect of the electronic space-charge on the distribution of potential between the electrodes has not been considered. A graphical method of determining the interelectrode times of transit under space-charge limited conditions has been given by the author in an earlier paper.

The work described in this paper has been carried out as part of the programme of the Radio Research Board, and acknowledgment is due to the Department of Scientific and Industrial Research for granting permission for publication. The author is also indebted to Mr. H. M. Bristow for assistance in the computations involved.

References.

(1) A. Scheibe, *Ann. d. Phys.* lxxiii. p. 54 (1924).
(2) H. Kapzov and S. Gevosdower, *Zeits. f. Phys.* xlv. p. 114 (1927).
(3) J. S. McPetrie, Radio Research Board Paper.

XLV. *Path and Stability of a Local Vortex moving round a Corner.* *By* Atsushi Miyadzu, *Assistant Professor of Hydraulics and Hydrodynamics, Tohoku Imperial University, Sendai, Japan**.

I. *Introduction and Summary.*

THE path of an irrotational vortex near a corner has constantly been studied † and is well known, but a local vortex maintained in a potential main flow round a corner has not been dealt with; no general conclusions, therefore, have as yet been published on this subject, so far as the present writer is aware.

In this paper, (1) the variation of the path of a local vortex depending upon the relative rotational direction

* Communicated by the Author.

† A. G. Greenhill, Quart. Journal, xv. p. 15; W. Barth, *Zeit. f. ang. Math. u. Mech.* p. 248 (1930).

and the strength of its circulation to the main flow *, and (2) the stability of equilibrium of the vortex have fully been treated of, with respect to the domain bounded by two straight lines, the inserted angle of which is $\alpha=\pi/n$.

The results † arrived at are summarized as follows :—

For $0<\alpha<\pi(\infty > n > 1)$.

(1) A vortex with a clockwise circulation at any specified point, in moving near a corner describes a closed curve which differs greatly with the relative strength of circulation to the main flow.

(2) A vortex with a counter-clockwise circulation, in the neighbourhood of a corner does not describe a closed curve but moves approximately, as if it were merely carried away by the main flow.

For $\pi<\alpha\leqq 2\pi(1>n\geqq 1/2)$.

(3) A vortex with a clockwise circulation moves round a sharp corner so far as the strength of circulation does not exceed a critical magnitude corresponding to the condition for equilibrium of the local vortex towards the main flow, but it does not move round the corner when subjected to a strength of circulation exceeding this limit.

(4) So far as a vortex with a counter-clockwise circulation is concerned, a similar result to that in (2) is observed.

(5) The locus giving the equilibrium position of a vortex is the line bisecting the angle α, and the equilibrium is reached when the main stream U and the strength of clockwise circulation Γ satisfy the relation

$$\Gamma=4\pi n\mathrm{U}\rho^{n},$$

where ρ is the distance of the vortex from the corner.

(6) The equilibrium is stable or unstable for the region $\alpha<\pi(n<1)$ or $\pi<\alpha\leqq 2\pi(1>n\geqq 1/2)$ with respect to the small deviation of its position.

For $\alpha=\pi(n=1)$.

* The term "main flow" is used in this paper for the flow due to U, which corresponds to the ordinary potential flow round a corner with no vortex in it.

† Conclusions are stated here under the conventional assumption that the main flow is taking place in a direction having the region under consideration on the left-hand side of the boundary as traced.

(7) A vortex moves always on the line parallel to the boundary in the direction of the main flow or against it. This follows from the expression $\Gamma \gtreqless 4\pi Uy$, y being the distance of the vortex from the boundary. $\Gamma = 4\pi Uy$ represents an equilibrium condition and a stability for a small deviation of a vortex from the equilibrium position is neutral.

II. *Determination of Path.*

The complex potential w for a uniform flow with a local vortex in it can be obtained by the so-called image method

Figs. 1A & 1B.

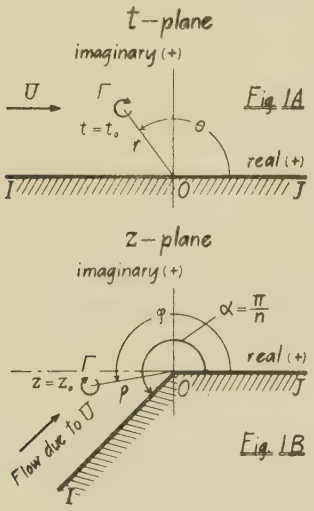

for a t-plane, which is taken as the upper half of an infinite domain bounded by a single straight line IOJ. in fig. 1A.

The flow with a local vortex, of the same strength of circulation Γ but relatively to the domain shown in fig. 1B ($\alpha = \pi/n$, $1/2 \leqq n < \infty$), becomes by merely transforming the t-plane to the z-plane defined by equation $t = z^n$ as follows:

$$w = -\frac{i\Gamma}{2\pi} \log[(z^n - z_0^n)/(z^n - \bar{z}_0^n)] - Uz^n, \quad . \quad . \quad (1)$$

where z_0 denotes the position of a vortex in the z-plane.

The complex potential w_v contributive to the motion of the vortex under consideration in the z-plane, is expressed, with subtraction of its own potential $-i\Gamma/2\pi \cdot \log(z-z_0)$ in equation (1), as *

$$\left.\begin{aligned} w_v &= -\frac{i\Gamma}{2\pi}\log[(z^n-z_0^n)/(z^n-\bar{z}_0^n)(z-z_0)]-\mathrm{U}z^n \\ &= \frac{i\Gamma}{2\pi}\log[(t^{\frac{1}{n}}-t_0^{\frac{1}{n}})(t-\bar{t}_0)/(t-t_0)]-\mathrm{U}t \end{aligned}\right\}. \quad (2)$$

If u and v are the velocity components of a vortex existing in the z-plane along the real and imaginary axes respectively, referring to any plane suffixed, they are determined as follows:—

$$-u_t+iv_t=\left(\frac{dw_v}{d\bar{t}}\right)_{t=t_0}$$

$$=\frac{i\Gamma}{2\pi}\left[\frac{t^{\frac{1}{n}-1}}{n(t^{1/n}-\bar{t}_0^{1/n})}-\frac{1}{(t-\bar{t}_0)}+\frac{1}{(t-t_0)}\right]_{t=t_0}-\mathrm{U}. \quad \ldots \quad (3)$$

Though the details are omitted here, it was possible to work out the result (4) for both an integral and a fractional positive number of $n(\mu/\lambda$, where μ and λ are positive integers).

$$\left[\frac{t^{\frac{1}{n}-1}}{n(t^{1/n}-\bar{t}_0^{1/n})}-\frac{1}{(t-\bar{t}_0)}\right]_{t=t_0}=\frac{(1-n)}{2nt_0} \quad \ldots \quad (4)$$

Hence the velocity components in connexion with the t-plane are found, putting $t_0=re^{i\theta}$, to be

$$\left.\begin{aligned} u_t &= -\frac{\Gamma}{4\pi r}\left[\frac{1-n}{n}\sin\theta+\frac{1}{\sin\theta}\right]+\mathrm{U} \\ v_t &= \frac{\Gamma}{4\pi r}\frac{1-n}{n}\cos\theta \end{aligned}\right\} \quad \ldots \quad (5a)$$

* For any subsequent consideration it may not be out of place to state here that the clockwise or the counter-clockwise circulation is represented by $+\Gamma$ or $-\Gamma$, and the main flow, due to U, towards the positive or the negative side of a real axis by $+\mathrm{U}$ or $-\mathrm{U}$, if Γ and U denote the positive constants in working out equations (2) and (3).

or

$$\left.\begin{aligned} -\frac{dr}{dt} &= \frac{\Gamma}{4\pi r}\cot\theta - \mathrm{U}\cos\theta \\ r\frac{d\theta}{dt} &= \frac{\Gamma}{4\pi r n} - \mathrm{U}\sin\theta \end{aligned}\right\}, \quad . \quad . \quad . \quad (5b)$$

from which

$$-\frac{dr}{r\,d\theta} = \frac{(\Gamma - 4\pi \mathrm{U} r\sin\theta) n\cot\theta}{\Gamma - 4\pi \mathrm{U} r n\sin\theta} \quad . \quad . \quad . \quad (6)$$

Integrating this, we get

$$\frac{\Gamma}{2\pi}\log(r\sin^n\theta) - 2n\mathrm{U}r\sin\theta = \mathrm{C}_1, \quad . \quad . \quad . \quad (7)$$

where C_1 is an integration constant. Let us now put $z_0 = \rho e^{i\varphi}$, and we obtain the relations $r = \rho^n$ and $\theta = n\phi$; the path of a local vortex existing in the z-plane has finally been determined as

$$\frac{\Gamma}{2\pi}\log(\rho\sin n\phi) - 2\mathrm{U}\rho^n\sin n\phi = \mathrm{C}, \quad . \quad . \quad . \quad (8)$$

where C is an integration constant.

III. *Graphical Representation.*

It is evident that, as special examples, the path of a vortex without the main flow becomes Cotes's spiral $\rho\sin n\phi = \text{const.}$ by putting $\mathrm{U} = 0$, and the stream line without a local vortex in it is represented by the curve $\rho^n\sin n\phi = \text{const.}$ by putting $\Gamma = 0$ in equation (8). It is also obvious that equation (8) becomes $\rho\sin\phi = \text{const.}$ or $y = \text{const.}$ for $n = 1$, where y is the distance of a vortex from the boundary. But the curves generally expressed by equation (8) have too varied profiles owing to the variation of both $\pm(\Gamma/\mathrm{U})$ and n for given ρ_0, ϕ_0 to lead us directly to the summarized conclusions without further detailed treatment. As a preliminary help for a fuller understanding of the typical varied paths of a local vortex in the neighbourhood of a corner, the direction of motion at any point will be now obtained.

Since angle ω between the radius vector and the tangent to the path is

$$\omega = \arctan\left(\rho\frac{d\phi}{d\rho}\right) = \arctan\left[\frac{4\pi n\mathrm{U}\rho^n\sin n\phi - \Gamma}{n\Gamma - 4\pi n\mathrm{U}\rho^n\sin n\phi}\tan n\phi\right], \quad \ldots \quad (9)$$

the direction of motion of a vortex at a point $\rho_0 e^{i\phi_0}$ in any specified region will be found for variation of $\pm(\Gamma/\mathrm{U})$, putting $\rho=\rho_0$ and $\phi=\phi_0$ with a given const. n in this

Fig. 2.

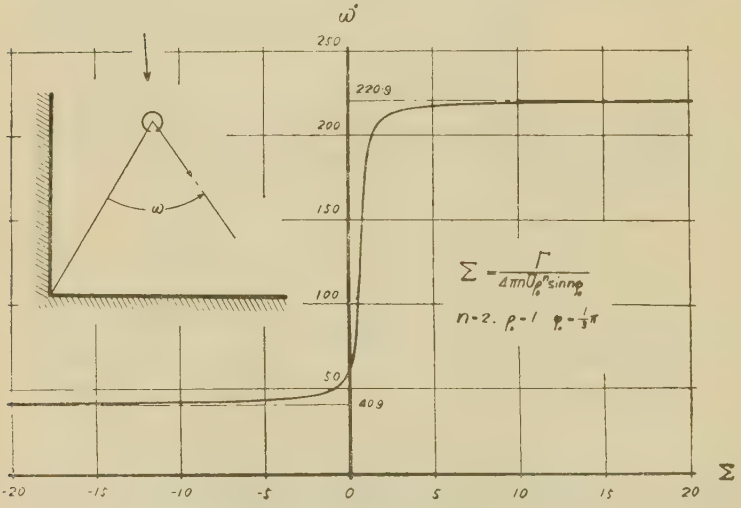

equation. If it is ambiguous to be directly determined uniquely, the determination of the velocity components leads us to the suitable value.

In this paper, in order to avoid complexity of statement $(\pm\Gamma)/\mathrm{U}$ has been considered as a variable to be changed in place of $\pm(\Gamma/\mathrm{U})$ without obscuring the general treatment.

As the typical examples for $n \gtrless 1$, only two cases are shown in fig. 2 and fig. 3, where $\pm\Sigma$ is used as a variable in place of $(\pm\Gamma)/\mathrm{U}$ for the sake of convenience of treatment.

The path of a vortex for the given value of Σ can be

traced from the $\rho-\phi$ curve satisfying equation (8), which is obtained after some tedious numerical calculations *.

Among several examples † with regard to n, treated for the purpose of deducing the summarized conclusions, the two in connexion with fig. 2 and fig. 3 are shown in fig. 4 and fig. 5 respectively. Fig. 4 A or fig. 5 A shows the direction of motion of a vortex at a point P ; this figure will serve to point out clearly the typical paths of a vortex shown in fig. 4 B or fig. 5 B without any plausible explanations.

Fig. 3.

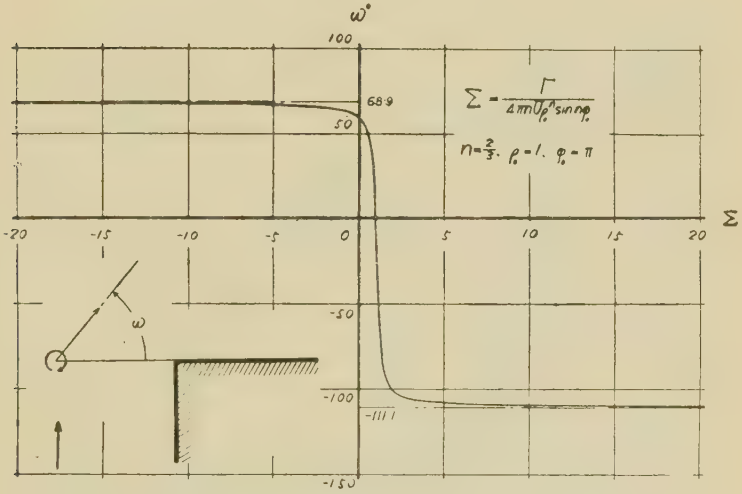

IV. *Equilibrium and Stability.*

The condition for the equilibrium of a local vortex towards the main flow is

$$-u_z+iv_z=\left(\frac{dw_0}{dz}\right)_{z=z_0}=0,$$

* Transform equation (8) into

$$\frac{F}{2\pi}(n-1)\log\frac{\rho}{\rho_0}=\frac{\Gamma}{2\pi}\log\frac{\xi}{\xi_0}-2U(\xi-\xi_0),$$

$$\xi=\rho^n\sin n\phi,$$

where $\rho_0 e^{i\phi_0}$ represents a given point on the path and $\xi_0=\rho_0{}^n\sin n\phi_0$. By obtaining ρ for the values of ξ properly assumed, ϕ can be determined corresponding to ρ thus decided from the above equations.

† The details will be published in Technology Reports of the Tohoku Imperial University, Sendai, Japan.

or

$$\left.\begin{aligned} u_z &= -\frac{\Gamma}{4\pi\rho}\left[(1-n)\sin\phi+\frac{n\cos(n-1)\phi}{\sin n\phi}\right] \\ &\qquad +\mathrm{U}n\rho^{n-1}\cos(n-1)\phi=0, \\ v_z &= \frac{\Gamma}{4\pi\rho}\left[(1-n)\cos\phi+\frac{n\sin(n-1)\phi}{\sin n\phi}\right] \\ &\qquad -\mathrm{U}n\rho^{n-1}\sin(n-1)\phi=0. \end{aligned}\right\} \quad (10)$$

Figs. 4A & 4B.

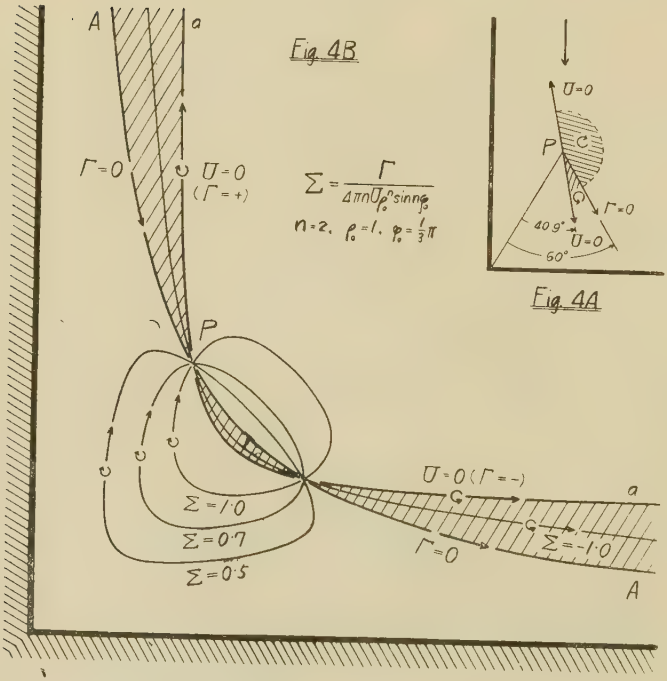

From which we get

$$(n-1)\sin 2n\phi=0.$$

For $n\neq 1, \sin 2n\phi=0$, or $\phi=\pi/2n$,

and consequently from equation (10),

$$\Gamma=4\pi n\mathrm{U}\rho^n.$$

This condition gives a curve such as PMM_1 shown in fig. 5B, and here conclusions (3) and (5) have been based.

For $n=1$ the equilibrium is not restricted for ϕ, and the condition $\Gamma=4\pi U\rho\sin\phi=4\pi Uy$ is only obtained where y is the distance of a vortex from a boundary, and a vortex moves in the direction of or against the main flow for $\Gamma<4\pi Uy$ or $\Gamma>4\pi Uy$, as is evident from the inquiry of the velocity component.

Figs. 5 A & 5 B.

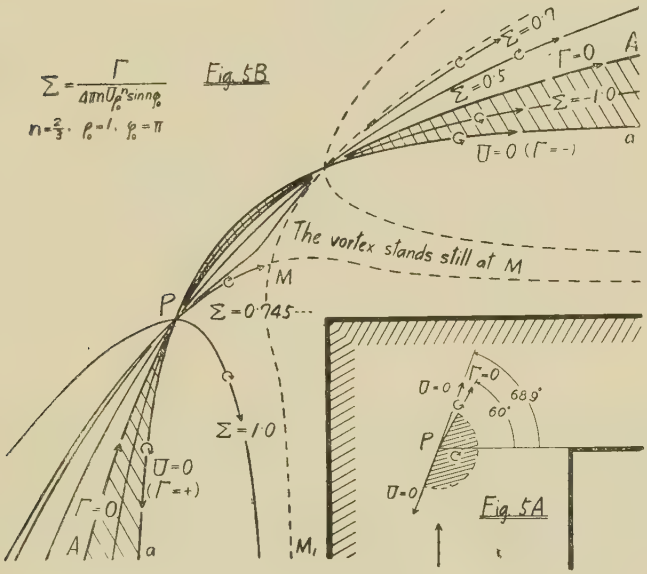

Let us denote the position of equilibrium by X_0, Y_0, and the disturbed one by $X_0+\xi$, $Y_0+\eta$ in Cartesian coordinates, with the assumption that both ξ and η are so small that the square and product of them are negligible, and the equations of motion of a vortex become

$$\left.\begin{aligned}\frac{d\xi}{dt}&=L\xi+M\eta\\ \frac{d\eta}{dt}&=N\xi-L\eta\end{aligned}\right\},\quad\ldots\ldots\quad(11)$$

where

$$\left.\begin{aligned} \mathrm{L}=\left|\frac{\partial u_z}{\partial \xi}=-\frac{\partial v_z}{\partial \eta}\right| &= -\frac{1}{2}n^2(n-2)\mathrm{U}{\rho_0}^{n-2}\sin\frac{\pi}{n}, \\ \mathrm{M}=\left|\frac{\partial u_z}{\partial \eta}\right| &= \frac{1}{2}n^2(n-2)\mathrm{U}{\rho_0}^{n-2}\cos\frac{\pi}{n}+\frac{1}{2}n^3\mathrm{U}{\rho_0}^{n-2}, \\ \mathrm{N}=\left|\frac{\partial v_z}{\partial \xi}\right| &= \frac{1}{2}n^2(n-2)\mathrm{U}{\rho_0}^{n-2}\cos\frac{\pi}{n}-\frac{1}{2}n^3\mathrm{U}{\rho_0}^{n-2}, \\ \xi=0,\ \eta=0 & \\ \Gamma=4\pi n\mathrm{U}{\rho_0}^n & \end{aligned}\right\}$$

and $$\rho_0=\sqrt{{\mathrm{X}_0}^2\pm{\mathrm{Y}_0}^2}.$$

Hence we get

$$\frac{d^2(\xi,\ \eta)}{dt^2}=(\mathrm{L}^2+\mathrm{MN})(\xi,\ \eta)=(1-n)n^4\mathrm{U}^2{\rho_0}^{2n-1}(\xi,\ \eta). \quad (12)$$

The coefficient of the right-hand side of this equation becomes $-$ or $+$ for $n>1$ or $n<1$; therefore the equilibrium is stable or unstable for the region $\alpha<\pi$ or $\alpha>\pi$.

For $n=1$ it is quite possible to deduce the following result by similar treatment, but with the condition $\Gamma=4\pi\mathrm{U}\rho_0\sin\phi_0$

$$\frac{d^2(\xi,\ \eta)}{dt^2}=0, \quad . \quad . \quad . \quad . \quad . \quad . \quad (13)$$

that is, the stability for a small deviation of a vortex from the equilibrium position is neutral with respect to the region having only a single straight boundary.

In conclusion, the writer wishes to express his hearty thanks to Prof. O. Miyagi for his kind advice and also to Mr. T. Tanabe for his help in numerical calculations.

Sendai.
March 20th, 1933.

XLVI. *Resonance in Coupled Pipes.*

By A. E. Bate, *Ph.D., M.Sc.**

Abstract.

The natural frequency of a resonator consisting of two coaxial cylindrical pipes of different diameters joined end to end, and closed at the larger end, was investigated

* Communicated by the Author.

theoretically by Aldis. The writer. using a series of such resonators closed at *either* end, found that the experimental results agreed closely with those obtained by Aldis's formula.

Further, the relationship is established between this formula and an empirical expression given by Cermak for this type of resonator, but with pipes equal in length.

I. *Introduction.*

THE results of this investigation confirm a theoretical formula, originally given by Aldis *, for the resonant tones of a compound pipe consisting of two pipes of different diameters joined end to end.

The resonators considered are shown in fig. 1 and had :

(*a*) The larger end closed.

(*b*) The smaller end closed.

(*c*) The larger end closed with the smaller pipe re-entrant.

(*d*) The smaller pipe closed and re-entrant.

The formula in question,

$$\tan 2\pi l/\lambda . \tan 2\pi \mathrm{L}/\lambda = (d/\mathrm{D})^2,$$

was proposed by Aldis for the type marked (*a*) and which he termed a bottle-pipe. The remaining forms are variations of (*a*), thus (*b*) is the same system as (*a*) with the pipe of smaller diameter closed; this is represented by Aldis's equation if D be understood to be the diameter of the closed end. In system (*c*) the (open) pipe is re-entrant so that l is negative, and the formula becomes

$$-\tan 2\pi l/\lambda . \tan 2\pi \mathrm{L}/\lambda = (d/\mathrm{D})^2.$$

The fourth combination is the same as (*b*) but is re-entrant.

II. *Experimental.*

The source of vibration was the organ-pipe previously described †; the resonating systems under test were

* Aldis, 'Nature,' p. 309, Aug. 30, 1924. (*See also* Irons, Phil. Mag. ix. p. 359, 1930.)

† Bate, Phil. Mag. viii. p. 750 (Nov. 1929); x. p. 617 (Oct. 1930).

placed at the end of this pipe remote from the mouth. The original method of frequency comparison—tuning-forks to each of which the pipe was adjusted to beat 4 times per second—was retained.

The organ-pipe was of diameter 5·4 cm. (internal) and with each of the other pipes, which will be referred to as X

Fig. 1

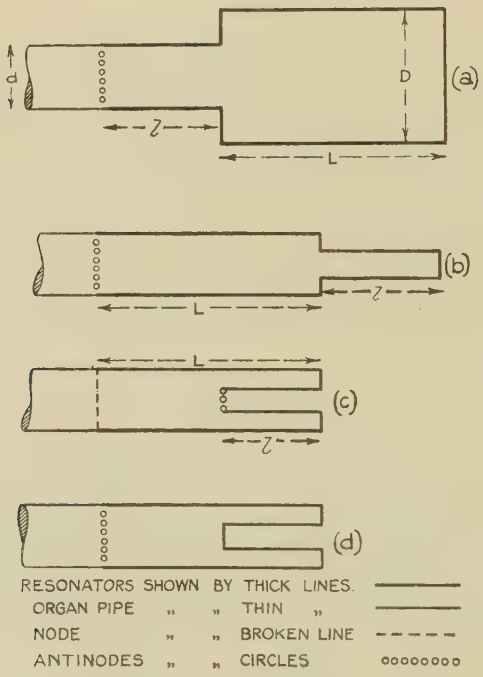

and Y, comprised the compound resonators. Particulars of these pipes are:

X, internal diameter	.....	7·6 cm.
Y, „	„	2·04 „
external	„	2·22 „

The ordinary pipe was used alone at first (stopped), and was *blown* * at the pressure necessary to give a frequency

* Bate, *loc. cit.*

of 260 c.p.s. The positions of the first and second nodes were then ascertained by adjusting the tightly fitting plunger to make the pipe *speak* at this frequency, and were found to be 25·1 and 90·9 cm. from the mouth of the pipe respectively. The antinode was thus 58 cm. from the mouth, and the wave-length 131·6 cm. Further experimental details and the results obtained with each type of resonator will now be considered under separate headings.

(1) *Pipes used*: *organ-pipe and X.*

The organ-pipe, unstopped, was fitted with the flange F, and the larger tube X, as in fig. 2. The flange, which

Fig. 2.

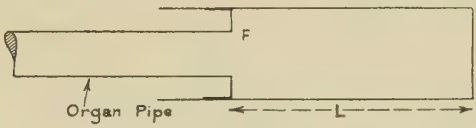

TABLE I.

Lengths of organ-pipe from mouth to flange F, and of pipe X required to give a frequency of 260 c.p.s.

Organ-pipe..	57·3	59·1	62·4	65·7	69·5	74·1	82·1	90·9 cm.
Pipe X	35·1	31·1	24·9	19·1	14·2	9.9	4·9	0·0 „
Total.....	92·4	90·2	87·3	84·8	83·7	84·0	87·0	90·9 „

was always retained at the end of the organ-pipe *, was placed in various positions with respect to the mouth of that pipe, and in each case the speaking length of the larger pipe (X) was adjusted until the original frequency was regained The lengths of the two pipes were obtained in each position, and are given in Table I., together with the total length of the combination.

The total length and the length of the organ-pipe are shown in fig. 3, plotted for each position against the length of the tube X. This curve indicates that when the length of the tube X was 32·9 cm. ($=\lambda/4$ for the note employed, 260 c.p.s.) the total length of the complete

* The organ-pipe consisted of several telescoping tubes.

pipe was 90·9 cm., which was the same as that of the organ-pipe when speaking alone, hence the flange F was at the antinode in this particular instance. It is reasonable to assume that, with the same frequency, the antinode would retain its position with respect to the mouth of the organ-pipe whatever the length of the pipe X—always provided that the antinode remains in the organ-pipe.

The portion of the pipe between the antinode and the closed end may be regarded as a bottle-pipe resonator.

The end-correction for the mouth of the resonator should be zero, for the sound waves at the antinode are

Fig. 3.

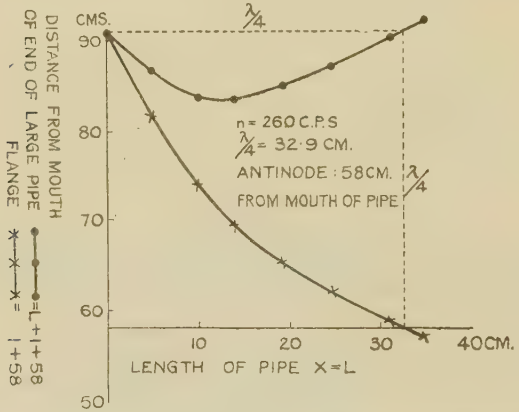

Relationship between positions of end of large pipe (closed), and flange, and the length of the larger pipe.

completely within the tube, and therefore are plane. It follows from Aldis's formula that the minimum length of the resonator occurs when the bottle and the pipe are equal in length, *i. e.*, when $l=L$, so

$$\tan^2 2\pi L/\lambda=(d/D)^2, \text{ whence}$$
$$\tan 2\pi L/\lambda=d/D=5\cdot4/7\cdot6=0\cdot71.$$

Substituting 131·6 cm. for λ in this value of the tangent, $L-l=12\cdot9$ cm. ; *i. e.*, the minimum value * of $L+l=25\cdot8$ cm. These figures agree with the experimental result read from the graph in fig. 3, and show that

* When $A=B$ in $\tan A . \tan B=\phi$ (a constant), $A+B$ is a minimum when ϕ is less than unity, and maximum when ϕ is greater than l.

the antinode does occupy its former position with respect to the mouth of the pipe for this value of l and L.

If, now, we assume that the antinode occupies this position for all positions of the flange in the larger pipe, we can obtain the lengths of the bottle-pipe portion by subtracting the length of the pipe below the antinode, 58 cm., from the total length of the complete pipe in each case. The values thus obtained from the results given in the last table are set out in Table II.; each pair of values was substituted in the formula for the purpose of calculating the ratio of the diameters shown in the third row. The actual ratio is 0·71.

The negative length of the pipe X indicates that the antinode enters the larger tube when the latter exceeds $\lambda/4$ in length, which is to be expected. This antinode

Table II.

Calculated ratio of diameters. [Actual value=0·71.]

Organ-pipe ..	−0·7	1·1	4·4	7·7	11·5	16·1	24·1	32·9
Pipe X.....	35·1	31·1	24·9	19·1	14·2	9·9	4·9	0·0
d/D	0·75	0·78	0·73	0·71	0·70	0·71	0·73	—

will be at a constant distance from the closed end now instead of from the open end of the organ-pipe, as before.

The calculated values of d/D agree closely with the actual value. Discrepancies arose when either of the pipe lengths were small; these are attributed to the possible small errors in measurement *, for such errors would have a considerable effect on the tangents of the smaller angles. In the last column d/D has no significance, as the length of the pipe X=0.

As stated above, when the antinode is in the larger tube it will remain at a distance equal to $\lambda/4$ from the closed end, and any change in the nodal system due to an adjustment in the position of the junction (the flange F) will be confined to the distance between the node and the antinode nearest the junction. This statement is true for all positions of the junction in the compound pipe.

* The measurements were true to the nearest mm., hence an error of 1 mm. may occur in the differences due to measurement alone

The experiment was repeated with frequencies of 388, 324, and 196 c.p.s.; the results of the former are shown in the graph in fig. 4, which is similar to the graph of 260 (fig. 3); this is also the case with the curves of the other frequencies, which are not shown. In each the junction was found to coincide with the antinode when the larger pipe was one-quarter wave-length long.

The maximum negative value of l for 324 c.p.s. was $-3{\cdot}9$ cm.; L was $33{\cdot}9$, giving $d/D=0{\cdot}71$; for 388 c.p.s., l and L were respectively $-3{\cdot}75$ and $29{\cdot}2$ cm., whence $d/D=0{\cdot}72$.

Fig. 4.

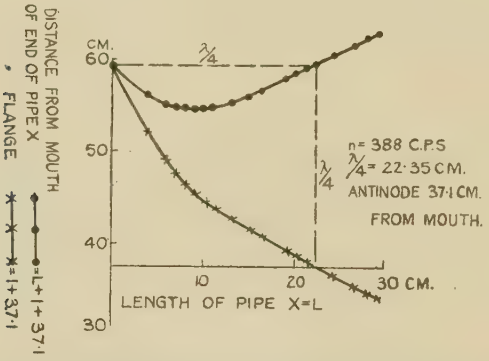

Relationship between the positions of the end of the large pipe (closed) and the flange, and the length of the larger pipe.

(2) *Pipes used*: *organ-pipe and Y, closed.*

The experiments were next repeated with the smaller pipes Y, of which there were four lengths, 20, 15, 10, and 5 cm. long respectively. These were attached, in turn, to the original pipe; the outer ends were closed. The results obtained with 260 c.p.s. are shown graphically in fig. 5. The curves are concave downwards: this is due to the fact that the sectional area of the "bottle," *i. e.*, the closed portion of the resonator, was less than that of the pipe. This is represented by Aldis's formula if D be taken to represent the diameter of the closed end, and d that of the open end. This value of $(d/D)^2$ is $7{\cdot}01$. The turning-point of the upper curve indicates that the maximum length of the bottle-pipe occurs when $L=l=25{\cdot}68$ cm. As the length of the longest of the small

diameter pipes (Y) was 20 cm., direct comparison cannot be made, but, owing to the reciprocal nature of L and l in the formula, four values were interpolated; the resulting curves show the maximum to agree with the calculated value.

Negative values for the closed pipe were obtained by inserting into the pipe a rod whose diameter equalled the internal diameter of the smaller pipes (fig. 1, *d*). The graph of the results indicates that the end of the rod coincides with the antinode when the rod projects one-quarter of the wave-length into the organ-pipe.

Fig. 5.

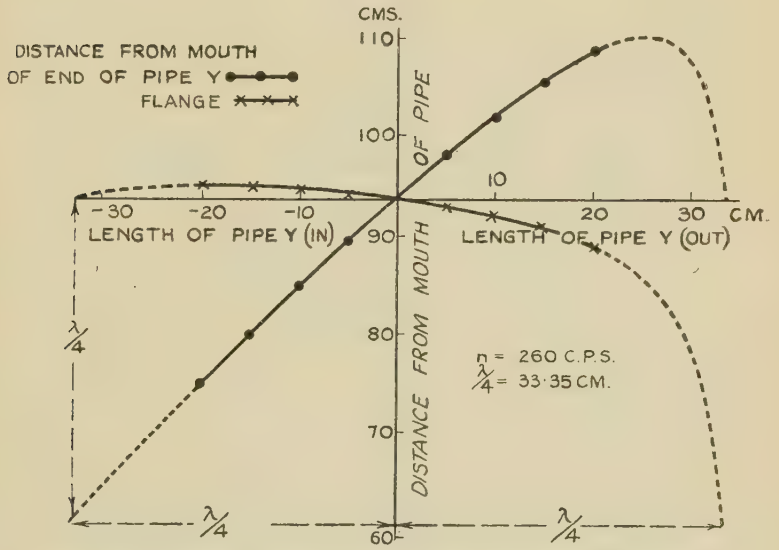

Relationship between positions of flange and end of small pipe (closed), and the length (re-entrant and normal) of the latter.

Similar results were obtained with a frequency of 324 c.p.s. (fig. 6).

(3) *Pipes employed: organ-pipe and Y, open.*

Since the small pipe was now open, it was necessary to regard it as the pipe of a bottle-pipe resonator which extended from the antinode at the mouth of Y to the node in the organ-pipe nearest the junction, for this node would correspond to the closed end of the bottle. The

ratio $(d/D)^2$ was less than unity, being 0·143, so the curves in the graphs of the results were concave upward (see second footnote). The graph in fig. 7 confirms this for a frequency of 260 c.p.s., and, if allowance be made for the end-corrections at the mouth, the calculated and experimental results are in agreement. For example, the calculated minimum lengths of the bottle and of the pipe are each 7·7 cm., whereas the curve shows the actual minimum length of the pipe to be 7·0 cm.; thus

Fig. 6.

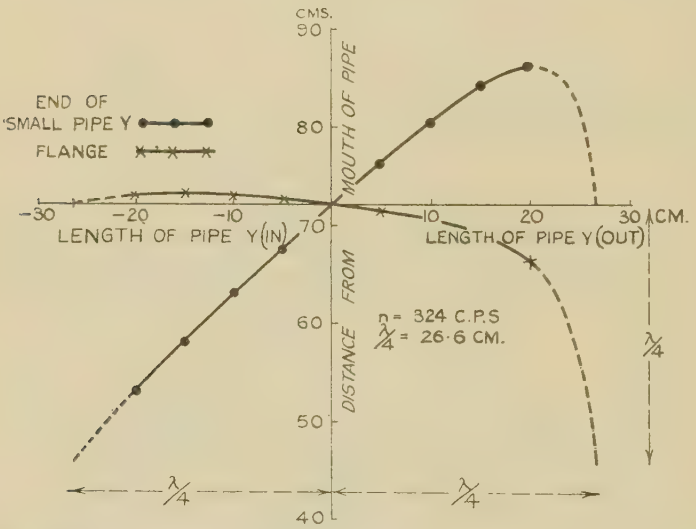

Relationship between positions of flange and end of small pipe (closed), and the length of the latter.

the end-correction was 0·7 cm., and this agrees with 0·66 R*, since R = 1·02 cm., to the nearest mm.

Negative values of l were obtained by fixing the small pipes, in turn, inside the organ-pipe, as in fig. 1, *c*. It will be seen that the total length of the two was zero when they were of equal lengths. This agrees with the results read from the curve (fig. 7), l being 7·7 cm., and indicates the end-correction of the unattached end of the small tube to be zero; this is to be anticipated, as the

* Bate, Phil. Mag. x. p. 621 (1930).

waves were plane in both tubes. Some correction is to be expected at the junction, however, since the latter communicates with the open air. At first it appeared that the absence of such a correction was caused by the increase in the ratio $(d/D)^2$ owing to the diminution in the effective sectional area of the larger tube by the *thickness* of the material of the smaller. This possibility received support from the fact that as any two such tubes become more nearly equal in diameter, the minimum

Fig. 7.

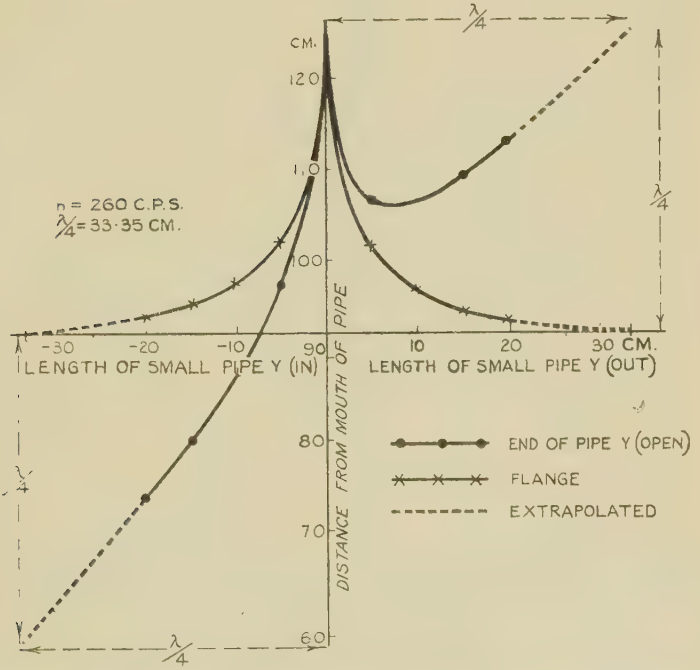

Relationship between positions of flange and end of small pipe (open), and the length of the latter.

total length increases (compare figs. 3 & 7). The ratio of the internal section of the small tube to that of the larger when the latter is reduced by an amount equal to the sectional area of the material of the smaller tube, however, was found to be 0·1465; and this, when substituted in the equation, gave $L = l - 7{\cdot}77$ cm. This almost agrees with the graphical result, and shows that there is

no appreciable end-correction for these values of l and L, which probably may be accounted for by the fact that the portion of the junction open to the air is not an antinode.

The corresponding results obtained with a frequency of 324 c.p.s. are shown in the graph (fig. 8); the shorter the wave-length the more nearly complete becomes the curve obtainable with the four smaller tubes.

Fig. 8.

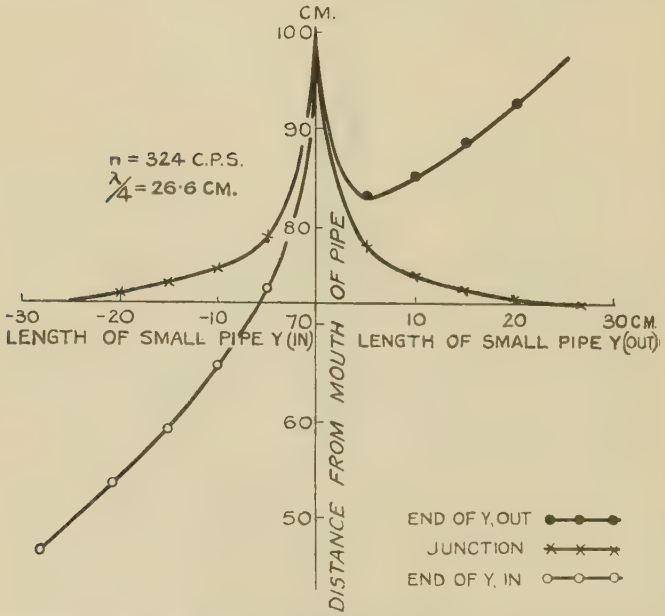

Relationship between positions of flange and end of small pipe (open) and the length of the latter.

III. *The Rohrflöte.*

When the stopped end of an organ-pipe is fitted with an open pipe of smaller diameter, as above, it constitutes a Rohrflöte (Ger.) or Flûte à Cheminée (Fr.) * Benton † gave the expression

$$(\tan 2\pi l/\lambda) / (\tan 2\pi L'/\lambda) = -(d/D)^2,$$

for the natural frequencies of such a pipe. L′ stands for

* Audsley, 'The Art of Organ Building,' vol. ii. p. 537.
† Benton, 'Nature.'

the length of the pipe, and includes the mouth correction ; the other terms retain their former significance.

$$L'=L+\lambda/4, \text{ whence } \tan 2\pi L/\lambda=-\cot 2\pi L'/\lambda,$$

which, substituted in Benton's equation, gives Aldis's equation.

IV. *Cermak's Work on Pipe Resonance.*

Cermak * has performed experiments on resonance in systems of coaxial tubes of various sectional areas. The major portion of his work concerned pipes arranged as bottle-pipe resonators, the frequencies of which he estimated by comparison with a sonometer. Values were estimated with various lengths of the pipe and bottle portions, but with the total length of each of the resonators equal in a particular group of experiments. Each experiment was performed first with one end and then with the other open. The results from each group showed that when the pipes were of equal length resonance occurred : (*a*) at the lowest frequency with the wide end closed ; (*b*) at the highest frequency with the narrow end closed.

Cermak gave the following empirical relationship between N, the frequency of the resonator when the two pipes were of equal length, and N_0, the fundamental frequency of a single pipe equal in length to the two, and in diameter equal to that of either :

$$N=N_0[1\pm(1-d/D)^{4/3}]$$

in which d and D now stand for *the diameters of the narrow pipe and the wide pipe respectively* ; the + sign is used if the narrow pipe be closed, the − if the wide end be closed. This formula represents the relationship closely when the wide end is closed, and is very near to the value obtained theoretically, for, when $l=L$ (including the end-correction of the open end) we may write, as before,

$$\tan 2\pi l/\lambda=d/D,$$

or

$$l=(\lambda/2\pi)\tan^{-1} d/D$$
$$=(\lambda/2\pi)(d/D-d^3/3D^3+d^5/5D^5\ldots).$$

But the wave-length λ_0 of the fundamental frequency of

* Cermak, *Ann. d. Phys.* p. 53 (1917).

a pipe of constant diameter and of length $2.l$ (including the end-correction) is $8.l$, hence

$$l=\lambda_0/8=(\lambda/2\pi)(d/\mathrm{D}-d^3/3\mathrm{D}^3+d^5/5\mathrm{D}^5\ldots)$$

or, since $\mathrm{N}/\mathrm{N}_0=\lambda_0/\lambda$,

$$\mathrm{N}=(4\mathrm{N}_0/\pi)(d/\mathrm{D}-d^3/3\mathrm{D}^3+d^5/5\mathrm{D}^5\ldots). \quad . \quad (\mathrm{A})$$

Cermak's expression expands to

$$\mathrm{N}=(4\mathrm{N}_0/3)(d/\mathrm{D}-d^2/6\mathrm{D}^2-d^3/27\mathrm{D}^3-\ldots), \quad . \quad (\mathrm{B})$$

when the negative sign is used, and closely resembles the expression (A).

When the small end is closed, (A) still holds if D/d be written for d/D. Cermak's expression with the positive sign, however, expands to

$$\mathrm{N}=(4\mathrm{N}_0/3)(3/2-d/\mathrm{D}+d^2/6\mathrm{D}^2+\ldots),$$

and this bears little resemblance to

$$\mathrm{N}=(4\mathrm{N}_0/\pi)(\mathrm{D}/d-\mathrm{D}^3/3d^3+\mathrm{D}^5/5d^5\ldots).$$

If Cermak's expression is re-written thus :

$$\mathrm{N}=\mathrm{N}_0[1-\{1-(d/\mathrm{D})^{\pm 1}\}^{1\cdot 3}],$$

in which the sign of the index is selected as before, it gives closer agreement between the theoretical and practical results when the small end is closed. For example, the values of N/N_0 for the experiments described in the first part of this paper were calculated each way, and the results were :

D closed.		*d* closed.		
Cermak.	Theoretical.	Cermak.	Theoretical.	Proposed.
0·81	0·76	1·19	1·32	1·30

In referring to the lengths of the pipe, the end-corrections must be accounted for ; if, however, the correction is ignored both with the compound pipe and the uniform pipe used for N_0, no serious error will arise, providing the diameters are small in comparison with the length of the pipes, or, if pipes of large diameter are used, providing the diameters are nearly equal.

The writer wishes to acknowledge helpful criticism on the part of Dr. Irons during the course of this work.

Northern Polytechnic,
London.

XLVII. *Note on the Stability of Saturn's Rings.* By C. G. Pendse, *B.A.*, *Downing College, Cambridge* *.

In the first part of his Adams Prize Essay †, "On the Stability of the Motion of Saturn's Rings," Maxwell investigated the stability of the motion of a rigid plane ring about a central homogeneous sphere in a plane passing through the centre of the sphere; and he deduced the instability of the motion of any conceivable rigid circular ring by considering the particular cases of the general results obtained on the assumption that the law of universal gravitation is applicable to the Saturnian system. As a particular case, and incidentally the most important particular case, he has deduced the instability of the motion of a uniform rigid circular ring. The purport of this note is to show that one cannot deduce the instability in question as a particular case of the general work, and that the general equations become meaningless in the case of the steady motion of a uniform circular rigid ring; the instability can, however, be proved by a slightly different method.

Let $\angle AGR=\theta$, $\angle BRK=\phi$, k=the radius of gyration of the ring about its centre of mass, $SR=r$.

Let the unit of mass be chosen in such a way as to make the constant of gravitation equal to unity; and let V denote the gravitational potential of the ring at S. V is a function of r and ϕ.

Maxwell obtained the general equations of motion of the ring in the form ‡

$$R\left\{2r\frac{dr}{dt}\frac{d\theta}{dt}+r^2\frac{d^2\theta}{dt^2}\right\}+(R+S)\frac{\partial V}{\partial\phi}=0, \quad . \quad . \quad (6)$$

$$R\left\{\frac{d^2r}{dt^2}-r\left(\frac{d\theta}{dt}\right)^2\right\}-(R+S)\frac{\partial V}{\partial r}=0, \quad . \quad . \quad . \quad (7)$$

$$Rk^2\left(\frac{d^2\theta}{dt^2}+\frac{d^2\phi}{dt^2}\right)-S\frac{\partial V}{\partial\phi}=0, \quad . \quad . \quad . \quad . \quad . \quad . \quad (8)$$

Then, according to Maxwell, in steady motion $\phi=$ con-

* Communicated by Dr. W. M. Smart.

† 'Scientific Papers,' vol. i. pp. 288–376.

‡ The numbers of the equations are Maxwell's numbers (pp. 298–299, *loc. cit.*).

stant, $\dot{\theta}$=constant=ω (say), r=constant=r_0. The equations (6), (7), (8) then become, in a steady state,

$$\left(\frac{d\theta}{dt}\right)^2 = -\frac{R+S}{Rr}\frac{\partial V}{\partial r} = \omega^2,$$

provided $\frac{1}{r}\frac{\partial V}{\partial r}$ is negative in the steady state, . . (9)

$$\frac{\partial V}{\partial \phi} = 0. \quad . \quad . \quad . \quad . \quad . \quad . \quad . \quad . \quad (10)$$

Then he put $r=r_0+r_1$, $\theta=\omega t+\theta_1$, $\phi=\phi_0+\phi_1$ for a slightly disturbed motion, where r_1, θ_1, ϕ_1 are small,

Fig. 1.

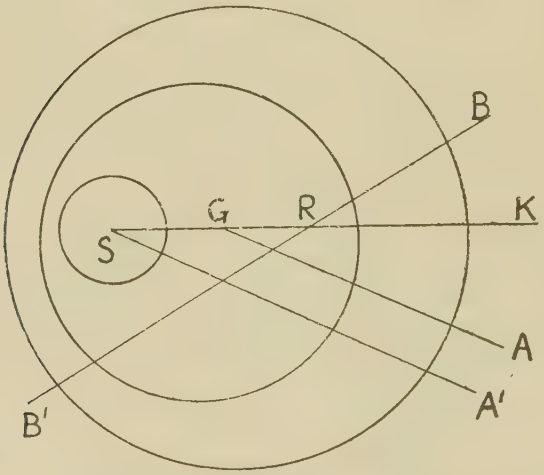

Maxwell's diagram in the general case *.

In fig. 1

G is the centre of mass of the ring and the planet.

R is the centre of mass of the ring and also its mass.

S is the centre of mass of the central body (Saturn) and also its mass.

GA is a direction fixed in the plane of the ring.

B'RB is a line fixed in the ring.

* Vol. i. plate v. (to face page 376).

ϕ_0 being the value of ϕ in the steady state ; and afterwards putting

$$L=\left(\frac{\partial^2 V}{\partial r^2}\right)_0, \quad M=\left(\frac{\partial^2 V}{\partial r \partial \phi}\right)_0, \quad N=\left(\frac{\partial^2 V}{\partial \phi^2}\right)_0;$$

the values of the left-hand sides being taken for the steady state, he obtained the equations (11), (12), (13) for r_1, θ_1, ϕ_1. From these equations he obtained the equation, (18), which contains the condition of stability, putting $\frac{dr_1}{dt}=nr_1$, $\frac{d^2r_1}{dt^2}=n^2r_1$, etc., and equations (19) contain the expressions for the coefficients A, B, C in equation (18). For stability n must be a pure imaginary.

In Problem V. he supposed that the ring is circular, and assumed the formula (21) for the line density of the ring, and introduced the coefficients f, g, h, etc. Taking a to be the radius of the ring, he then obtained the equations (24) for L, M, N in terms of R, a, f, g, h. Considering the mass-acceleration of the whole ring he derived the relation

$$Ra f\omega^2=RS\frac{f}{a^2}.$$

Neglecting R in comparison with S, the equation of stability reduces to

$$R^2a^4f^2\left[(1-f^2)n^4+(1-\frac{5}{2}f^2+\frac{1}{2}f^2g)\,n^2\omega^2+\left(\frac{9}{4}-6f^2-\frac{1}{4}g^2-\frac{1}{4}h^2+2f^2g\right)\omega^4\right]=0,$$

which reduces to equation (28) of Maxwell if $R^2a^4f^2$ is left out.

Now for a uniform ring $f=g=h=0$, and the equation then becomes

$$n^4+n^2\omega^2+\frac{9}{4}\omega^4=0, \quad . \quad . \quad . \quad . \quad . \quad (29)$$

which gives complex values to n^2, and hence denotes instability, according to Maxwell.

In 'Traité de Mécanique Céléste,' t. ii., Tisserand followed Maxwell's method in every detail, and arrived at equation (29). In 'Figures d'equilibre d'une masse fluide' (chapter viii.) Poincaré used a slightly different

method, and arrived at the equation $\omega^4-\omega^2+\frac{9}{4}=0$ for the case of a uniform rigid circular ring, and thence concluded that the steady motion is unstable.

Now, in the case of steady motion of a uniform rigid circular ring, R, S, and G will coincide, and consequently θ will have no meaning in the steady state. The same applies to ϕ. Consequently equations (6), (7), (8) will become meaningless in the steady state. Since $f=g=h=0$ for a uniform rigid ring, the equation $Raf\omega^2=RS\frac{f}{a^2}$ reduces to the form $0=0$ (f cannot be divided out).

Fig. 2.

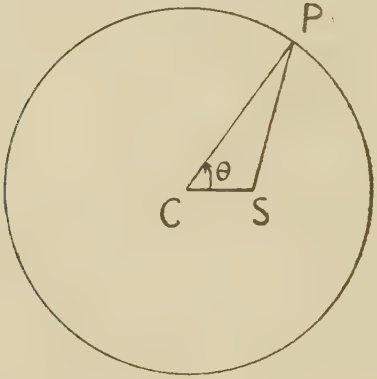

For the same reason the equation (29) cannot be arrived at in the particular case by cancelling $R^2a^4f^2$ from both sides of the equation from which it is derived by putting $f=g=h=0$ and leaving out $R^2a^4f^2$.

The important point is that this state of relative equilibrium may be either static or dynamic. Secondly, it is impossible to determine ω^2 in terms of R, S, and a for a uniform circular ring; for the sum of the mass-accelerations of the ring vanishes, and also the total gravitational force on the ring due to the attraction of the central body, when R and S coincide, is zero; finally, equation (29) of Maxwell cannot arise.

Hence one comes to the conclusion that the whole scheme breaks down for a uniform circular ring.

A proof of the instability of the steady motion of a uniform circular ring about a homogeneous spherical body will now be given.

In fig. 2 let R be the mass of the ring and let C be its centre. Let S be the mass of the central body and also its centre, and let V be the gravitational potential of the ring at S.

In the steady state S coincides with C and the ring rotates uniformly about C. We consider a disturbance in the plane of the ring.

Let a=radius of the ring, CS=r, $\angle$PCS=θ.

We suppose that r is small, and hence find the value of V, neglecting the terms of order $\frac{r^3}{a^3}$. We have

$$V = \frac{2R}{2\pi a}\int_0^\pi \frac{a\,d\theta}{(a^2-2ar\cos\theta+r^2)^{\frac{1}{2}}}$$

$$= \frac{R}{\pi a}\int_0^\pi \left\{ P_0(\cos\theta)+\frac{r}{a}P_1(\cos\theta) + \frac{r^2}{a^2}P_2(\cos\theta+)\ldots \right\} d\theta \text{ in terms of Legendre Polynomials.}$$

$$= \frac{R}{\pi a}\int_0^\pi \left\{ P_0(\cos\theta)+\frac{r^2}{a^2}P_2(\cos\theta) \right\} d\theta \text{ up to } \frac{r^2}{a^2}$$

$$= \frac{R}{a}+\frac{R}{\pi a}\frac{r^2}{a^2}\int_0^\pi \tfrac{1}{2}(3\cos^2\theta-1)\,d\theta$$

$$= \frac{R}{a}+\frac{R}{4a^3}r^2.$$

Hence the force on the central body due to the gravitation of the ring

$$= S\frac{\partial V}{\partial r} \text{ along CS},$$

$$= \frac{RS}{2a^3}r \text{ along CS}.$$

The acceleration of S relative to Newtonian axes is, therefore, $\frac{R}{2a^3}r$ along CS. The force on the ring due to the gravitation of the central body reduces, by Newton's

third law, to a force $\frac{RS}{2a^3}r$ along SC. Hence the acceleration of C relative to Newtonian axes is $\frac{S}{2a^3}r$ along SC.

The acceleration of C relative to S is therefore

$$\frac{S+R}{2a^3}r \text{ along SC.} \quad . \quad . \quad . \quad . \quad . \quad . \quad \text{(I.)}$$

Let Sx, Sy be rectangular axes in the plane of the ring and parallel to Newtonian axes, and let x, y be the coordinates of C relative to S.

Equation (I.) then means

$$\ddot{x} = \frac{S+R}{2a^3}x, \quad \ddot{y} = \frac{S+R}{2a^3}y \quad . \quad . \quad . \quad . \quad \text{(II.)}$$

Equations (II.) denote instability, and the motion departs more and more from its steady state till the approximations are no longer valid.

Another point is worth noticing. The spin of the ring does not figure anywhere in the above work, and, in fact, it remains constant for any disturbance in the plane of the ring, *i. e.*, even though r is made so large that the approximations made above cease to be valid. For it is easy to see that on account of symmetry the force on the ring due to the gravitation of the sphere is along SC ; hence the angular momentum of the motion of the ring relative to C about C remains constant for these displacements, large as they may be.

I am indebted to Prof. H. F. Baker, Prof. G. R. Goldsbrough, and Dr. W. M. Smart for helpful suggestions.

XLVIII. *Influence of Temperature on the Diamagnetism of certain Liquids.* *By* Mohd Abdul Azim, *M.Sc., Sir George Anderson Scholar*, S. S. Bhatnagar, *D.Sc., F.Inst.P., University Professor of Chemistry, and* Ram Narain Mathur, *M.Sc.**

SINCE the Langevin theory of diamagnetism came into vogue, a vast amount of work has been done which shows, contrary to this theory, that diamagnetism is also influenced by temperature. Honda [1], in his

* Communicated by the Authors.

classical work on the susceptibilities of elements, found that in many elements the diamagnetism varied with temperature. Similar observations have been made by Ishiwara[2], Sucksmith[3], and Ashworth [4]. Oxley [5] showed that a sudden change in the value of magnetic susceptibility is observed when the substances get fused. In most liquids the susceptibility decreases with temperature. The only case which has been studied with great accuracy where the susceptibility shows a slight increase with temperature is that of water [6]. In a previous paper from this laboratory R. N. Mathur[7] emphasized the observations of Bhatnagar that the thermal variations of susceptibilities were, in general, greater in the case of the aromatic compounds, and the most particularly noticeable substance with respect to this property was nitro-benzene. Interest in work of this nature has been enhanced by the observations of K. S. Krishnan and Bragg[8], who have established that the whole of the work of Oxley on the influence of temperature on the susceptibility at the melting-point requires to be repeated on single crystals. A study of liquids which shows a definite increase in the value of χ with temperature and accurate observations on the thermal decrease of susceptibility in case of other liquids deserve special attention, particularly where the variations of their dipole moments with temperatures have been accurately studied. A comparison of these thermal variations of susceptibilities with other properties such as magnetic birefringence, association, dissociation, and polymerization has opened up a new field of work of great interest and importance.

Experimental.

The apparatus employed during this investigation was similar to that used by Bhatnagar and Mathur[9], with this modification, that the narrow tube in between the pole-pieces of the electromagnet was also double-jacketted Readings at any temperature of the liquid under investigation were taken by circulating water from a large thermostat in the outer jackets round the tube and the reservoir. As the readings of the meniscus are taken through the outer tube and water, it is necessary that the outer jacket and the water flowing through it be clear and transparent.

As the differences between the displacements of the meniscus at different temperatures are in general small, a micrometer eye-piece was employed to register the change. Another precaution found necessary was to definitely fix the position of the pole-pieces as well as the tube. In order to accomplish this a stout brass piece, with a hole in the centre to admit the tube, was fixed on to the pole-pieces of the electromagnet. Further, a fine mark was etched on the narrow tube, thus fixing its position between the poles of the electromagnet. For every reading at every temperature the meniscus was brought to the same position in the field by raising or lowering the reservoir.

Scrupulous care is also necessary in cleaning the tube and the reservoir to prevent any faulty movements of the meniscus owing to wetting difficulties. Another necessary precaution taken was to set the micrometer eye-piece exactly in line with the meniscus at right angles to the narrow tube. Before recording observations it is necessary that the temperature of the liquid should become constant. When the temperature becomes constant, the meniscus in the microscope becomes steady, or tends to rise in case of volatile liquids due to evaporation.

Other precautions taken are the same as those described in the previous papers from these laboratories on the subject.

Before commencing the investigation the apparatus was standardized with respect to water ($\chi = -0{\cdot}72 \times 10^{-6}$ at 20° C.). The values of the magnetic susceptibility at different temperatures have been calculated by the equation

$$\chi = \frac{2\theta g}{H^2} + \chi_a \frac{\rho_a}{\rho},$$

where

χ = specific susceptibility of the liquid ;
χ_a = specific susceptibility of air ;
ρ_a = density of air ;
θ = mean displacement of the meniscus.

The values of ρ_a in the above equation for different temperatures were taken from standard Tables, and the values of ρ were determined experimentally. The values of χ_a at different temperatures can be calculated without

appreciable error by Curie's law, as the diamagnetism of nitrogen and argon in air is almost negligible [7].

The results obtained are shown in Tables I.–XX.

TABLE I.

Nitro-benzene.

$\chi = -0{\cdot}499 \times 10^{-6}$ at 20° C. (Oxley).

Temperature, ° C.	Density.	Susceptibility, $-\chi \times 10^6$.
25	1·1986	0·496
30	1·1936	0·492
40	1·1836	0·487
50	1·1735	0·482
60	1·1635	0·477
70	1·1536	0·472
75	1·1435	0·469

TABLE II.

Benzo-nitrile.

$\chi = -0{\cdot}650 \times 10^{-6}$ (Pascal).

Temperature, ° C.	Density.	Susceptibility, $-\chi \times 10^6$.
20	1·0060	0·650
30	0·9992	0·645
30	0·9911	0·639
50	0·9808	0·636
60	0·9727	0·630
75	0·9600	0·625

TABLE III.

Ethyl-benzene.

Temperature, ° C.	Density.	Susceptibility, $-\chi \times 10^6$.
20	0·8684	0·750
30	0·8615	0·748
40	0·8530	0·747
50	0·8435	0·746
60	0·8361	0·743
70	0·8275	0·742
75	0·8255	0·741

TABLE IV.

Pseudo-cumene.

Temperature, °C.	Density.	Susceptibility, $-\chi \times 10^6$.
20	0·8767	0·845
30	0·8685	0·842
40	0·8611	0·841
50	0·8530	0·837
60	0·8457	0·834
75	0·8341	0·829

TABLE V.

Mesitylene.

Temperature, °C.	Density.	Susceptibility, $-\chi \times 10^6$.
20	0·8638	0·682
30	0·8557	0·680
40	0·8476	0·679
50	0·8393	0·677
60	0·8310	0·676
75	0·8158	0·674

TABLE VI.

Toluene.

$\chi = -0{\cdot}730 \times 10^{-6}$ (Pascal).

Temperature, °C.	Density.	Susceptibility, $-\chi \times 10^6$.
20	0·8670	0·730
30	0·8548	0·727
40	0·8426	0·724
50	0·8338	0·721
60	0·8251	0·718
75	0·8096	0·714

TABLE VII.

Xylene Meta.

Temperature, °C.	Density.	Susceptibility, $-\chi\times10^6$.
20	0·8662	0·741
30	0·8581	0·738
40	0·8500	0·736
50	0·8418	0·734
60	0·8335	0·731
75	0·8216	0·728

TABLE VIII.

Aniline.

Temperature, °C.	Density.	Susceptibility, $-\chi\times10^6$.
20	1·0220	0·700
30	1·0134	0·696
40	1·0048	0·692
50	0·9964	0·688
60	0·9878	0·684
70	0·9788	0·680

TABLE IX.

O-nitro-toluene.

$\chi=-0\cdot532\times10^{-6}$ (Pascal).

Temperature, °C.	Density.	Susceptibility, $-\chi\times10^6$.
20		0·532
30		0·527
40	Densities taken	0·522
50	from	0·518
60	W. H. Perkin.	0·514
75		0·510

Table X.

Iodo-benzene.

$\chi = -0{\cdot}471 \times 10^6$.

Temperature, ° C.	Density.	Susceptibility, $-\chi \times 10^6$.
20	1·8287	0·475
30	1·8138	0·470
40	1·7989	0·466
50	1·7841	0·463
60	1·7692	0·459
75	1·7445	0·454

Table XI.

Bromo-benzene.

Temperature, ° C.	Density.	Susceptibility, $-\chi \times 10^6$.
20		0·482
30		0·476
40	Densities taken	0·472
50	from Landolt	0·467
60	Bornstein Tables.	0·464
75		0·459

Table XII.

Cyclo-hexane.

Temperature, ° C.	Density.	Susceptibility, $-\chi \times 10^6$.
20	0·7755	0·810
30	0·7672	0·810
40	0·7592	0·809
50	0·7515	0·808
60	0·7435	0·808

TABLE XIII.

Carbon Tetrachloride.

$\chi = -0{\cdot}430 \times 10^{-6}$ (Pascal).

Temperature, ° C.	Density.	Susceptibility, $-\chi \times 10^6$.
20	1·5879	0·430
30	1·5780	0·430
40	1·5648	0·431
50	1·5528	0·432
60	1·5420	0·432

TABLE XIV.

Benzene.

$\chi = -0{\cdot}712 \times 10^{-6}$ (Ishiwara).

Temperature, ° C.	Density.	Susceptibility, $-\chi \times 10^6$.
20	0·8802	0·712
30	0·8697	0·708
40	0·8603	0·702
50	0·8500	0·696
60	0·8301	0·692

TABLE XV.

Chloro-benzene.

$\chi = -0{\cdot}639 \times 10^{-6}$ (Pascal).

Temperature, ° C.	Density.	Susceptibility, $-\chi \times 10^6$.
20		0·639
30		0·633
40	Densities taken	0·626
50	from Landolt	0·620
60	Bornstein Tables.	0·614
75		0·606

TABLE XVI.

Water.

$\chi = -0{\cdot}720 \times 10^{-6}$ (Ishiwara and Piccard).

Temperature, °C.	Density (Ramsay and Shields).	Susceptibility, $-\chi \times 10^6$.
25	0·9983	0·720
30	0·9958	0·721
40	0·9923	0·722
50	0·9882	0·723
60	0·9834	0·724
70	0·9779	0·725
75	0·9749	0·726

TABLE XVII.

Iso-butyl Alcohol.

Temperature, °C.	Density.	Susceptibility, $-\chi \times 10^6$.
30	0·7950	0·810
40	0·7889	0·812
50	0·7788	0·813
60	0·7707	0·814
75	0·7545	0·816

TABLE XVIII.

Butyl Alcohol.

Temperature, °C.	Density.	Susceptibility, $-\chi \times 10^6$.
30	0·8038	0·800
40	0·7953	0·802
50	0·7871	0·803
60	0·7789	0·804
75	0·7621	0·806

TABLE XIX.

Propyl Alcohol.

Temperature, °C.	Density.	Susceptibility, $-\chi \times 10^6$.
30	0·7982	0·771
40	7904	0·773
50	0·7816	0·774
60	0·7728	0·775
75	0·7598	0·777

TABLE XX.

Iso-propyl Alcohol.

Temperature, °C.	Density.	Susceptibility, $-\chi \times 10^6$.
30	0·7786	0·788
40	0·7698	0·790
50	0·7617	0·791
60	0·7509	0·792

Discussion of Results.

The results recorded in the tables show clearly that the liquids under discussion can, in general, be divided into three types :—

(1) Those in which the effect of temperature is practically negligible (*cf.* Tables XII. and XIII., which refer to the case of cyclo-hexane and carbon tetrachloride).

(2) Those in which there is a definite increase in the value of χ with temperature, *e. g.*, water, isobutyl alcohol, butyl alcohol, propyl alcohol, and isopropyl alcohol (Tables XVI. to XX.).

(3) Those in which there is a decrease in susceptibility, and these constitute the largest number in this investigation (*cf.* Tables I. to XI.).

Several interesting points emerge from a closer examination of these results. For example, one is immediately struck with the fact that substances in class (1) are

characterized by the non-polar and symmetrical nature of their molecular arrangement. Substances in class (2) are all noted for their polarizability and association. Substances in class (3) are almost all aromatic compounds, and this decrease in χ with temperature has something to do with the aromatic structure.

During recent years it has become increasingly recognized, from the work of Van Vleck [10], Bitter, and Honda, that the magnetic susceptibilities can be given by an expression of the type

$$\chi = \chi_P + \chi_D \text{ (Honda)},$$

or

$$\chi = \chi_P + \chi_S - \chi_D \text{ (Van Vleck)},$$

where χ_P and χ_D refer to the paramagnetic and diamagnetic contributions towards the susceptibility χ. According to Van Vleck in case of diamagnetics, the molecules of which have no initial magnetic moment, χ_P arises from want of symmetry of the molecules, and hence disappears when the molecules possess spherical symmetry. This would explain the behaviour of carbon tetrachloride and cyclo-hexane admirably. In general, however, χ_P will exercise its influence in the case of poly-atomic molecules and as its value decreases with temperature, the net result will be that the value of the diamagnetic susceptibility of the molecule as a whole will tend to increase with rise in temperature. Thus it follows from these observations that an electrically polarized molecule will have a small additional paramagnetic moment whose value decreases with rise of temperature. The diamagnetic susceptibility of such a molecule will therefore tend to increase with rise of temperature. In the case of water Johner [11] has often made attempts to calculate the effect on the paramagnetic moment of the polarized water molecules. The observed increase in the value of χ between about 0° and 100° C. was, however, found to be about ten times greater than what could be accounted for on the polarization hypothesis.

A more careful examination of the results reveals the fact that the order of increase in the values of χ is almost the same both in alcohols and water, and it is therefore natural to expect some sort of a common explanation for the effect in the two cases. The degree of association

and its variation with temperature for these liquids is shown in Table XXI.

It is clear from the table that the changes in the degree of association between 0° C. and the boiling-points are approximately of the same order of magnitude in each case. For example, in the range of temperature (30°–75°) the percentage change in the values of χ is 0·693 in the case of water, 0·70 in the case of butyl alcohol, 0·716 in the case of iso-butyl alcohol, and 0·75 and 0·77 in the case of propyl and iso-propyl alcohols. These facts strongly suggest that the increase of χ with temperature is connected with the thermal change of association.

Reverting to the case of liquids which show a thermal

TABLE XXI.

Substance.	Degree of association at 0° C.	Degree of association at boiling-points.	Boiling-points.
Propyl alcohol.....	3·26	2·17	97·17
Iso-propyl alcohol	4·14	2·17	82·28
Butyl alcohol	3·77	1·71	117·71
Iso-butyl alcohol.....	5·61	1·83	107·88
Water	4·18	2·70	100·00

decrease of χ, the significant fact is that these compounds are almost all aromatic in character. The aromatic compounds have one or two distinctive features of their own which have helped us in explaining their behaviour with respect to the thermal variation of χ. First of all one is struck with the fact that the aromatic compounds, as a rule, crystallize out much more easily than the aliphatic compounds. Secondly, these compounds, and particularly nitro-benzene, exhibit a very high magnetic birefringence as compared with the aliphatic substances. Magnetic birefringence seems to be connected with orientation effects of the kind which are a first step towards crystallization. For example, it has been shown that liquid crystals which lie midway between the crystalline and the liquid states exhibit even higher magnetic birefringence than nitro-benzene. A comparison

of the temperature coefficient of the Cotton-Mouton constant and the percentage change of χ with temperature shown in Table XXII. reveals interesting relationships.

For example, the naphthalene compounds which show a large variation of χ with temperature have also a high magnetic birefringence and high coefficient of change for the Cotton-Mouton constant. Among the mono-substitution products of benzene, the case of halogen derivatives is particularly interesting. The values of Cotton-Mouton constant and the percentage changes in the value of χ are in the same order. It is also interesting to note that the higher the value of the dipole moment, the greater seems to be the percentage change in χ with

Table XXII.

Substance.	Formula.	Cotton-Mouton constant.	Temperature coefficient of Cotton-Mouton constant.	Percentage change of χ between 20°–75° C.
Nitro-benzene	$C_6H_5NO_2$	100·0	$\frac{1}{138}$ (6·4–53·9)	5·4
Chloro-benzene.....	C_6H_5Cl	28·8	$\frac{1}{139}$ (5·2–55·1)	5·26
Iodo-benzene	C_6H_5I	24·8		4·35
Bromo-benzene	C_6H_5Br	25·7	$\frac{1}{144}$ (4·7–54·7)	4·80
Bromonaphthalene .	$C_{10}H_7Br$	99·0	$\frac{1}{218}$ (5·7–52·4)	5·94
Pseudo-cumene	$C_6H_3(CH_3)_3$	28·0	$\frac{1}{143}$ (5·1–54·5)	1·85

temperature. For example, the dipole moment of nitro-benzene is as high as $3{\cdot}89\times10^{-18}$. Nitro-benzene has also a very high value for the Cotton-Mouton constant and for the thermal variation of χ. The order of dipole moments for the halogen derivatives is $1{\cdot}61\times10^{-18}$ for chloro-benzene, 1·51 for bromo-benzene, and 1·30 for iodo-benzene. The order for the Cotton-Mouton constant and percentage change in the thermal variation of χ is also the same. The significance of this fact becomes apparent when we take into consideration the fact that the tendency towards association is related to the strength of the dipole moment of the associating molecules. For example, J. Rolinski [12] has shown that the stronger the dipole moment the greater is the tendency towards

association, and this view has been confirmed by Debye and Keesom [13], and by J. Errera [14] in Brussels.

It appears likely that in the expression $\chi=\chi_P+\chi_D$ a factor for susceptibility due to crystalline structure or orientation effects should be included, particularly for molecules which show a large change of χ with temperature. Its significance can be judged from the fact that the aromatic substances which show this phenomenon are also characterized by high values of magnetic birefringence and dipole moments. They are also remarkable regarding their facility to crystallize.

Magnetic birefringence is considered as being due to the orientation of the molecules by the magnetic field owing to the magnetic anisotropy of the molecules. The aliphatic substances have, as a rule, very low anisotropy and, consequently, very low magnetic birefringences [15]. They are also, as a rule, more difficult to crystallize. The effect of temperature is to disturb this orientation, with a result that the value of the Cotton-Mouton constant decreases, the tendency to crystallize becomes less marked, and the contribution of orientating tendencies towards χ decreases considerably.

References.

(1) Honda, *Ann. der Physik.* xxxii. p. 1027 (1910).
(2) Ishiwara, Tohoku Univ. Sci. Reports, ix. p. 231 (1920).
(3) Sucksmith, Phil. Mag. li. p. 21 (1926).
(4) Ashworth, ' Nature,' cv. p. 645 (1920).
(5) Oxley, Phil. Trans. Roy. Soc. ccxiv. p. 109 (1914).
(6) Piccard, Johner, and Cabrera, *Compt. Rend.* cxci. p. 589 (1930).
(7) R. N. Mathur, Indian Journ. Phys. vi. p. 207 (1930).
(8) K. S. Krishnan and Bragg, ' Nature,' Supplement, May 7, 1927.
(9) Bhatnagar and Mathur, Phil. Mag. (7) x. p. 101 (1930).
(10) Van Vleck, Phys. Rev. xxxi. p. 587 (1928); *also cf.* Farquharson, Phil. Mag. xiv. p. 1005 (1932).
(11) Johner, Dissertation Bern.; see also Helv. Phys. Acta, iv. 3–4, pp. 238–280 (1930).
(12) J. Rolinski, *Physikal Z.* xxix. pp. 658–667 (1928).
(13) Debye and Keesom, ' Molecular Association,' by J. Errera, p. 101.
(14) J. Errera, *Zeitschr. f. phys. Chemie,* cxxxviii. p. 332 (1928); cxl. p. 273 (1929).
(15) C. V. Raman and K. S. Krishnan, Proc. Roy. Soc. London A, cxiii. p. 511 (1927).

University Chemical Laboratories,
University of the Punjab,
Lahore, India.

XLIX. *On the Radiation of Metal Surfaces bombarded by Positive Alkali Ions.* *By* H. Mayer, *D.Sc., University of Cernauti (Roumania)* *.

Introduction.

IF positive ions approach the surface of a metal it might be expected that some radiation should be emitted when they are neutralized. J. J. Thomson † discusses the influence that this radiation may have in setting free secondary electrons from the cathode of a glow discharge. Since that time this assumption can be found in many theoretical discussions on the mechanism of a glow discharge.

Some experiments have been made to detect the radiation, but such results as have been obtained cannot be regarded as a direct proof of its existence as the conclusions are drawn from secondary phenomena ‡.

This work was undertaken in the hope of obtaining a direct experimental proof of the existence or non-existence of radiation emitted during the neutralization of positive alkali ions hitting a surface of a metal of low work function. Naturally the experimental conditions are totally different from those existing in glow discharges, and caution is required in the application of the results of this work to glow-discharge phenomena.

According to Oliphant and Moon§ there is a finite probability that a positive ion approaching a metal surface will capture an electron from the metal before making contact, and give an excited atom. The distance at which this neutralization becomes probable is calculated as lying within $4 \cdot 10^{-8}$ cm. The velocity of the ions being generally higher than 10^5 cm./sec., an exciting atom so produced will collide with the surface after less than 10^{-12} sec. The time of relaxation being of the order of 10^{-8} sec., it is highly improbable that this excited atom will emit radiation by loss of its potential energy while moving towards the cathode. Therefore, we can

* Communicated by Prof. A. M. Tyndall, D.Sc.

† J. J. Thomson, Phil. Mag. (6) xlviii. p. 1 (1924).

‡ Taylor, *ZS. f. Phys.* xlv. p. 620 (1927); Proc. Roy. Soc. cxvii. p. 508 (1928).

§ M. L. E. Oliphant and P. B. Moon, Proc. Roy. Soc. A, cxxvii. p. 388 (1930).

expect emission of radiation only if ions are reflected from the metal surface, *i.e.*, if they are moving away from it.

Well-known experiments show that positive alkali ions, hitting a metal surface of electron work function ϕ higher than the ionization potential of the ion, leave the surface largely as positive ions; neutralization does not occur if $V_i < \phi$. This means that neutralization is impossible at any distance when alkali ions approach a clean metal surface such as platinum or tungsten; but if the surface of a metal of high electron work function becomes covered with an absorbed gas layer or if its surface is that of an alkali metal itself, neutralization in the manner described above becomes probable.

Fig. 1.

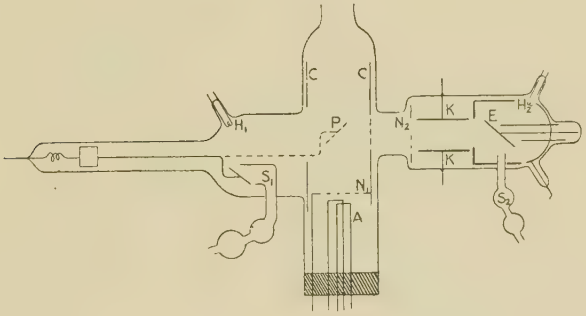

Apparatus and Experimental Method.

The investigation has been carried out in two ways. Initially a photoelectric cell was used to detect the radiation; later, when it was noticed that the radiation becomes visible at higher ionic velocities, the observations were continued spectroscopically.

The first apparatus, consisting of a pyrex-glass tube with all seals of glass and tungsten, is shown in fig. 1. The positive ions coming from the Kunsman source A, and accelerated to the desired velocity by the field between the grid N_1 and A, strike the metal surface of the plate P. P could be moved by magnetic control from the position shown with a dotted line to that with a full line in order that it might be covered with alkali metal provided by vapour from the side tube S_1. The field from the cylinder C

concentrates the positive ions upon the plate P and prevents them from penetrating in the direction of the photoelectric cell occupying the right-hand part of the tube. The grid N_2 and the condenser K prevent positive ions or secondary electrons from reaching the plate E connected to a Compton electrometer of a sensitivity of about 8000 mm. per volt. The plate E could also be covered with alkali layers from S_2. Both plates E and A could be heated by electron bombardment from the tungsten filaments H_1 and H_2. All metal parts except P and E (platinum) were made of pre-degassed nickel sheet and tungsten wires. The pressure was measured by means of a McLeod gauge (10^{-6} mm. Hg) and an

Fig. 2.

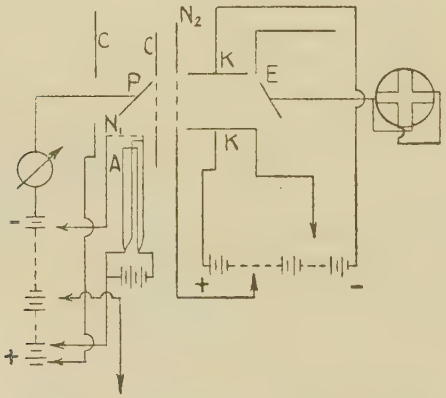

ionization gauge. The apparatus having no ground joints, could be degassed in an electric oven at about 500° C. The electrical connexions are shown in fig. 2, and do not need comment.

Results.

(A) *Photoelectric Method.*

After carefully degassing the whole apparatus and selecting the potentials to be applied to C, N, and K, in order to prevent ions and secondary electrons coming from P from reaching the photoelectric cell, a very thin layer of alkali metal was deposited on both plates P and E. It was then found that as soon as positive ions

hit the surface of P there is a photoelectric current from E. A more quantitative study was then undertaken, the results of which may be seen from the curves given

Fig. 3.

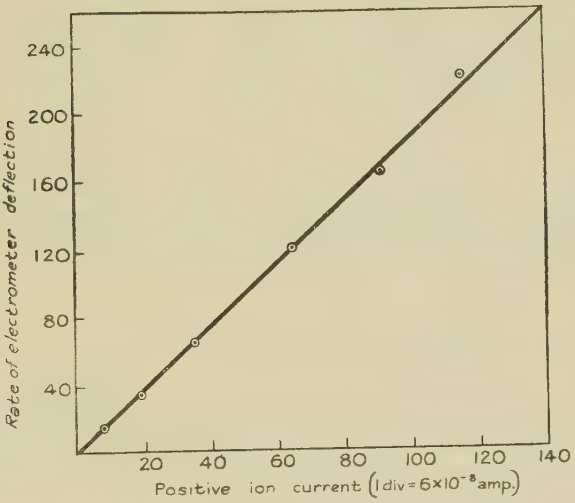

Fig. 4.

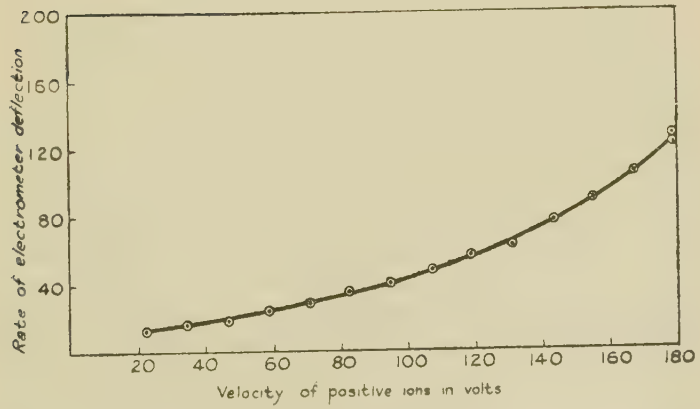

in figs. 3 and 4. The first shows the intensity of this radiation (measured by the photoelectric current) as a function of the current intensity of the positive ions with constant velocity (154 volts); it should be noted

that there is a direct proportionality between the intensity of the radiation and the number of positive ions hitting the surface of P; the secondary electron emission from P, due to the impact of the positive ions, and therefore the electron part of the total current measured in this experiment, is negligible. In fig. 4 the intensity of the radiation is plotted against the velocity of the positive ions, the curve being very similar to curves one obtains by plotting the secondary electron emission against the velocity of the ions in the same velocity interval*.

It should be noted that even in these first experiments there was sometimes no photoelectric current, especially immediately after rigorously degassing and cleaning the plate P by electron bombardment, or after covering it with thick alkali metal layers.

(B) *Visual and Spectroscopic Observations.*

In the course of these experiments it was found that there was even a visible although very feeble glow upon the surface of the plate P when bombarded by ions†. Therefore, after removal of the photoelectric cell, a quartz window was fixed in front of the plate P whereby the surface of P could be viewed tangentially. This had not been possible before owing to the presence of the cylinder. In most of the following experiments the relatively thick plate P was also replaced by a thin metal foil (Pt, Cu, or Al) which could be heated electrically.

After degassing the whole apparatus at about 500° C. until there was an almost constant residual pressure of about 10^{-7} mm. Hg, it was observed, without any further special treatment of the plate P, that immediately the ions of a velocity of several hundred volts strike P a very feeble thin layer of light appeared on the surface. The thickness of this layer was generally only a small fraction of a millimetre; at the highest velocities used in these experiments ($\sim$3000 V) it was about one millimetre. The colour was yellowish if sodium ions struck the metal

* A. L. Klein, Phys. Rev. xxvi. p. 804 (1925); W. J. Jackson, Phys. Rev. xxviii. p. 524 (1926). No radiation could be detected below a velocity of about 60 V either in the first or the second method.

† The writer is obliged to Mr. M. L. E. Oliphant for kindly informing him, after the results with the photoelectric cell were obtained, that this radiation has been observed by him and his collaborators on a platinum surface with ions of much higher velocity and current intensity.

surface, almost violet for potassium ions, and bluish-violet for cæsium ions. With potassium and cæsium ions the colour and weak intensity made visual observations almost impossible and, therefore, most of the experiments have been carried out with sodium ions.

For low velocities of the ions the D-line only is visible in the spectroscope; for higher velocities some lines in green and blue also appear. Potassium and cæsium ions give, in most cases, a very weak D-line and the violet lines of potassium line 4044 (47) Å. and cæsium 4555 (93) Å. respectively.

If the foil P is now heated white-red, the surface glow and the observed lines become weaker and weaker and finally disappear completely. The time from the beginning of the heating until the complete disappearance of the radiation amounts to only a few minutes for a platinum foil; when P is of copper foil it must be heated much longer, *i. e.*, two hours and more, before the radiation disappears. If, after complete disappearance of the radiation, the heating current is interrupted, but the positive ion bombardment continued, the radiation appears again after a few minutes. At first it is extremely feeble but becomes stronger as time passes. Once P is in the state in which no radiation is emitted, a wait of many hours without heating or bombardment has no effect, though a short exposure to the positive ion current will cause the phenomenon to reappear.

From these results, which can be repeated indefinitely, we conclude that there is no radiation if the positive ions hit a perfectly clean metal surface such as platinum or copper. Further, that this radiation does not depend so much upon a gas-covered surface as upon a layer of alkali ions or of alkali atoms which is formed by bombarding the surface with positive alkali ions for some time.

Both the intensity of the radiation and the breadth of the layer of light depend upon three factors: (*a*) the intensity of the current of positive ions, (*b*) the energy of the ions, (*c*) the surface conditions.

By increasing the intensity of the current, or the velocity of the ions, the breadth, as also the intensity of the radiation, grows, and when the surface conditions are best for the latter the breadth, too, has a maximum.

The influence of the surface conditions can be seen

best from the following experiments. After rigorously cleaning and degassing the foil P until the radiation had completely disappeared, the surface was covered with very thin layers of alkali metal of increasing thickness. The observed variation of the intensity of the radiation (intensity of ion-current and velocity of the ions being constant) with thickness of the alkali layer takes the form of the curve in fig. 5. Naturally the values of the intensity and thickness cannot be given, as it was not possible to measure them in these experiments; but

Fig. 5.

it may be mentioned that no trace of a visible layer of alkali was observed at the maximum of the light intensity, and the thickness of the alkali layer was only a fraction of a millimetre when the radiation disappeared.

It is possible to reverse the above experiment. After covering P with a thick layer of alkali metal, the heating current was switched on so that the alkali was evaporated and the thickness of the layer diminished. Plotting the intensity of the radiation against the time the curve one obtains is of the same form as that in fig. 5.

If potassium ions hit a sodium layer the D-line appears and becomes so intense that it is quite impossible

to observe the characteristic potassium radiation *. This result is important as regards the interpretation of the phenomena.

The intensity of the radiation increases from platinum to copper to aluminium, the velocity of the positive ions and the current intensity being constant. Owing to the weakness of the radiation on platinum it was easier to photograph its spectrum on copper and aluminium. After exposures of some hours (as long as the emission from the Kunsman sources lasted) the spectrum of the radiation caused by sodium ions between 5880 and 4500 Å. shows in both cases the known lines of the main series and of the first secondary series. The intensity of the lines except the D-line is very small, but the lines appear to be sharp. An aluminium surface gives also the aluminium doublet 3990; it is well known, from experiments in glow discharges, that if the cathode is of aluminium the spectrum of the discharge also shows this doublet. It is very hard to clean the aluminium surface from all traces of oxide, so that the appearance of the aluminium doublet seems to be the same phenomenon as observed by Stark and Wendt †.

Discussion.

As regards the interpretation of these results it is first necessary to keep in mind the conditions under which the experiments described above have been performed, *i. e.*, the high vacuum ($\sim 10^{-6}$ mm. Hg), the carefully degassed apparatus, and the small intensities of the positive ion current ($\sim 10^{-6}$ amp.). Therefore, it seems impossible to interpret the observed radiation in terms of the Günther-Schulze and Keller ‡ experiment. Considering the low pressure, the mean free path being of the order of 10^{-4} cm., the formation of a sodium vapour cloud in front of the plate P due to impact of positive ions is hardly conceivable. Besides, it would be impossible to explain the variation of the intensity of the radiation with the thickness of the layer of alkali metal upon

* Sometimes, when sodium ions hit a thick layer of sodium metal, a very weak residual radiation was observed.

† J. Stark u. G. Wendt, *Ann. d. Phys.* xxxviii. p. 678 (1912).

‡ A. Günther-Schulze u. F. Keller, *Zeits. f. Phys.* lxxv. p. 105 (1932), and lxxi. p. 246 (1932).

the surface of P_1, especially the disappearance of the radiation on a thick layer.

It seems that there is more connexion between the writer's experiments and those of Stark and Wendt * and of Ohlon †, as follows from the explanation given below.

If one compares the dependence of the radiation upon the experimental conditions with the dependence of the electron emission upon the same factors whether thermionic, photoelectric, or caused by impact of positive alkali ions ‡, we find a very pronounced parallelism, especially as regards the variation of the electron work function as a function of an adsorbed electropositive metal layer §. From this we might draw the conclusion that the observed radiation is due to neutralization of the positive ions, its intensity being largest when the neutralization is most probable, *i. e.*, when the electron work function is a minimum. But, as there is no time as shown above for radiation, by an ion neutralized before actually making contact with the metal surface, we have to assume that the observed radiation is due to ions becoming neutralized after reflexion. There has been little work done on reflexion of positive ions ||. Of course, the maximum observed amount of 4 per cent. reflected ions would be more than sufficient to give the observed intensity of radiation, considering that the threshold of perception of the human eye in the yellow region of the spectrum amounts to about 200 quanta per sec., and for low-velocity ions the intensity of the radiation was just near this limit.

However, there are serious objections to this explanation of the origin of the observed radiation. First of all, there is no experimental evidence at all of any dependence of the coefficient of reflexion of positive ions upon the thickness of alkali layers. As the radiation disappears on thick alkali layers, we should have to

* J. Stark u. G. Wendt, *loc. cit.*

† S. Ohlen, *Verh. d. D. Phys. Ges.* xx. p. 9 (1918).

‡ W. J. Jackson, *loc. cit.*; J. Klein, *loc. cit.*

§ Langmuir and Kingdon, Proc. Roy. Soc. lxi. p. 107 (1925); J. A. Becker, Phys. Rev. xxviii. p. 341 (1926); Bell Telephone Reprint, B. 412 (1929): B. 649 (1932); P. Lukirsky, A. Sosina, &c., *Zeits. f. Phys.* lxxi. p. 306 (1931); R. Suhrmann, *Phys. Zeits.* xxxii. p. 929 (1931).

|| W. J. Jackson, *loc. cit.*; J. Klein, *loc. cit.*

assume that there is very little reflexion of positive ions in this case; this seems to be very improbable. Secondly, there is little experimental evidence for an increased reflexion of positive ions when the velocity of the ions increases *. Thirdly, Jackson finds that there is no measurable reflexion of positive ions from aluminium surfaces, whereas in the present experiments, as mentioned above, the intensity of the radiation was highest in this case. Lastly, it would be almost impossible to explain why potassium ions striking a thin deposit of sodium give the characteristic sodium radiation. At the same time, it may be that the small residuum of radiation, observed sometimes when sodium ions strike a thick sodium deposit, is due to reflected ions.

It seems, therefore, that not only the condition $V_i > \phi$, but at least a second condition must be fulfilled in order to obtain radiation. As the experiments show, this second condition is neither fulfilled on a clean metal surface of high work function such as platinum, nor on surfaces of low work function such as the alkalis. In the writer's opinion, this second condition requires the existence of adsorbed ions ("adions") on the surface hit by ions.

If a metal surface of high work function becomes covered with atoms of low ionization potential V_i, so that $\phi > V_i$, a part of these atoms will exist as adions on the surface. There are a whole series of experiments and results which clearly show the existence of these adions †. It is important to note that even in a monatomic layer of alkali atoms adsorbed on such a surface there are still some adions, although now the work function of this covered surface may be less than the ionization potential of the adsorbed atoms. Thus, if cæsium is gradually supplied to a tungsten surface until a single layer of cæsium is formed, the work function decreases from its initial value 4·6 V to about 1·6 V ‡, the ionization potential of cæsium being about 4 V. From this we draw the conclusion that the emission of electrons is governed by the value of the work function ϕ', which is the sum of the work function of the clean

* R. B. Sawyer, Phys. Rev. xxxv. p. 124 (1930); R. W. Gurney, Phys. Rev. xxxii. p. 467 (1928), &c.

† See, for instance, J. A. Becker, *loc. cit.*

‡ J. A. Becker, *loc. cit.*

tungsten surface and of the potential of the double layer; whereas the formation of adions is determined by the work function ϕ of the clean surface only.

On this view the origin of the observed radiation would be as follows. Adatoms and adions upon the surface are "evaporated" by impact of the positive ions. If the electron work function of the metal, which is decreased by the layer of adions, becomes smaller than the ionization potential of the "evaporating" ions, the ions may extract electrons from the metal, and may be neutralized by them as long as they are within a distance of about 10^{-7} cm. from the surface. During their path the observed radiation is emitted.

This interpretation embraces all results obtained in the writer's experiments. First of all, it is now intelligible why the radiation disappears on thick alkali metal layers. Although $\phi < V_i$, there is in this case no neutralization which is followed by radiation, because there are no adions upon the surface of an alkali metal. The variation of the intensity as a function of the thickness of the alkali layer can also be understood, as both electron work function and the number of evaporating ions per sq. cm. show an analogous variation with the concentration of alkali atoms and ions upon the surface. The electron work function has a minimum and the electron emission a maximum if the layer is monatomic, whereas the evaporation of ions has a maximum at a concentration of about 0·1 of a monatomic layer *. Somewhere between these two extremes the intensity of the radiation must reach its maximum, but it is not possible to define the point more exactly.

The existence of the radiation immediately the ions strike surfaces not especially degassed and cleaned, is in agreement with the results of Richardson †, Barton ‡, and others, which show that there are always sodium and potassium ions or atoms upon such surfaces.

If the velocity of the oncoming ions increases, we must assume, according to our views, that the "evaporating" ions will have a higher velocity or "temperature." Therefore the distance they travel in the time of relaxa-

* J. A. Becker, *loc. cit.*

† O. W. Richardson, Proc. Roy. Soc. lxxxix. p. 507 (1904).

‡ H. A. Barton, G. B. Harnwell, and C. H. Kunsman, Phys. Rev. xxvii. p. 739 (1926).

tion will be longer and the breadth of the layer of light upon the surface will increase, just as the experiment shows. It is interesting to determine from the experimental data the mean temperature of the spots from which the local evaporation takes place. According to Kapitza *, the secondary electron emission, due to impact of positive ions, is a thermionic phenomenon. Oliphant and Moon † have calculated from their experimental data the mean temperatures of the spots struck by 600 V potassium ions. For platinum the obtained value is of the order of 60,000° K.

If the views expressed above as regards the mechanism of the observed radiation are right, it is possible to estimate from the experimental data of this paper the mean temperature of the spots struck by 600 V. sodium ions. The thickness of the layer of light for the highest velocities of the positive ions used in the experiments (3000 V $= 5 \cdot 10^8$ mm./sec.) was about 1 mm. For 600 V ions we obtain a thickness of 0·4 mm. in good accordance with the observations. The time of relaxation for the D-lines being about $4 \cdot 10^{-8}$ sec. ‡, we can assume that practically the whole decrease of the intensity to zero takes place within about 10^{-7} sec. Putting the breadth of the layer equal to 0·4 mm., we obtain a velocity of the evaporating ions of $4 \cdot 10^6$ mm./sec. or a temperature of about 30,000° K. for sodium ions hitting platinum. The accordance with the value mentioned above is satisfactory, considering the accuracy of the estimates.

Summary.

(*a*) Alkali ions striking surfaces of platinum, copper, and aluminium give a characteristic radiation of the line spectrum of the alkali atom. The luminous layer sits on the surface as a thin skin.

(*b*) The influence of the surface conditions of the bombarded metal of the intensity of the current and of the velocity of the positive ions upon this radiation have been studied.

* P. L. Kapitza, Phil. Mag. xlv. p. 989 (1923).

† Oliphant and Moon, *loc. cit.*

‡ H. Kerschbaum, *Ann. d. Phys.* lxxix. p. 465 (1926); Ellet and Wood, J. Opt. Soc. Amer. x. p. 427 (1925).

(*c*) A possible explanation of the origin of this radiation is given.

The problem arose from discussions with Professor Badarau (Cernauti). I am indebted to the Rockefeller Foundation for the grant of a fellowship which enabled me to complete the work in the Wills Physical Laboratory at Bristol. I wish to express my thanks to Professor A. M. Tyndall for his encouragement and help, and to the staff of that laboratory for their assistance.

L. *Crystal Parameters of Four Metals when under Reduced Pressure. By* Professor E. A. Owen, *M.A., and* E. L. Yates, *M.Sc., University College of North Wales, Bangor* *.

[Plates XV. & XVI.]

IN a previous paper † an account was given of the measurement of the crystal parameters of a number of metals. As most metals occlude large quantities of gas, the precaution was taken to heat the materials *in vacuo* before the X-ray photographs were taken in air at atmospheric pressure. It was felt, however, that this procedure was not entirely satisfactory, as the measurements might yield different values of the parameters if the materials were heated and allowed to cool *in vacuo*, and the photographs taken without removing the material from its evacuated enclosure.

In the present paper an account is given of the measurements made with a precision camera specially designed for high temperature work, the camera being mounted in an enclosure which could be evacuated. The arrangement was such that the specimen under investigation could be heated to any desired temperature up to about 600° C., whilst it was mounted on the camera, and the pressure inside the camera was maintained at about 0·001 mm. Hg. By this means gases occluded by the materials were to some extent removed, and there was no danger, when once they were removed,

* Communicated by the Authors.

† Owen and Yates, Phil. Mag. xv. p. 472 (1933).

that they would be taken up again, as was the case when the photographs were taken in air at atmospheric pressure after the heat treatment *in vacuo*.

Measurements were made of the crystal parameters of spectroscopically pure gold, platinum, palladium and rhodium. These were the same specimens as were previously used to determine the parameters of these metals.

Apparatus.

The precision camera differed in construction from that employed in our previous investigations. It was made of invar and was constructed in two parts, the part on which the film was laid being thermally insulated by means of silica from the part carrying the powdered material under investigation. The specimen was mounted on thin aluminium foil, which was heated by the aid of a small furnace situated directly behind and in contact with a thick copper sheet backing the foil. On the surface of the copper sheet was soldered the nickel-nichrome thermocouple junction, which served to record the approximate temperature of the specimen. Between the foil carrying the specimen and the curved camera surface was placed a thin sheet of mica of known thickness to reduce the temperature gradient across the foil and copper sheet.

The camera was mounted in a robustly-built brass box, three of whose sides were water-cooled. The wires carrying the heating current and the thermocouple wires passed through vacuum-tight plugs in one of the remaining sides. A photograph of the camera in elevation and mounted in its enclosure is reproduced in fig. 1 (Pl. XV.).

Special heat-resisting X-ray films were employed, but in this investigation the films had not to withstand very high temperatures, as the temperature of the part of the camera in contact with the film was less than 50° C., even when the specimen was heated to the highest temperatures.

The effective radius of the camera was 51·55 mm. This was measured with a Hilger travelling microscope, and checked by means of a micrometer screw which had been calibrated with the aid of a standard end-gauge, the length of which was approximately equal to the

diameter of the camera. The radius was checked frequently during the course of the work.

The measurement of the films and the corrections applied for shrinkage were carried out precisely as previously described, the only difference being that several fiducial marks were now engraved on the camera to test whether the shrinkage took place evenly over the whole length of the film. The error of measurement was of the same order as in the previous measurements *.

Method of Procedure.

The method of procedure was to mount the specimen on the camera, which in turn was mounted in its enclosure. Then the furnace was brought up to touch the copper sheet backing the specimen. This furnace was wound on mica and covered with alundum cement, which was shaped to the back of the camera.

A photograph was first taken in air at atmospheric pressure when the specimen was at room-temperature. The next photograph was taken after the enclosure had been evacuated to a pressure of about 0·001 mm. Hg, with an oil pump, the specimen again being kept at atmospheric temperature. Before the third photograph was taken the enclosure was evacuated, the specimen heated for a certain interval at a given temperature, and then allowed to return slowly to atmospheric temperature. The exposure was made whilst the vacuum was maintained, and the specimen was kept at room-temperature. About two hours' exposure was usually required for each photograph. Throughout the investigation copper radiation was employed, and the wavelengths were assumed to have the following values: $K\alpha_1 = 1{\cdot}537395$ Å. and $K\alpha_2 = 1{\cdot}541232$ Å. †.

Results.

The measurements of the films yielded the results shown in the following table. The photographs taken with palladium and rhodium are shown in fig. 2 (Pl. XVI.). All the parameters are reduced to 18° C., and are corrected

* The expression for the maximum error due to all sources was wrongly entered in our previous paper. In this expression the product-terms, as well as the square-terms, should be included under the square root. The actual limits of error given in the paper were, however, greater than those calculated from the full expression.

† Siegbahn, 'Spektroskopie der Rontgenstrahlen,' 1931.

Treatment of reflecting powder.	Temperature (° C.).	Arc (mm.).	λ.	Reflecting planes.	Parameter (Å.). Obs.	Corr.	Calc. at 18° C.
GOLD.							
No heat treatment; exposure made *in vacuo*.	9	79·34	α_1	(511)	$4{\cdot}0693_4$	$4{\cdot}0696_0$	$4{\cdot}0699_4$
		73·64	α_2	(333)	$4{\cdot}0689_3$	$4{\cdot}0691_9$	
Heated to 300° C. for 2 hrs.; cooled and exposed *in vacuo*.	9	79·30	α_1	(511)	$4{\cdot}0692_7$	$4{\cdot}0695_3$	$4{\cdot}0700_4$
		73·80	α_2	(333)	$4{\cdot}0692_2$	$4{\cdot}0694_8$	
					Mean	value =	$4{\cdot}0699_9$ Å.
PLATINUM.							
No heat treatment; exposure made in air.	18	114·36	α_1	(422)	$3{\cdot}9154_1$	$3{\cdot}9157_0$	$3{\cdot}9157_5$
		110·72	α_2		$3{\cdot}9155_0$	$3{\cdot}9157_9$	
No heat treatment; exposure made *in vacuo*.	9	114·23	α_1	(422)	$3{\cdot}9150_6$	$3{\cdot}9153_5$	$3{\cdot}9156_7$
		110·55	α_2		$3{\cdot}9150_6$	$3{\cdot}9153_5$	
Heated to 400° C. for 2½ hrs.; cooled and exposed *in vacuo*.	12	114·39	α_1	(422)	$3{\cdot}9154_9$	$3{\cdot}9157_8$	$3{\cdot}9159_9$
		110·71	α_2		$3{\cdot}9154_7$	$3{\cdot}9157_6$	
					Mean	value =	$3{\cdot}9158_0$ Å.
PALLADIUM.							
No heat treatment; exposure made in air.	18	101·12	α_1	(422)	$3{\cdot}8819_5$	$3{\cdot}8821_1$	$3{\cdot}8822_2$
		97·02	α_2		$3{\cdot}8821_7$	$3{\cdot}8823_3$	
No heat treatment; exposure made *in vacuo*.	10	101·00	α_1	(422)	$3{\cdot}8817_5$	$3{\cdot}8819_1$	$3{\cdot}8823_0$
		96·86	α_2		$3{\cdot}8818_1$	$3{\cdot}8819_7$	
Heated to 100° C. for 1 hr.; cooled and exposed *in vacuo*.	11	101·15	α_1	(422)	$3{\cdot}8820_2$	$3{\cdot}8821_8$	$3{\cdot}8825_7$
		97·02	α_2		$3{\cdot}8821_7$	$3{\cdot}8823_3$	
Heated to 300° C. for 4 hrs.; cooled and exposed *in vacuo*.	12	101·17	α_1	(422)	$3{\cdot}8820_6$	$3{\cdot}8822_2$	$3{\cdot}8824_2$
		96·91	α_2		$3{\cdot}8819_2$	$3{\cdot}8820_8$	
					Mean	value =	$3{\cdot}8823_8$ Å.
RHODIUM.							
No heat treatment; exposure made in air.	18	51·55	α_1	(422)	$3{\cdot}7954_7$	$3{\cdot}7956_2$	$3{\cdot}7956_4$
		42·65	α_2		$3{\cdot}7955_1$	$3{\cdot}7956_6$	
No heat treatment; exposure made *in vacuo*.	8	51·38	α_1	(422)	$3{\cdot}7952_5$	$3{\cdot}7954_0$	$3{\cdot}7956_0$
		42·17	α_2		$3{\cdot}7950_5$	$3{\cdot}7952_0$	
Heated to 400° for 1½ hrs.; cooled and exposed *in vacuo*.	9	51·28	α_1	(422)	$3{\cdot}7951_3$	$3{\cdot}7952_8$	$3{\cdot}7955_2$
		42·19	α_2		$3{\cdot}7950_7$	$3{\cdot}7952_2$	
					Mean	value =	$3{\cdot}7955_9$ Å.

for deviation from Bragg's Law. The values taken for the coefficients of thermal expansion of the metals are the same as those assumed in our previous paper.

In addition to the heat treatment to which the specimens were subjected for the present measurements, they had already received a certain amount of heat treatment during the previous investigation carried out with them. Throughout the six months that elapsed between the two investigations, the materials had been exposed to the atmosphere. The present results show that during this period the metals had not absorbed an appreciable amount of gas, since in each case the parameter of the material in its initial state did not differ by more than the experimental error from the parameter of the material after it had been subjected to further heat treatment *in vacuo*.

The fact that the values of the parameters recorded in this paper confirm the values which we have already published for these four elements shows that the method of procedure previously adopted is capable of yielding reliable results.

Summary.

A design of precision camera suitable for the investigation of materials at high temperatures *in vacuo* is briefly described. The parameters of four spectroscopically pure elements, namely, gold, platinum, palladium and rhodium, were measured with this camera. Each specimen was heated *in vacuo* to a high temperature, and was maintained at this temperature for a definite period of time. It was then allowed to cool slowly to atmospheric temperature and exposed *in vacuo* to the X-rays. The values of the parameters under these conditions confirmed those previously published for these elements.

LI. *Explanation of the FitzGerald Contraction in Optics.* *By* Prof. Alex. Larmor, *M.A.*, *Londonderry**.

THE following abbreviated statements are taken from the elementary text-books, viz.:—

Einstein gives a chapter on the behaviour of rods and clocks in motion. He shows from the Lorentz equations

* Communicated by Sir Joseph Larmor, D.Sc., F.R.S.

that a rod when moving in the direction of its length is shorter than when at rest, and does not discuss the matter further.

Lorentz says that the contraction of the rod is a real contraction.

Eddington says that nothing whatever has happened to the rod. Its apparent contraction is due to a change in the relation of the rod to the observer, and he illustrates by diagrams in the geometry of the world of four dimensions.

These conflicting views can, I think, be partially reconciled by a simple explanation, on the basis of the existence of rays, which appears to clear up the whole matter without invoking the world of four dimensions.

The idea of the length of a rod implies a unit of length to compare it with. If there is no change in the rod, but if the unit of measurement changes in length when the rod changes from rest to motion, then the length of the rod, as measured by this unit, changes. *The natural unit of length for all measurements, including lengths of rods introduced into the system, is a wave-length of standard homogeneous light belonging to the system.* A length in the system is intrinsically expressed by the number of wave-lengths, in its direction, which it covers. In short, the frame of reference is the complex of all the possible light-rays within the system. One calls the lengths thus measured *optical* lengths. For a system at rest the optical lengths agree with those given by a measuring rod, but when the system is moving with uniform velocity v it is a matter for investigation (from the Lorentz equations) whether they do or do not agree.

In applying the equations of transformation in order to compare the lengths in an unchanging material system when in motion with the lengths when at rest one is really adopting, in each case, the wave-length of light within the system as the unit of length, and therefore comparing the *optical* lengths—a simple fact which seems to have been overlooked by Einstein, Lorentz, and Eddington.

Much has been written about the FitzGerald contraction during the last forty years, but it can hardly be said that any very simple explanation has been advanced. It follows from the Lorentz equations, and it has been left at that, without troubling to enquire too closely what

that might imply. Of course any explanation of the contraction must be founded on these equations, but it should be borne in mind that, as the Michelson-Morley experiment is an interference experiment, it forcibly suggests the appropriateness of measuring the lengths of the two paths of the split beam in wave-lengths (*i. e.*, taking their optical lengths), and that a rational explanation of the result of the experiment should clearly show that the apparent contraction is based upon this unit of measurement.

It therefore becomes important to make a detailed examination into the proper interpretation of the equations of transformation without introducing artificial sets of apparatus, such as rods and clocks, which are not intrinsic to the material system moving in space and time that is under consideration. One may claim that such procedure will lead to rational (as opposed to formal) explanations of the phenomena implied by these equations. Such detailed examination, I find, leads to the conclusion that when a source of light is moving with uniform velocity v the "phase" travels in the direction of the motion of the source with velocity $c \Big/ \sqrt{1-\frac{v^2}{c^2}}$ and the amplitude (energy) with velocity $\sqrt{1-\frac{v^2}{c^2}}\,.c$, so that the wave-length for that direction, which is an affair of phase, is $\lambda \Big/ \sqrt{1-\frac{v^2}{c^2}}$, where λ is the wave-length when the source is at rest; while for propagation in the direction at right angles to the direction of motion of the source the "phase" and the energy both travel with velocity c, and for propagation in that direction the wave-length is λ. It follows that, when the wave-length is the unit of measurement, a rod of length l will appear to have length $\sqrt{1-\frac{v^2}{c^2}}\,.l$ when it points in the direction of the motion of the source, but to have length l when it points at right angles to that direction.

In order to justify these statements let us enquire what form the wave-front from a moving source of light takes when it is referred to the space coordinates

x, y, z of the fixed system and the time t' of the moving system.

Let x, y, z, t and x', y', z', t' be the coordinates of a point on the wave-front in the fixed and the moving systems respectively.

If we set $t'=$constant in the equation for change of frame of reference as regards time, viz., $t'=\beta\left(t-\frac{vx}{c^2}\right)$, we get the wave-front of the source in the moving system. Multiply both sides of the equation by c, and substitute r for ct and $r\cos\theta$ for x, and we have the polar equation of the wave-front, referred to the source as pole and to the direction of motion as prime radius, the coordinates r, θ being those of the fixed system, viz.,

$$\sqrt{c^2-v^2}.t'=r\left(1-\frac{v}{c}\cos\theta\right),$$

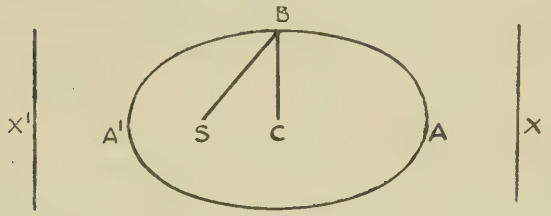

which is identical with the ellipse

$$\frac{l}{r}=1-e\cos\theta$$

of semi-axes a, b and semi latus-rectum l, it

$$e=\frac{v}{c},\quad l=\sqrt{c^2-v^2}.t'=\sqrt{1-\frac{v^2}{c^2}}.ct'=\beta^{-1}.ct', \text{ say,}$$

whence it is easily deduced that

$$a=\beta ct',\quad b=ct'.\quad \mathrm{SC}=\beta vt',\quad \mathrm{SB}=\beta ct',\quad \text{and}\quad \mathrm{CX}=\frac{c^2}{v}.\beta t'.$$

It follows that the source is passing through the fixed point S when $t'=0$, so that when $t'=0$ the phase is at S; when the time is t' the phase has reached the ellipse and the source is at C, the phase of the ray proceeding in the direction of motion has reached A and that of the ray proceeding in the direction at right angles to the direction of motion has reached B. As viewed

from the fixed system the phase of the former ray has apparently travelled the distance

$$SA=SC+CA=\beta vt'+\beta ct',$$

but, as viewed from the moving system (*i. e.*, relatively to C), it has only travelled the distance $CA=\beta ct'$. The discrepancy between these distances, viz., $\beta vt'$, is accounted for by "Doppler effect."

The phase of the ray propagated at right angles to the direction of motion has travelled the distance $SB=\beta ct'$ in the fixed system, but only a distance $CB=ct'$ in the moving system. The difference of these distances is exactly accounted for by the "angle of aberration," SBC.

It is interesting to note that when the wave-front of the moving source is expressed in terms of the coordinates x, y, z, t' it becomes a prolate spheroid whose longer axis is in the direction of motion, and that its directrix planes are the de Broglie waves which travel relatively to the source with velocity c^2/v in the coordinates x, y, z, t, which are thus also included in this point of view.

This geometrical figure, if the calculated distances can be properly interpreted, should give the key to the meaning of the Lorentz equations. If $\beta\tau'$ is taken as the atomic period of the source of light in the moving system, then, since $CA=c.\beta t'$, $CB=c.t'$, the wave-lengths in these directions are in the ratio $\beta : 1$, so that, if l be the length of an unchanging rod, its optical length when placed along CA is $\sqrt{1-\frac{v^2}{c^2}}\times$ its optical length when placed along CB. If we were to put $t'=t$, the latter would be the optical length of the rod when at rest. It should be noted, however, that if $\beta\tau'$ is taken as the atomic period, c will be the velocity and the light will arrive sooner at B than at A, so that the ellipse will not be a wave-front.

We therefore reject this interpretation and, in order to make the ellipse a wave-front, we associate β with c (instead of with t'), so that the "phase" of the light travels parallel to CA with velocity βc (which is greater than c), and, if so, the amplitude (energy) travels parallel to CA with velocity $\beta^{-1}c$. (If this were not the mode of propagation in the moving system, the energy, on a quantum basis, would change with the frame of reference, as will appear presently.)

Since the optical length $CA=\beta c.t$, the optical unit of length, or wave-length, for propagation along CA is $\lambda'=\beta\lambda$, where λ is the wave-length when the source is at rest. For propagation in the direction CB we have $CB=ct$, so that $\lambda'=\lambda$.

We are thus led to the FitzGerald contraction on the view that when a source of light changes from rest to motion in the direction CA with uniform velocity v, the phase of the light moves, relative to the source, faster than the amplitude in that direction, there being no change in the atomic period of the source, but, since $\lambda'=\beta\lambda$, all optical distances parallel to CA are increased in the ratio $\beta : 1$.

Adopting this view, we see that since the velocity of the phase relative to C is βc instead of c, the number of waves that cross a fixed plane in one second is $\nu'=\beta\nu$, where ν is the number when the source is at rest.

It will be observed that as we pass from the coordinates x, y, z, t of the resting system to the coordinates x, y, z, t' of the moving system the distances

$$SC=\beta vt', \quad CA=\beta ct', \quad \text{and} \quad CX=\beta\frac{c^2}{v}t'$$

show that the several velocities v, c and c^2/v become βv, βc, and $\beta c^2/v$ respectively. This suggests an interpretation of the light-quantum. We have seen that the phase of the light travels relative to C with the velocity βc, and, therefore, that the energy travels with velocity $\beta^{-1}c$. In an interference experiment the Fresnel pattern is formed so that darkness occurs where the lengths of the paths of the interfering rays differ by an odd multiple of $\frac{1}{2}\lambda'$, the velocities along the paths being βc. When v/c is small this differs very little from the velocity $\beta^{-1}c$ of the energy.

If the quantity h in a plane-wave of light be regarded as the energy per wave-length λ' of its path, then $h\nu'$ is energy emitted by the source per second. Also, since the velocity of the " phase " is βc instead of c, it follows that the frequency is $\nu'=\beta\nu$, so that the quantum $h\nu$ when the source is at rest becomes $\beta h\nu$ when the source is in motion, in agreement with the usual relation, for

$$\lambda'=\beta\lambda, \quad \text{so that} \quad \frac{h\nu'}{\lambda'}=\frac{h.\beta\nu}{\beta\lambda}=\frac{h\nu}{\lambda},$$

i. e., the energy per wave-length is the same (as it ought to be) whether expressed in the coordinates x, y, z, t' or x, y, z, t.

It follows that the energy which crosses a fixed plane in one second is $h\nu$, whether the source is at rest or moving.

Likewise, since

$$\text{momentum} \times c = \text{energy} = h\nu,$$

it follows that the momentum carried across a fixed plane in one second is $h\nu/c$.

The scheme would also appear to give a reasonable account of the inertia coefficient of a particle of mass m_0 when it moves with uniform velocity v, and of the associated quantum relations.

On passing from the coordinates x, y, z, t to x, y, z, t' we have seen that v becomes βv, so that momentum $m_0 v$ becomes $\beta m_0 v$. The physicist, who is concerned with the preservation of the relations of momentum and energy in the moving system, associates the factor β with m_0, and on developing he arrives at the relations

$$m_0 = \frac{\mathrm{E}}{c^2}, \quad \text{and} \quad m = \beta m_0 = \beta \frac{\mathrm{E}}{c^2}, \text{ etc.}$$

We have now to endeavour to interpret the significance which is to be attached to E on our theory. When the mass m_0 is moving with velocity v it is the source of the de Broglie waves, which are phase waves travelling with velocity $\beta c^2/v$ relative to C, the corresponding energy waves travelling with velocity $c^2 \div \beta c^2/v$, i. e., $\beta^{-1} v$ relative to C. If h is the energy in the train of waves per wave-length of a de Broglie wave in the coordinates x, y, z, t, then the energy crossing a fixed plane in one second is $h\nu$ in these coordinates. When we pass from the coordinates x, y, z, t to the coordinates x, y, z, t', the frequency ν becomes the frequency $\nu' = \beta\nu$, and at the same time the length λ of the de Broglie wave becomes $\lambda' = \beta\lambda$. Thus $\frac{h\nu'}{\lambda'} = \frac{\beta h\nu}{\beta\lambda} = \frac{h\nu}{\lambda}$, so that the energy per wave-length of the de Broglie wave is conserved. Thus, when we say that the momentum of a particle of mass m_0 moving with velocity v is $m_0 v = \frac{\mathrm{E}}{c^2} v$, the interpretation of E would be $h\nu$, viz., the

energy of the waves which cross a fixed plane in one second, and the interpretation of the momentum would be the momentum which is carried across a fixed plane by these waves in one second.

All this accords with the view that the mass (energy) of a body resides in the æther outside it, and that as the body moves from one place to another it is accompanied by æthereal waves.

Minkowski's famous challenge would, perhaps, on this view lose something of its impressive character. It would, seemingly, be replaced by the statement that when a source of æther waves (a material body or a source of light) is moving with uniform velocity v (in the coordinates x, y, z, t), the phase of the waves moves faster, in the direction of v, than the amplitude (energy). The world of four dimensions would be illusory.

Holywood, Co. Down.
May 20.

LII. *Some Electrocapillary Experiments.* *By* I. G. Walters, *Washington Singer Laboratories, University College, Exeter* *.

1. *Introduction.*

THE only direct method for the determination of a single potential difference between an electrolyte and a metal-electrode is that based upon an evaluation of the electrocapillary curve of mercury. From the nature of the curve it is deduced that the surface tension at the mercury-electrolyte surfaces passes through a maximum as an increasing negative potential is applied to the mercury side of the interface, and at the maximum it is assumed that the charge on the mercury, and hence the potential difference across the mercury-electrolyte interface, must be zero. Thus the value of the applied potential difference corresponding to the maximum of the electrocapillary curve should determine the potential difference existing across the interface. In some cases this is not so. When capillary active ions are adsorbed at the interface the double

* Communicated by Professor F. H. Newman, D.Sc.

layer of ionic adsorption is superposed upon the Helmholtz electrical double layer. It is generally assumed that the adsorption potential vanishes in the case of capillary active salts, especially if they are chlorides, nitrates, sulphates, etc., of the alkalis. Probably it is more correct to state that in these cases the adsorption potential is less than 5 millivolts, which is about the degree of accuracy to which the Lippmann maximum on the electrocapillary curve can be measured. It has been suggested by Frumkin *, however, that even in cases when there is no adsorption of ions, and when the metal is not charged by any exchange of ions, there might yet be at the interface a potential difference of contact.

According to Gibbs † the interfacial potential difference brings about a change in the concentration of the mercury ions about the electrode. Gouy ‡ and Frumkin § have developed theories which are combinations of Lippmann's theory and Gibbs's relation for the lowering of the surface tension by adsorbed substances. Frumkin's equation contains two terms, one of which represents the normal effect and the second the effect of the adsorption of capillary active ions. Butler || shows that Gibbs's equation by itself is inadequate to account for the electrocapillary curve anomalies, and holds that an electrostatic effect should be included. Krüger ¶ also explained the anomalies of the electrocapillary curves on the adsorption theory, and showed that they increase with increasing stability of the corresponding complex salts. The relationship, however, does not hold generally, since the stability of complex salts increases in the following order :—nitrates, sulphates, iodides, and cyanides, whereas the maximum surface tension of mercury in normal solutions of the nitrate, sulphate, iodide, and cyanide of potassium are 98·95, 100·17, 94·0, and 96·6 C.G.S. units, respectively.

Whatever the theory may be the capillary active substance not only lowers the maximum surface tension, and therefore the maximum point of the electrocapillary

* *Zeits. phys. chem.* ciii. p. 43 (1922).
† 'Scientific Papers,' vol. ii.
‡ *Ann. d. Phys.* vii. p. 129 (1917).
§ *Loc. cit.*
|| Proc. Roy. Soc. A, cxiii. p. 594 (1927).
¶ *Zeits. Elektroc.* xix. p. 681 (1913).

curve, but also displaces the curve to the right or left, the direction of displacement depending upon which of the ions, anions, or kations are active. The actual direction may be predicted in the following manner :— If the anions alone are active that surface of the electrical double layer which falls in the solution will be decidedly richer in anions than it would be if they were inactive ; hence the interfacial tension, and therefore the rising branch of the curve, is strongly depressed, as is also the region of the maximum.

Corresponding to the falling branch of the curve the inactive kations predominate in the solution surface layer, so that the depression produced by the anions disappears, and the curve then coincides with that found for capillary inactive electrolytes; but at the maximum point of the curve no change in the surface tension, and therefore no change in the concentration of the solution can occur upon a change in the potential difference, and so the mercury surface must carry a negative charge at the maximum point in order to balance the tendency of the anions to adsorption, which, if it occurred, would change the concentration of the solution. The case of the capillary active kations is exactly the converse; both the falling branch of the curve and its maximum are strongly depressed, and the mercury must have a positive charge at the maximum point.

2. *Experimental.*

After various experimental tests it was found that the vertical capillary tube type of electrometer was more satisfactory than the type in which a jet dips into the electrolyte. In all cases the purity of the mercury and cleanliness of the internal glass surface had a decided influence on the regularity and consistency of the mercury meniscus movement.

The first measurements were made with aqueous solutions of potassium chloride of various concentrations, the strengths varying from a saturated solution to one of 0·02 normal concentration. The value of the maximum surface tension corresponded to 0·522 volt for a saturated solution, and the potential difference at the maximum increased as the solution became weaker. In addition the electrocapillary curves were flatter in shape with the more dilute solutions and there was less maximum

displacement of the meniscus. The movement of the latter was slow, and the surface tension required some considerable time to reach a steady value after the potential difference had been established. This slowness of movement has been attributed by various workers to the high electrical resistance of the electrolyte in the capillary, especially when the solution is very dilute; but it is difficult to accept such an explanation. However high an electrical resistance may be in magnitude any charge rapidly leaks through it, and the weakest of electrolytic solutions cannot be termed of very high resistance. More probably the explanation lies in the fact that with the very dilute solutions, the number of ions being comparatively small, the relative changes in ionic concentration at the interface as the potential difference is applied are small, so that the surface tension changes, if they depend upon ionic concentration, must also be comparatively small. This would account for the flatness of the curve. Moreover the ions in these dilute solutions will be more hydrated than in the more concentrated solutions, and will thus move more slowly through the liquid. Thus even when a potential difference is applied across the interface the resultant movement of the ions in the solution towards the interface must be slow, and therefore the concentration changes in the vicinity of the interface take place slowly, so that the surface tension only assumes its final value after a considerable interval. Sticking of the meniscus will undoubtedly tend to become more marked with this slow movement. At concentrations below 0·02 normal it was impossible to obtain any consistent movements.

In order to see if the electrical conductivity played any part in the erratic movement of the meniscus a small trace of acid was added to the electrolyte and also hydrogen gas was bubbled through it. No effect was observed.

In all these measurements the meniscus was followed towards the maximum depression both for the ascending and descending branches of the curve. Thus the position of the maximum could be verified when travelling in the reverse direction, *i. e.*, when the applied potential difference was being decreased. Also it was found that if the curve was obtained by continually increasing the

applied potential difference in the same direction there was a lag of the meniscus after passing the maximum point. This is also explained by the small change in surface tension in the neighbourhood of the maximum and can be eliminated by working towards the maximum from both branches of the curve.

Fig. 1.

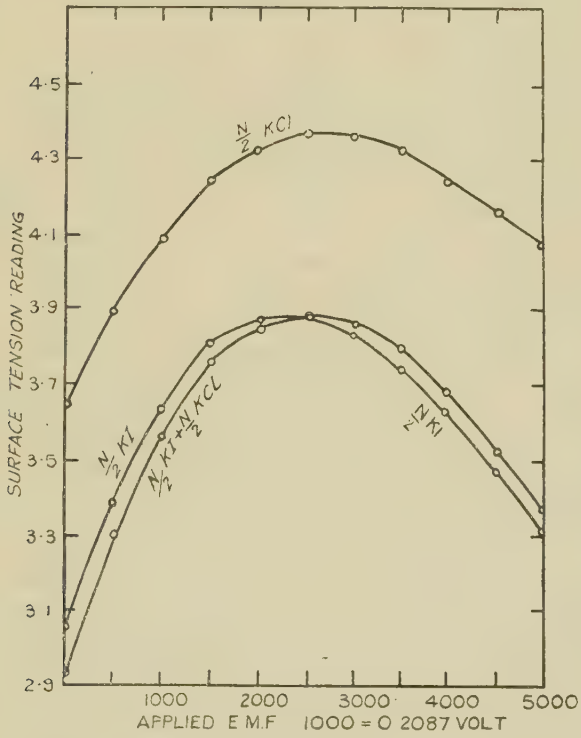

In a second series of experiments the electrocapillary curves for aqueous solutions 0·5 normal KCl, 0·5 normal KI, and a mixture of these two solutions were determined. The results are shown in fig. 1, the potential difference at the maxima corresponding to 0·5 N KCl, 0·573 volt, 0·5 N KI, 0·475 volt and mixture, 0·521 volt.

The curves for the potassium iodide and the mixture are similar in shape and distinct from that for potassium chloride, the mixture curve is displaced to the right

of the iodide curve over its entire length, and the potential difference corresponding to its maximum is slightly higher in value than that for the iodide solution. The predominant factor in the mixture is evidently the capillary active iodide ions which are adsorbed at the interface to the exclusion of the chloride ions. This is in general agreement with the principle that of two substances present in a solution the one which lowers the surface tension at the interface will always be attracted thereat to the exclusion of the other constituent.

With the mixture it was found that if the two mercury electrodes were short-circuited the steady position of the meniscus was only attained after a considerable time interval. If it were slightly displaced by applying a small potential difference the meniscus "jerked" into a new position and then slowly returned to its steady reading. This type of movement suggests the adjustment of ionic concentration at the interface when the latter is disturbed.

The determination of the capillary curves for electrolytes in non-aqueous solutions is subjected to the same difficulties that occur with weak aqueous solutions. Gouy * found that when he used a Lippmann electrometer with alcoholic solutions the capillary jet soon developed a "sticking effect." Davis † noted a similar difficulty with the fine jet, the small mercury meniscus only retaining its mobility for a few minutes. This has also been confirmed by the present writer. Newbery ‡, using the vertical type of capillary tube, determined the absolute potential of mercury in a saturated alcoholic solution of sodium chloride, and found from the maximum of the electrocapillary curve that the same potential existed as in a saturated aqueous solution, viz., NaCl (saturated aqueous solution) 0·483 volt, NaCl (saturated alcoholic solution) 0·485 volt. Similar results were obtained with ammonium chloride.

Lapworth § suggested that the absolute potential of a metal in a saturated solution of a given salt is the same whether the solvent be water or some other solvent

* *Ann. Chim. Phys.* xxix. p. 145 (1903).
† Phil. Mag. xiii. p. 1188 (1932).
‡ Journ. Chem. Soc. cvii. p. 852 (1915).
§ *Ibid.* p. 852 (1915).

provided that each ion involved has the same affinity for water as for the other solvent, for if a concentration cell is made up with similar electrodes in the two saturated solutions there will be no tendency for the salt to migrate in either direction. Hence, neglecting boundary potentials, which may, of course, be considerable, the absolute electromotive force of such a cell would be zero. Reasoning from the fact that transference numbers of all ions at present investigated, with the exception of the hydrogen ion, have the same values in alcohol as in water, Lapworth concluded that the above condition is probably fulfilled in the case of solutions of sodium chloride in alcohol and in water.

Wiid * has extended these observations, and his researches show that this equality will hold generally in cases where there is partition equilibrium between the two phases.

Buckley and Hartley † measured the standard electrode potentials of eight elements in methyl alcohol, and compared the results with the corresponding values in water. There was fairly close agreement between the two sets of values, although all the monovalent metals were rather more electropositive in methyl alcohol than in water.

Now if the process of ionization were solely the separation of a charged atom from the electrode, as postulated in the original Nernst theory, it might be expected that the electrode potentials should be independent of the solvent. However, there is little doubt that the passage of an ion from the crystal lattice into solution is accompanied by its association with a certain number of solvent molecules. Hence the electrode potential of an element represents the difference in the free energy content of the ions in the lattice and in a solvated condition. One would expect, therefore, individual differences between the electrode potentials in the two solvents corresponding to the varying affinities of the molecules of the two solvents for the same ion. Thus, on the whole, some differences, even if small, would be expected between the potential differences corresponding to the maximum in the electrocapillary curves of alcoholic and aqueous solutions of any given electrolyte.

In the present work the electrocapillary curve for

* *Zeits. phys. chem.* ciii. p. 43 (1922).
† Phil.Mag. viii. p. 320 (1929).

a saturated solution of potassium chloride in methyl alcohol was determined, the result being shown in fig. 2. As compared with the curve for a saturated aqueous

Fig. 2.

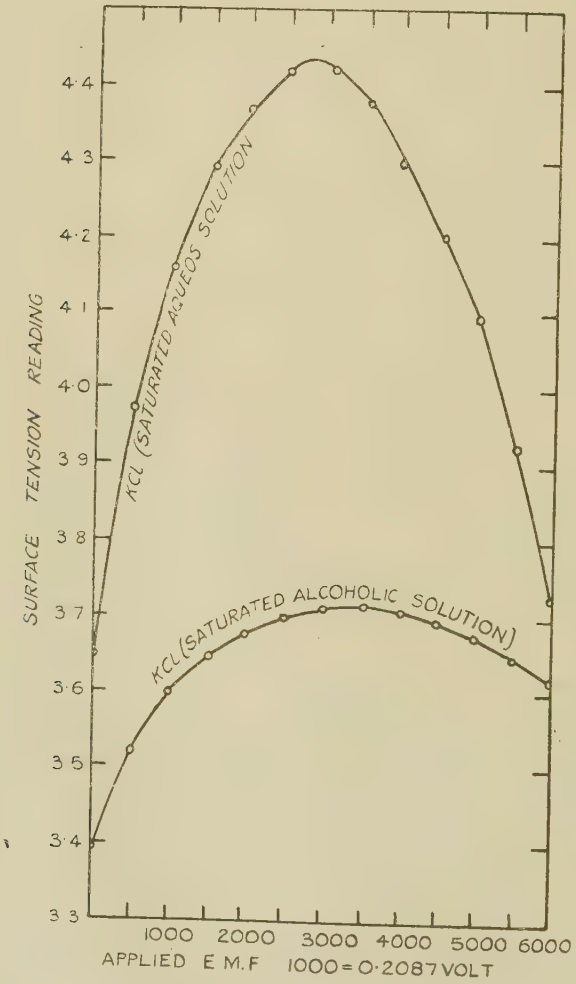

solution of the same salt the maximum is greatly depressed, as one would expect from the relatively small concentration of the salt in the alcoholic solution, and, in addition, the curve is much flatter. Both of these

results can be satisfactorily explained, as previously mentioned, by the very small ionic concentration in the alcoholic solution. The maximum of the curve corresponds to 0·64 volt as compared with 0·522 volt for the saturated aqueous solution. This difference lies in the same direction as the results obtained by Buckley and Hartley for univalent metals. Owing to the flatness of the alcoholic curve the determination of its maximum point is not an easy matter.

No experimental difficulty was encountered with the uniform capillary and alcoholic solutions, although the movements of the meniscus, corresponding to the descending part of the curve, were more regular than those corresponding to the ascending portion.

This work was carried out under the direction of Professor Newman.

LIII. *The Intensities of the Spectra emitted by High-Frequency Discharges in Helium.* *By* J. E. Keyston, *Magdalen College, Oxford* *.

1. A SERIES of investigations have recently been carried out in the Electrical Laboratory, Oxford, in order to determine the way in which the intensity of the light emitted from the uniform columns of high-frequency and direct-current discharges in helium varies with the gas pressure. With the aid of a theory of the uniform columns of discharges given by Townsend † it is possible to estimate the energies of electrons which excite the various parts of the helium spectrum from the results of these experiments.

Hitherto the measurements of the intensity of the light have been made by means of colour-filters and photoelectric cells. This method of measurement has certain disadvantages which considerably limit its range of application ; they are :—

(*a*) Only two of the strongest lines of the visible helium spectrum, viz., λ 5876 Å and λ 5016 Å, can be

* Communicated by Prof. J. S. Townsend, F.R.S.

† J. S. Townsend, Phil. Mag. ix. p. 1145 (1930) ; xi. p. 1112 (1931) ; xii. p. 745 (1932).

separated from neighbouring strong lines by means of colour-filters.

(*b*) Similarly only that part of the continuous spectrum which lies between the wave-lengths 5876 Å and 5016 Å can be measured.

(*c*) At pressures greater than 15 or 20 millimetres the band spectrum becomes prominent and contributes appreciably to the radiation passing through some of the filters.

(*d*) The intensity of the band spectrum cannot be measured by this method, as it is impossible to separate the bands by means of filters from neighbouring strong lines.

(*e*) Measurements cannot conveniently be extended to the ultra-violet part of the spectrum.

The spectrophotometric measurement of the intensity of the light emitted from the uniform column, which is described in the following pages, was therefore undertaken with a view to measuring the intensities of the line, band, and continuous spectra both in the visible and in the ultra-violet parts of the spectrum.

A qualitative study of the photographs of the spectra emitted by high-frequency and direct-current discharges in helium at different pressures revealed many points of interest which have already been discussed in a previous paper *.

2. The theory of the uniform columns of discharges is applicable both to the positive column of a direct-current discharge and to the uniform column of a high-frequency discharge. The high-frequency discharge in a wide electrodeless tube was used in these experiments, since the gas remains perfectly pure in an electrodeless tube even when it is considerably heated by the current.

The discharge-tube T (fig. 1) was a quartz cylinder of 3·9 cm. internal diameter and 40 cm. long. The external sleeve electrodes S_1 and S_2 were connected to an oscillatory circuit as shown in fig. 1. The circuit was loosely coupled to a high-frequency generator. Oscillations of 110 metres wave-length were used throughout the experiments. The method of measuring the

* J. E. Keyston, Phil. Mag. xv. p. 1162 (1933).

electric force in the uniform column of the discharge was the same as described in previous papers *.

The current in the discharge-tube was measured by the current induced in two small loops of wire supported on an ebonite holder in a vertical plane passing through the axis of the discharge-tube. This method of measuring high-frequency currents has been described by Townsend and Pakkala †.

A quartz tube A, with a side-tube B containing metallic calcium, was included between the tap X and the discharge-

Fig. 1.

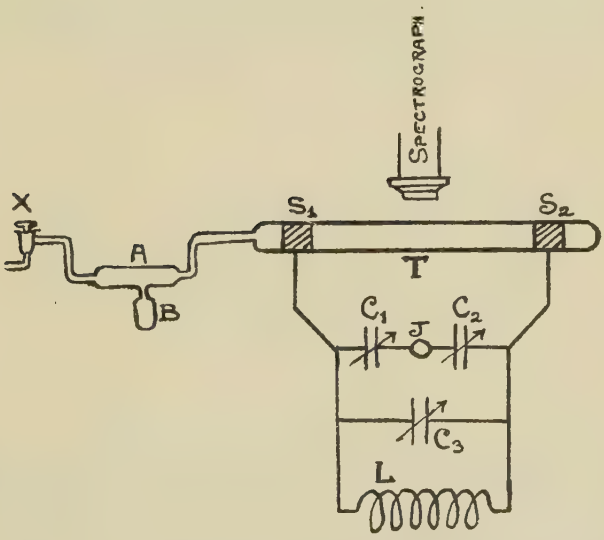

tube T. The calcium was heated strongly and a thin layer was deposited on the walls of the tube A, which absorbed any impurity that may have been given off from the taps during the course of the experiments.

The helium gas was prepared from thorianite, it was passed over palladium black to remove any traces of hydrogen which it might contain, and other impurities were removed by keeping the gas in tubes containing charcoal cooled with liquid air.

* J. S. Townsend and W. Nethercot, Phil. Mag. vii. p. 599 (1929).
† J. S. Townsend and M. H. Pakkala, Phil. Mag. xiv. p. 418 (1932).

3. The photographs of the discharge were taken with a Bellingham and Stanley spectrograph having a horizontal slit. Ilford hypersensitive panchromatic plates were used for photographing the yellow and red part of the spectrum, and Ilford iso-zenith and golden iso-zenith plates for the green, blue, violet, and ultra-violet parts of the spectrum.

The spectrum of the uniform column was photographed at various gas pressures with the same current in the discharge-tube and the same time of exposure on one plate. Thus a series of images of each line with different densities were obtained on the same plate. In order to determine the variation in the intensity of illumination I from the variation in density D of the images it is necessary to impress on the same plate a spectrum

Fig. 2.

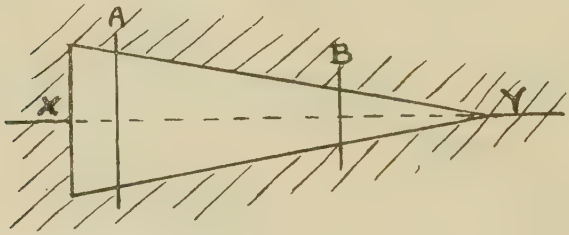

of known intensities from which the relation between I and D can be deduced at any desired wave-length. This calibration was carried out by two different methods.

In the first method the rectangular slit of the spectrograph was replaced by a slit shaped as shown in fig. 2. This slit was illuminated by a uniform source of continuous radiation which consisted either of a high-frequency discharge in a quartz tube containing pure argon at about 40 mm. pressure, or of the diffused radiation from a filament lamp.

The axis of the slit XY was horizontal and about 9 mm. long, and the width at the end X was 1·25 mm. Two fine wires, A and B, 5 mm. apart, were fixed across the slit at right angles to XY.

The variation of density across the image of the continuous spectrum, photographed through this slit, was measured for each wave-length by means of a micro-

photometer. The relation between the intensity of illumination I and the density D of the image was then obtained on the assumption that the intensity I at every point of the image was proportional to the corresponding width of slit. Having also found the densities D_1, D_2, D_3 etc. of the images of a line in the spectrum of the gas at different pressures, the corresponding intensities I_1, I_2, I_3 etc. of the line were therefore obtained in arbitrary units.

For the second method of calibration a set of flat metal disks were made which were drilled with a symmetrical pattern of holes as shown in fig. 3, all the holes on any one disk being of the same diameter. Each of these disks could be fitted over the end of the collimator of the spectrograph, between the collimator lens and the

Fig. 3.

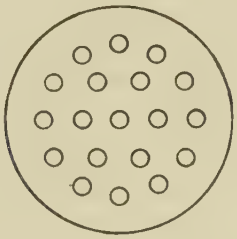

prism and at right angles to the parallel beam of rays emerging from the collimator. The diameters of the holes varied from one disk to the other, but the centres of the holes occupied precisely the same relative positions on each disk. Under constant conditions of illumination of the slit the intensity of the light falling on the photographic plate varies directly as the area of the holes in the disk. Thus by using in turn disks bored with holes of 4 mm., 3 mm., 2 mm., and 1 mm. diameter the intensity of illumination could be varied in the ratio 16 : 9 : 4 : 1. The four photographs thus obtained give the changes in the density D corresponding to known changes in I for the plate.

This method of calibration has the advantage that no continuous spectrum is used to compare with the lines, but, on the other hand, it has the disadvantage

that the number of exposures which has to be made on each plate is increased.

As a final check on the accuracy of both methods of calibrating the photographic plates, the continuous spectra photographed with the triangular slit were calibrated by means of the perforated disks. It was thus found that the increase in the intensity of the light due to an increase in the area of the holes in the disks had exactly the same effect on the photographic plates as a corresponding increase in the width of the slit.

4. It is a disadvantage of the spectrophotometric method of measuring intensities as compared with the colour-filter method that much larger currents have to be employed in the former than in the latter. With the filter method the intensity of the light is sufficient to be measured accurately when the current in the discharge-tube is 2 or 3 milliamperes, but the proportion of the light from a given source that passes through a spectrograph of small aperture is so small, that it is necessary to use currents of 20 to 30 milliamperes in order to avoid inconveniently long times of exposure. For currents of this order there is a considerable increase in the temperature of the gas, and the mean electric force in the uniform column is not quite independent of the current.

The results of measurements of the mean electric force in the uniform column at 10, 20, and 30 milliamperes are given in Table I. For pressures from 3 mm. to 40 mm. the force was found to be practically constant for currents smaller than 10 milliamps. The forces are much smaller at the lower pressures, and the method of measuring the force in the uniform column becomes inaccurate. Thus the values of the forces obtained for the three lowest pressures given in Table I. can only be considered to be approximate determinations.

5. *Results of Measurements of Intensity : The Line Spectrum.*—The variation of intensity with current at constant pressure of the gas was measured for several lines. Currents of 15 milliamperes and 30 milliamperes were used, and the ratio of the intensity at 30 milliamperes to the intensity at 15 milliamps. was found in all cases to lie between 2·25 to 1 and 2·0 to 1. The slight departure from strict proportionality between

current and intensity is due to the increase in temperature of the gas.

The intensities of seven prominent lines of the helium spectrum were measured at the pressures given in Table II. This range was covered by taking photographs at three successive pressures on each of four plates. The results of the measurements are given in Table II. The intensity of each line at 7 mm. pressure is taken as 100 units. The pressures, p, of the helium are given in millimetres of mercury and the root mean square electric force Z in the uniform column is given in volts per centimetre. The mean energy of agitation, E, and the velocity, W, in the direction of the electric force, corresponding to different

TABLE I.

Pressure in mm.	Force Z in volts/cm.		
	i=30 ma.	i=20 ma.	i=10 ma.
40	51·5	53·0	54·0
30	41·5	42·0	42·0
20	30·2	30·8	31·6
13	22·5	23·0	23·5
7	13·6	14·6	15·0
4	8·4	8·9	9·8
1·5	3·75	4·0	4·6
0·78	3·1	3·7	4·1
0·32	2·55	3·0	3·4

values of the ratio Z/p, have been found by Townsend and Bailey *. The values of E_1 which they obtained are given in volts in Table II. and the values of W in centimetres per second.

It can be seen that the intensities of all the lines increase as the pressure decreases from 40 mm. to 0·78 mm., and that the rate of increase of intensity is much greater than the rate of increase of E_1. Between 0·78 mm. and 0·10 mm. the intensities of all the lines pass through maximum values.

6. The above results are very similar to those obtained by Townsend and Jones † by the colour-filter method, and may be explained similarly by the following hypothesis.

* J. S. Townsend and V. A. Bailey, Phil. Mag. xlvi. p. 657 (1923).
† J. S. Townsend and F. Ll. Jones, Phil. Mag. xii. p. 815 (1931).

In order to excite any particular line of the helium spectrum by collision with a helium atom, an electron must possess an energy greater than a certain value E_x, which is known as the excitation potential of the line. The mean energy E_1 of the electrons in the discharge is much less than E_x ($E_x \sim 23$ volts, $E_1 \sim 3$ volts), and a small change in E_1 will cause a large change in the number of electrons with energies greater than E_x; the increase in the intensity of the lines is therefore much greater than the increase in the mean energy E_1.

If the distribution of energies of the electrons about the mean energy were known, the number of collisions

Table II.

				Intensity.						
p.	Z/p.	E_1.	$W \times 10^{-4}$.	λ 5876 2^3P-3^3D.	λ 4471 2^3P-4^3D.	λ 3889 2^3S-3^3P.	λ 3188 2^3S-4^3P.	λ 4713 2^3P-4^3S.	λ 5016 2^1S-3^1P.	λ 6678 2^1P-3^1D.
40	1·29	2·58	96	12	10	9	<9	—	13	12
30	1·38	2·76	99	19	18	17	—	—	21	19
20	1·51	3·02	105	34	27	27	—	—	35	33
13	1·73	3·46	115	58	50	50	46	48	58	57
7	1·94	3·85	125	100	100	100	100	100	100	100
4	2·10	4·10	132	148	220	163	220	220	155	145
1·5	2·50	4·60	150	252	540	334	616	594	418	261
0·78	4·0	5·63	235	340	675	367	920	772	668	340
0·32	8·0	—	—	187	585	550	1200	868	1600	303

in which the energies of the electrons are greater than E_x could be calculated, and this number should be proportional to the observed intensity of the line. The results deduced from a formula for the distribution may therefore be compared with the results of the experiments.

7. There are several causes which give rise to inequalities in the energies of electrons moving under a constant force, and it is impossible to find from theoretical considerations any simple formula for the distribution. The effects which determine the distribution of the energies of the electrons have been discussed by Townsend *. He showed that the differences in the

* J. S. Towsend, Phil. Mag. ix. p. 1145 (1930).

amounts of energy transferred in collisions, which give rise to the Maxwellian distribution in ordinary gases, have much less effect in causing inequalities in the energies of electrons; but there are other causes, due to the motion of the electrons in the field of force, which give rise to other inequalities in the energies and to a type of distribution which is different from the Maxwellian distribution. It has been found that a formula representing this type of distribution of energies of the electrons gives satisfactory results in the case of neon * but that it leads to values of the excitation potentials of helium which are much too low.

In the case of helium it is found that better agreement with the known values of the excitation potentials is obtained by assuming that the distribution of the energies of the electrons may be expressed by the following formula (1), which closely resembles the Maxwellian formula :—

$$\frac{N_x}{N} = \phi\left(\frac{E_x}{E}\right) = A\sqrt{\frac{E_x}{E}}\,\epsilon^{-\frac{3}{2}\cdot\frac{E_x}{E}}, \quad . \quad . \quad . \quad (1)$$

where N is the total number of electrons, E is their mean energy of agitation, N_x is the number of electrons having energies greater than E_x, and A is a constant.

With this formula the mean energy E of the electrons which excite a line of the spectrum can be calculated from the intensities I_1 and I_2 at pressures p_1 and p_2 by the equation

$$\frac{I_1}{I_2} = \frac{p_1 W_2}{p_2 W_1} \cdot \frac{\phi\left(\frac{E_x}{E_1}\right)}{\phi\left(\frac{E_x}{E_2}\right)} \quad . \quad . \quad . \quad . \quad . \quad . \quad (2)$$

The values of E_x obtained in this way from the results given in Table II. are given in Table III. The corresponding value of E_x for the yellow line λ 5876 Å, obtained by Townsend and Jones from measurements with colour-filters in the range of pressure from 13 to 3 millimetres was 22·4 volts.

The effect of large inelastic losses of energy by the electrons on the distribution increases as E_1 increases, and for pressures less than about 5 mm. (where $E_1 < 2Z/p$)

* P. Johnson, Phil. Mag. xiii. p. 487 (1932).

may lead to inaccuracies in the formula (1); this may account for the difference between the values of E calculated for the range 7 mm. to 0·78 mm. and the values calculated for the range 20 mm. to 7 mm.

It can be seen that for the range 7 mm. to 0·78 mm. the value of E_x for the singlet line 5016 Å (2^1S-3^1P) is considerably greater than the value of E_x for the corresponding triplet line 3889 Å (2^3S-3^3P), which has nearly the same excitation potential. This can be explained from considerations arising out of the difference between the excitation functions of singlet and triplet lines which have been discussed in a previous paper.

TABLE III.

Wave-length of line in Å.	Spectroscopic excitation potential.	Excitation energies in volts.		
		Pressure 40 to 20 mm.	Pressure 20 to 7 mm.	Pressure 7 to 0·78 mm.
5876	22·96	22·5	22·6	34·4
4471	23·62	21·9	24·8	40·0
3889	22·89	23·1	24·8	35·0
3188	23·59	—	—	42·5
4713	23·40	—	—	41·1
5016	22·97	21·8	22·4	39·9
6678	22·96	22·1	22·9	34·4

8. It has been assumed in the calculations that the probability of excitation is the same for all electrons whose energies are above the excitation potential. Experiments made by Hanle * show, however, that the probability of excitation of a line varies considerably with the energy of the electrons which excite it. He found that over a considerable range of energies E of the electrons immediately above the excitation potential E_x the probability of excitation is approximately proportional to $(E-E_x)$. On the assumption that this relation holds for all energies E of the electrons, which are greater than the excitation energy, the formula (1) becomes

$$\frac{N_x}{N}=\phi\left(\frac{E_x}{E}\right)=B\sqrt{E}(E_x+E)\epsilon^{-\frac{3}{2}\cdot\frac{E_x}{E}} \quad . \quad . \quad . \quad (3)$$

The values of E_x calculated from this formula are given in Table IV. These values differ by only two

* W. Hanle, *Zeits. f. Physik.* lvi. p. 94 (1929).

or three volts from the values of E_x calculated on the assumption that the probability of excitation is constant for all electrons whose energies are greater than the minimum energy of excitation.

9. *The Band Spectrum.*—Measurements were made of the intensity of the bands at the wave-lengths 6400 Å and 4650 Å. Since the individual lines of the bands could not be resolved with the small spectrograph, the intensity of all the lines in each band was integrated by using a wide slit. The bands therefore appeared as wide lines in the photographs.

The intensities of the bands at constant pressure were measured with currents of 15 and 30 milliamperes.

TABLE IV.

Excitation energies in volts of λ 5876 Å.

	Pressure 40 to 20 mm.	Pressure 20 to 7 mm.	Pressure 7 to 0·78 mm.
Probability of excitation $=k$	22·5	22·6	34·4
Probability of excitation $=k(E-E_x)$	20·6	20·4	31·3

The ratio of the intensity at 30 milliamperes to the intensity at 15 milliamperes was found to lie between 1·8 and 1·95 to 1. This shows that the intensity is almost exactly proportional to the current. The fact that the exact ratio of 2 to 1 was not obtained is probably due to the increase of temperature of the gas in changing the current from 15 to 30 milliamperes.

The change in intensity of the helium bands with the pressure is given in Table V. At pressures less than 7 mm. the intensities of the bands were too small to be measured accurately.

10. Assuming the bands to be emitted by diatomic molecules of helium, it is necessary to make some further assumption concerning the concentration of molecules in the gas in order to calculate the energies E_x of the electrons which excite the bands from a formula for the distribution of energies of the electrons.

The values of E_x obtained from the formula (1) by assuming that the concentration of molecules is proportional to the square of the pressure are given in the first row in Table VI., and the values obtained by assuming the concentration to be directly proportional to the pressure are given in the second row. The results of the calculation support the former assumption, since they lead to values of E_x for the two ranges of pressure, which differ less from one another than the values obtained on the latter assumption. The figures show

TABLE V.

Pressure in mm.	Intensity of bands.	
	λ 6400 Å.	λ 4650 Å.
40	300	260
30	285	250
20	240	220
13	180	170
7	100	100

TABLE VI.

Excitation energies in volts.

	λ 6400 Å.		λ 4650 Å.	
	Pressure 40 to 20 mm.	Pressure 20 to 7 mm.	Pressure 40 to 20 mm.	Pressure 20 to 7 mm.
Concentration of molecules $\sim p^2$	15·7	14·2	16·4	15·0
Concentration of molecules $\sim p$	7·5	4·4	8·2	5·2

that the excitation potential of the band spectrum is considerably lower than the excitiaton potential of the line spectrum.

11. The results of these measurements of the intensity of the band spectrum are very different from those obtained by Weizel *. He found, from measurements of the radiation emitted when large currents are passed

* W. Weizel, *Zeits. f. Physik.* li. p. 330 (1928); lix. p. 320 (1929).

through capillary tubes containing helium, that the intensity of the band spectrum did not change appreciably with the pressure, and also that the intensity of the bands was proportional to the square of the current. In order to explain his observations Weizel put forward the hypothesis that the molecules of helium are formed by the combination of one normal and one metastable helium atom. The experiments described above are not in accordance with this hypothesis, as it was found that the intensities of the bands were directly proportional to the current. The simplest explanation of this result is that there is a small proportion of molecules present in the normal state of the gas.

12. *The Continuous Spectrum.*—The variations in the intensity of continuous spectrum of helium, with the current and the pressure of the gas, have been measured by Townsend and Pakkala *. Their experiments were made with colour-filters and were confined to the part of the continuous spectrum between the principal green and yellow lines. They found that the intensity of the continuous spectrum varied directly as the current when the currents were of the order of 2 or 3 milliamperes. Spectrophotometric measurements of the continuous spectrum at the wave-lengths 3500 Å and 3000 Å show also that the intensity varies directly as the current for currents between 15 and 30 milliamperes.

The change in the intensity of the continuous spectrum with the pressure was measured for a range of wave-lengths of about 10 Å on either side of the wave-lengths 3500 Å and 3000 Å. The results of these measurements are given in Table VII.

13. The energies E_x of the electrons which excite the continuous spectrum have been calculated from formula (1) on the following two assumptions :—firstly, that the continuous spectrum is emitted by helium particles whose concentration is proportional to the square of the pressure, and, secondly, that it is emitted by helium particles whose concentration is directly proportional to the pressure. The values of E_x obtained by making these assumptions are given in the first and second rows

* J. S. Townsend and M. Pakkala, Phil. Mag. xiv. p. 418 (1932).

respectively in Table VIII. There is good agreement between the value 9·4 volts obtained for the range 20 to 7 mm. and the value of 10 volts which was calculated in the same way by Townsend and Pakkala from their measurements with colour-filters for the range 12·5 to 3 mm.

TABLE VII.

Pressure in mm.	Intensity of continuous spectrum.	
	λ 3000 Å.	λ 3500 Å.
40	160	160
30	153	
20	140	140
13	122	
7	100	100

It can be seen that if the continuous spectrum is emitted by the helium atom the excitation potential is much lower than the excitation potential of the line spectrum.

If it be supposed that there are molecules of helium present in the normal state of the gas the continuous

TABLE VIII.

Excitation energies in volts of continuous spectrum at wave-lengths 3500 Å. and 3000 Å.

	Pressure 40 to 20 mm.	Pressure 20 to 7 mm.
Concentration $\sim p^2$	18·2	19·2
Concentration $\sim p$	7·1	9·4

spectrum might be attributed to molecules as far as the observations of the intensity in the uniform column are concerned. This conclusion, however, is not confirmed by observations of the light from the cathode glow, where it was found that the band spectrum is very strong but no continuous spectrum can be observed.

I wish to thank Professor J. S. Townsend for much valuable help and advice throughout the course of this investigation. My thanks are also due to Professor H. H. Plaskett and to Professor H. L. Brose for permitting me to use their microphotometers, and to the Department of Scientific and Industrial Research for a Senior Research Award which has enabled me to carry out this investigation.

LIV. *An X-Ray Investigation of Crystals of Stilbene and Tolane.* *By* Mata Prasad, *D.Sc.**

CRYSTALS of stilbene ($C_6H_5CH=CHC_6H_5$) and tolane ($C_6H_5C\equiv CC_6H_5$) have been examined photographically by X-rays, using the rotating and oscillating single crystal method. Previous measurements made by Sir William Bragg and K. Lonsdale (Yardley) on the ionization spectrometer gave, for the dimensions of the unit cells,

$$a=12{\cdot}20\text{ Å.};\ b=5{\cdot}72\text{ Å.};\ c=16{\cdot}00\text{ Å.};\ \beta=113^\circ\ 48'$$

for stilbene, and

$$a=12{\cdot}80\text{ Å.};\ b=5{\cdot}68\text{ Å.};\ c=15{\cdot}74\text{ Å.};\ \beta=114^\circ\ 56'$$

for tolane.

These dimensions are similar to those found for azobenzene ($C_6H_5N=NC_6H_5$) by Prasad (Phil. Mag. x. p. 311, 1930), which were

$$a=12{\cdot}65\text{ Å.};\ b=6{\cdot}06\text{ Å.};\ c=15{\cdot}60\text{ Å.};\ \beta=114^\circ\ 24',$$

and again the space-group is C_{2h}^5, with four molecules to the unit cell.

Stilbene crystals have also been examined by Becker and Rose (*Zeit. f. Physik*, xiv. p. 369, 1923) and by J. Hengstenberg and H. Mark (*Zeit. f. Krist.* lxx. p. 283,

* Communicated by the Author.

1929). The unit cell given here is the same as that of Hengstenberg and Mark, and the dimensions are in good agreement with theirs.

As in the case of azobenzene, an approximate symmetry about the (201) plane was observed. This was shown both by the geometrical relations and by the similarity between the intensities of reflexion of corresponding planes. In all these three compounds, therefore, the crystals show a pseudo-orthorhombic symmetry, and may be referred to an approximate orthogonal cell. For stilbene and tolane the dimensions are $a=12{\cdot}20$ Å.; $b=5{\cdot}72$ Å.; $c=29{\cdot}0$ Å. and $a=12{\cdot}80$ Å.; $b=5{\cdot}68$ Å.; $c=28{\cdot}4$ Å. respectively; in each case β is nearly 90°. The indices $(h'k'l')$ of planes referred to the orthogonal cell are related to those (hkl) of the original monoclinic cell by the relation

$$h'=h, \quad k'=k, \quad l'=2l+h.$$

A large number of reflexions were observed and visual estimations of intensities made, and it was found that in the majority of cases the reflexions from $(h'k'l')$ and $(h'\bar{k}'l')$ planes were of the same intensity.

This approximate orthogonal symmetry is confirmed by the magnetic measurements of crystals of stilbene by Krishna, Guha, and Banerjee (Phil. Trans. A, ccxxxi. p. 259).

From the similarity of the results on the crystals of azobenzene with those on stilbene and tolane, it can be inferred that the molecules in the unit cells lie in the same way, with their lengths along the [20$\bar{1}$] axis. The length of the cell along the [201] direction in the case of tolane is exactly the same as in azobenzene. It appears, therefore, that the linkings (—N=N—) and (—C≡C—) are equivalent in length, within the errors of experiment. The (—C=C—) linking is somewhat longer.

Davy Faraday Laboratory,
Royal Institution, London,
and
Chemical Laboratories,
Royal Institute of Science, Bombay.

LV. *The Thermal Aspects of Carburation, with special reference to the Vaporization of Ethyl Alcohol.* By James Small, *B.Sc., Ph.D., Carnegie Teaching Fellow, The James Watt Engineering Laboratories, The University of Glasgow* *.

THE carburetter fitted to any internal combustion engine fulfils two main functions. Firstly, it measures out the requisite amount of fuel, and secondly, it mixes the fuel with the air necessary for its combustion. Practically all the analytical treatment which has been given to the carburetter has been confined to the first of these aspects of its action, which presents a hydrodynamic problem. In a sense this aspect is of primary

Fig. 1.

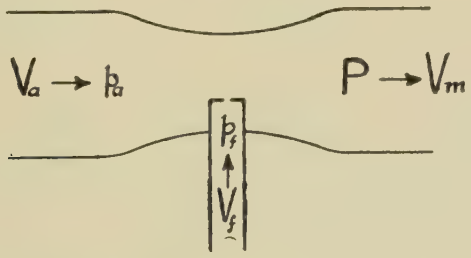

importance; but the second function of the carburetter is almost as important, for the thermal condition of the combustible mixture leaving the carburetter is a factor controlling not only the power and the efficiency of the engine under conditions of normal running, but also its manœuvrability, as, for instance, in "starting from cold." This is a thermodynamic problem.

Let fig. 1 represent the choke-tube of a carburetter and a simple jet supplying the fuel. The air enters the system at pressure p_a with velocity V_a, while the fuel enters at pressure p_f with velocity V_f. While the volumes v_a and v_f of air and fuel enter the system, let a volume v_m of the mixture leave the system with pressure P and velocity V_m. Let m_a and m_f be the masses of the

* Communicated by Professor W. J. Goudie, D.Sc.

constituents passing through the system in the given time. The work accounted for by the passage of the air into the main is $p_a v_a$, and by the passage of the fuel, $p_f v_f$. In the same time the work associated with the passing of volume v_m of the mixture out of the system is $\mathrm{P}v_m$.

Let I_a, I_f, and I_m be the internal energies respectively of the constituents entering the system and the mixture leaving, and let there be no exchange of heat with the surroundings, then the energy equation becomes

$$p_a v_a + \mathrm{I}_a + \frac{m_a \mathrm{V}_a^2}{2g} + p_f v_f + \mathrm{I}_f + \frac{m_f \mathrm{V}_f^2}{2g} = \mathrm{P}v_m + \mathrm{I}_m + \frac{(m_a + m_f)\mathrm{V}_m^2}{2g}$$

or

$$\mathrm{H}_a + \mathrm{H}_f = \mathrm{H}_m + \frac{(m_a + m_f)\mathrm{V}_m^2}{2g} - \left(\frac{m_a \mathrm{V}_a^2}{2g} + \frac{m_f \mathrm{V}_f^2}{2g}\right),$$

where H_a, H_f, and H_m are the total heats of the air, fuel, and mixture respectively, and $\mathrm{H} = \mathrm{I} + pv$.

While a solution of the hydrodynamic problem is dependent upon the fluid velocities, these are of little account in applying the above equation to the solution of the thermal problem; for we do not study the condition of the mixture at the throat of the choke-tube, but as it enters the engine. The kinetic energies are, therefore, relatively small, and the equation may be written

$$\mathrm{H}_a + \mathrm{H}_f = \mathrm{H}_m.$$

That is to say, the total heat of the mixture is the sum of the total heats of the fluids before mixing. Applying the laws of mixtures, we have also the volume v_m of the mixture equal to the volume of each constituent as it exists at its partial pressure in the mixture.

The fuels in general use in internal combustion engines are of a complex nature, and it is, therefore, not feasible in a given case to arrive at the true condition of the air-fuel mixture. It is of importance, however, to study the *characteristics* of the mixture. The difficulties met with in the alcohol engine are typical in greater or less degree of the difficulties met with in the carburation

of liquid fuels in general. It is, therefore, proposed to examine in the first place the thermal side of the carburation of pure ethyl alcohol.

A *total heat–moisture content* chart has been devised by Mollier in connection with atmospheric hygrometry*. This type of chart depends on the fact that at low pressures the total heat of dry water vapour is very nearly a linear function of temperature only. The thermal properties

TABLE I.

Thermal Properties of Ethyl Alcohol.

$t°$ C.	Liquid specific heat (mean).	Liquid or sensible heat. Cals./gr. or C.H.U./lb.	Latent heat of vaporization. Cals./gr. or C.H.U./lb.	Total heat of dry saturated vapour. Cals./gr. or C.H.U./lb.
−40	0·501	−20·0	223·7	203·7
−30	0·508	−15·2	222·7	207·5
−20	0·515	−10·3	221·9	211·6
−10	0·522	− 5·2	221·0	215·8
0	0·535	0	219·8	219·8
10	0·538	5·4	218·8	224·2
20	0·545	10·9	217·4	228·3
30	0·552	16·6	216·2	232·8
40	0·562	22·5	215·0	237·5
50	0·575	28·7	213·0	241·7
60	0·585	35·1	210·2	245·3
70	0·600	42·0	205·3	247·3
80	0·612	49·0	203·0	252·0

of the common liquid fuels are not nearly so well established as those of water and steam, but it is found that to some of them, including ethyl alcohol, the same linear law applies, to a sufficient degree of approximation.

The Thermal Properties of Ethyl Alcohol.—The tensions of the saturated vapours of various combustible substances as measured by different observers are collected in the International Critical Tables (vol. iii.), and in the same publication (vol. v.) is to be found some

* Mollier, Z.V.D.I., July 20, 1929.

information regarding liquid specific heats and latent heats of evaporation; but direct observations of the specific heats of the vapours are extremely scanty.

The only figures available for the specific heat of the vapour of ethyl alcohol are those given by Regnault and by Dixon and Greenwood. The former gives 0·453 for the range 108° C. to 220° C., and the latter authorities give 0·406 at 90° C.

Table I. has been constructed from the information available on the thermal properties of ethyl alcohol, and it will be found that very nearly at all pressures within the range given, $H_f = 220 + 0{\cdot}43t$, where H_f calories per gramme or C.H.U. per lb. is the total heat of the dry vapour and $t°$ C. is its temperature. The value 0·43 is reasonably consistent with the above-mentioned values for the specific heat of the vapour. If 1 lb. of air is mixed with x lb. of fuel, then the total heat of $(1+x)$ lb. of the mixture is given by $H_m = 0{\cdot}24t + x(220 + 0{\cdot}43t)$, where 0·24 is the specific heat of air at constant pressure.

Construction of the Total Heat–Fuel Content *Chart or Carburation Chart.*

Let P be the total pressure of the mixture of air and fuel and let p_a and p_f be their respective partial pressures in the mixture. If M_a and M_f are the molecular weights of the air and fuel, and if x lb. of fuel is associated with 1 lb. of air, then, provided the air is unsaturated,

$$x = \frac{M_f}{M_a} \cdot \frac{p_f}{P - p_f},$$

where $P - p_f = p_a$.

If p_f' is the saturation pressure corresponding to the temperature $t°$ C. of the mixture, then the weight of fuel which saturates the lb. of air at a given total pressure is

$$x' = \frac{M_f}{M_a} \cdot \frac{p_f'}{P - p_f'} \quad . \quad . \quad . \quad . \quad . \quad . \quad (1)$$

If the quantity of fuel per lb. of air is greater than this, then the excess is present in the liquid form.

The chart (fig. 2) contains lines of constant fuel content. These are vertical and equally spaced. It contains, also, lines of constant temperature diverging towards the

Fig. 2.

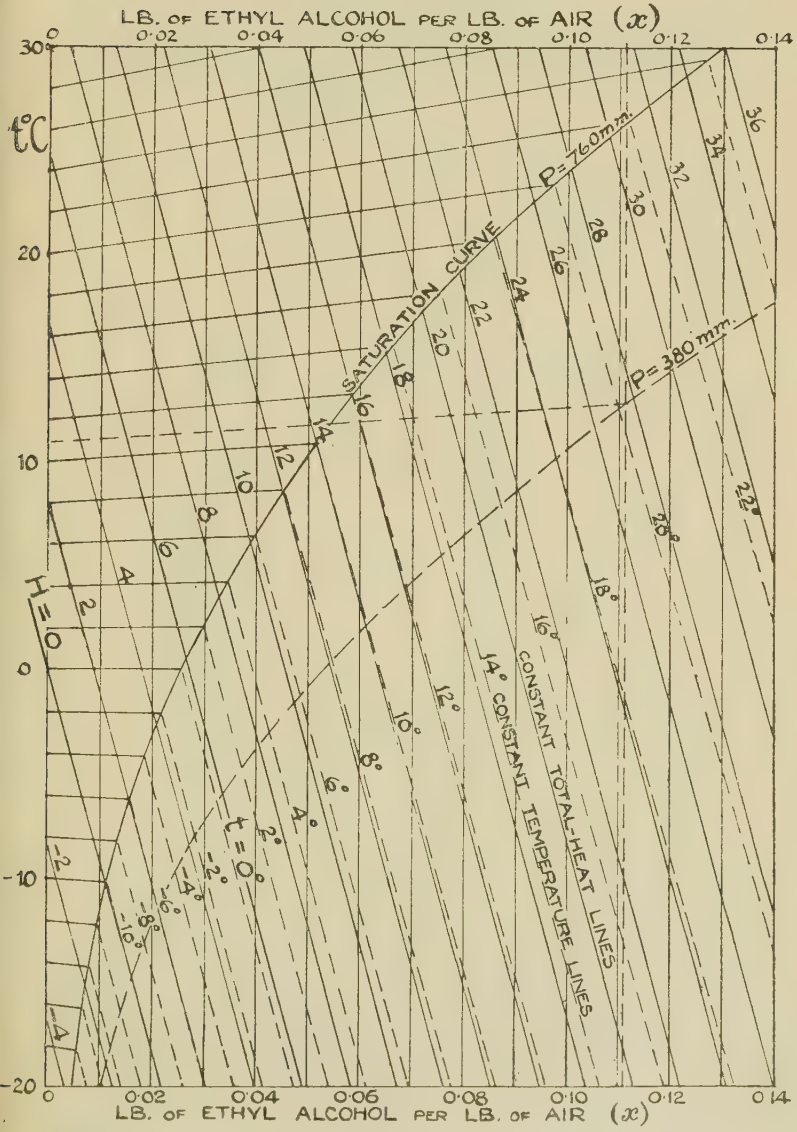

CARBURATION CHART FOR ETHYL ALCOHOL

right in the dry region at such a rate as to keep the lines of constant total heat parallel and equally spaced.

Since the total heat of the mixture of 1 lb. of air with x lb. of fuel takes the form $H=at+x(b+ct)$, then, for equal increments ΔH of H at given values x_1 and x_2 of x,

$$\Delta H=a[\Delta t]_{x_1}+cx_1[\Delta t]_{x_1},$$

$$\Delta H=a[\Delta t]_{x_2}+cx_2[\Delta t]_{x_2},$$

and

$$\frac{[\Delta t]_{x_1}}{[\Delta t]_{x_2}}=\frac{a+cx_2}{a+cx_1}.$$

If $x_1=0$,

$$[\Delta t]_{x=x}=\frac{a}{a+cx}[\Delta t]_{x=0}.$$

TABLE II.

Vapour Tensions of Ethyl Alcohol.

$t°$ C.	p'. mm. Mercury.	p'. lb./in.^{2}
−40	0·39	0·0075
−30	1·04	0·0201
−20	2·50	0·0483
−10	5·6	0·1082
0	12·2	0·2358
10	23·6	0·4562
20	43·9	0·8486
30	78·8	1·5232
40	135·3	2·6153
50	222·2	4·2951
60	352·7	6·8177
70	542·5	10·487
80	812·6	15·706

Hence the constant-temperature lines are made to diverge so that the space-scale (*i. e.*, vertical distance for each degree) at $x=x$ is $\frac{a+cx}{a}$ times the space-scale at $x=0$.

Typical values of the vapour tensions of ethyl alcohol are given in Table II.*

* International Critical Tables, vol. iii. p. 215 *et seq.*

By taking p_f' at different temperatures and substituting the values in the expression for x' (equation (1)) along with a chosen constant value of P, points are obtained on the saturation curve corresponding to the total pressure P.

Choosing 28·97 as the virtual molecular weight of air, we have for ethyl alcohol

$$x' = \frac{46{\cdot}05}{28{\cdot}97} \cdot \frac{p_f'}{P - p_f'}$$

$$= 1{\cdot}59 \cdot \frac{p_f'}{P - p_f'}.$$

Thus, when P = 760 mm., we have,

$t°$ C.	p_f'. mm.	$\frac{p_f'}{P - p_f'}$.	$x' = 1{\cdot}59 \frac{p_f'}{P - p_f'}$.
−20	2·5	0·00330	0·00525
−15	3·6	0·00483	0·00768
−10	5·6	0·00743	0·01180
− 5	8·3	0·01103	0·01754
0	12·2	0·0163	0·0259
5	17·3	0·0233	0·0371
10	23·6	0·0321	0·0510
15	32·2	0·0443	0·0704
20	43·9	0·0614	0·0976
25	59·0	0·0842	0·1340
30	78·8	0·1157	0·1840

A point above the saturation curve represents a dry mixture of fuel and air, and a point below the curve represents a wet mixture. No matter what the extent of the wetness may be, so long as the temperature is constant the partial pressure exerted by the fuel is constant, and the total heat of the wet mixture is given by $H = at + x'(b + ct) + h_f(x - x')$, where h_f is the liquid heat per lb. of fuel and x' the fuel-content for saturation at temperature t, while x is the actual fuel-content. This enables us to draw the constant-temperature lines in the wet field.

The *Total Heat–Fuel Content* Chart or Carburation Chart for Ethyl Alcohol (fig. 2) shows the saturation curve drawn for a total pressure of 760 mm. It will be seen that for most practical purposes the temperature-lines in the wet region might be taken as parallel to the lines of total heat. This approximation makes it possible to extend the usefulness of the chart by drawing in a number of saturation curves corresponding to different total pressures. In fig. 2 the broken curve is that corresponding to saturation at half an atmosphere of total pressure. The temperature-lines in the dry region at this low pressure are to be imagined extended to this broken line ; but the distribution of temperature in the wet region is now altogether different from that for the original saturation curve. It is determined by the points of intersection of the upper temperature lines with the broken curve, and by lines drawn from them parallel to the total heat lines.

The vertical broken line in fig. 2 corresponds to a fuel-content of 0·111 lb., which is the theoretically correct amount to burn in 1 lb. of air.

An examination of fig. 2 reveals some interesting characteristics of the vaporization process.

Suppose that the carburetter has been so designed as to supply 0·111 lb. of ethyl alcohol per lb. of air, both constituents being at 15° C. The total heat of the air is $0{\cdot}24 \times 15 = 3{\cdot}6$ C.H.U., and the liquid heat of the fuel (see Table I.) is $0{\cdot}111 \times 8{\cdot}1 = 0{\cdot}9$ C.H.U. Therefore the total heat of the mixture initially is 4·5 C.H.U. If mixing takes place at atmospheric pressure it will be seen, on reference to the chart, that at 4·5 C.H.U. of total heat only 0·022 lb. of the alcohol can be vaporized, that is, only about one-fifth of the amount leaving the carburetter, and the temperature is depressed to −1·7° C.

Since it is the proportion of *vaporized* fuel in the fuel-air mixture that determines the ignitability of the charge, and since the aim is, therefore, to have all of the fuel vaporized, preheating is necessary. If the air only is preheated, and if it is assumed that the chemically correct mixture of fuel and air is used, to what temperature must the preheating be carried ?

Let the temperature of the heated air be t° C. The total heat of the constituents before mixing is, therefore, $0{\cdot}24t + 0{\cdot}9$.

From the chart it is seen that, at one atmosphere, the total heat required for a dry saturated mixture is practically 31 C.H.U. and the temperature is nearly 22° C.

By equating, $0{\cdot}24t+0{\cdot}9=31$, we obtain $t=125°$ C. (257° F.).

In passing it may be mentioned that a similar analysis of methyl alcohol shows that the preheat temperature of air for the vaporization of the chemically correct proportion of that fuel at atmospheric pressure is 195° C. (383° F.).

With these figures before us it is seen how desirable it is to introduce into power-alcohol a considerable proportion of ordinary hydrocarbon fuel as in done in practice.

The Explanation of some Carburetter Phenomena.

The vaporizing conditions in the carburation of alcohol are widely different as to temperature, partial pressure, and total heat from those in the petrol engine. But the general characteristics of the process are the same in both cases.

The Strangler Valve.—The strangler valve is a device by means of which, when the engine is "starting from cold," the air-flow through the carburetter is so throttled that a considerable vacuum is induced in the region of the fuel-jet. Of itself the introduction of liquid fuel is ineffective, for it is the relative amount *vaporized* per lb. of air, and not the total weight of fuel thrown into the air-stream, that determines the ignitability of the charge. The aid which the strangler valve affords in starting the engine comes from secondary effects which can only be studied with the help of the carburation chart.

Let us suppose, for example, that, due to partial preheating, 19·6 C.H.U. of total heat are available. This at 760 mm. total pressure would evaporate 0·071 lb. of ethyl alcohol (fig. 2), and the temperature of the mixture would be 15° C., which we may regard as the temperature of the atmosphere. But if by such means as a strangler valve the pressure in the induction system is reduced to half an atmosphere (380 mm.), *the same total heat* not only evaporates 0·082 lb. of ethyl alcohol per lb. of air used, but results in a temperature of 6° C. Due to this low temperature, heat flows from the surroundings (for example the metal walls of the induction passages,

which are at atmospheric temperature) into the charge. If this flow of heat were to continue until the temperature again approximated to 15° C., then the amount of the increase in total heat would be such as to vaporize easily the requisite proportion of fuel for combustion.

This flow of heat set up by the refrigerating action of the carburation process is also effective in the case of the ordinary hydrocarbon fuels.

The serious practical objections to flooding the induction system, and the cylinders, with liquid fuel in starting an engine with the aid of the strangler are too well known to require mention here. It seems clear that ease in starting can be achieved without such flooding. If, while the air-strangler is closed in order to induce a low pressure in the carburetter system, the flow of fuel is at the same time restricted to what is necessary to give a normal air/fuel ratio, the same ignitability of the charge is obtainable as is achieved by the destructive flooding of the cylinders.

This point is further illustrated by the skeleton diagram (fig. 3). Let it be assumed that the total heat H_1 initially available would cause at atmospheric pressure P_1 the evaporation of x_1 lb. of the fuel and maintain the mixture at atmospheric temperature T_1. These conditions are represented by the point A. But if the pressure be reduced to P_2 the amount evaporated at the same total heat increases to x_2, and the temperature drops to T_2, these conditions being represented by the point B. If sufficient time were allowed for the mixture to rise to T_1, then the total heat would rise to H_2, and if the correct amount of fuel, x' lb., is present per lb. of air, the conditions at point C are such as to afford a fully vaporized, and even superheated, mixture.

A practical application of this effect is found in a method for starting an alcohol engine from cold. The throttle is tightly closed, and the engine is primed with a little fuel. The crank-shaft is turned slowly and then quickly. The engine picks up with certainty on the third or fourth compression stroke *. The low pressure induced during the suction-stroke no doubt sets up a low temperature and causes an inflow of heat which renders the evaporation sufficient for ignition.

* "Starting on Alcohol." Report of Australian Fuel Comm. Journal of Soc. of Automotive Engineers, November 1921.

The charts, it must be noted, refer to conditions of thermal equilibrium, and, as the vaporizing process takes time, it may be that equilibrium is not attained before the mixture of fuel and air enters the engine. It is therefore necessary to provide conditions which leave a considerable margin in favour of the attainment of the required quality of the charge. For instance, preheating should be carried to a temperature higher than that suggested by theoretical considerations. The attainment of thermal equilibrium depends upon the rate of evaporation of the fuel. This is a matter which will be touched upon later.

Fig. 3.

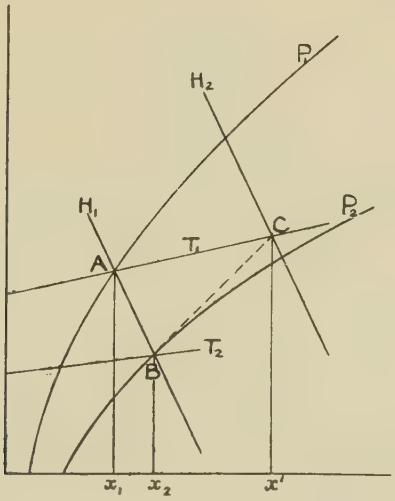

The chart reproduced in fig. 4 is a development of fig. 2. The saturation conditions at various total pressures are represented by the curves. The temperatures in the dry region at any given pressure are represented by the straight diverging lines above and to the left of the saturation curve corresponding to that pressure; but temperatures in the wet region may be taken as represented approximately by straight lines drawn parallel to the total heat lines from the points of intersection of the above-mentioned diverging lines with the saturation curve.

Quantitative analyses of the type represented by fig. 3 can now be carried out on fig. 4.

Fig. 4.

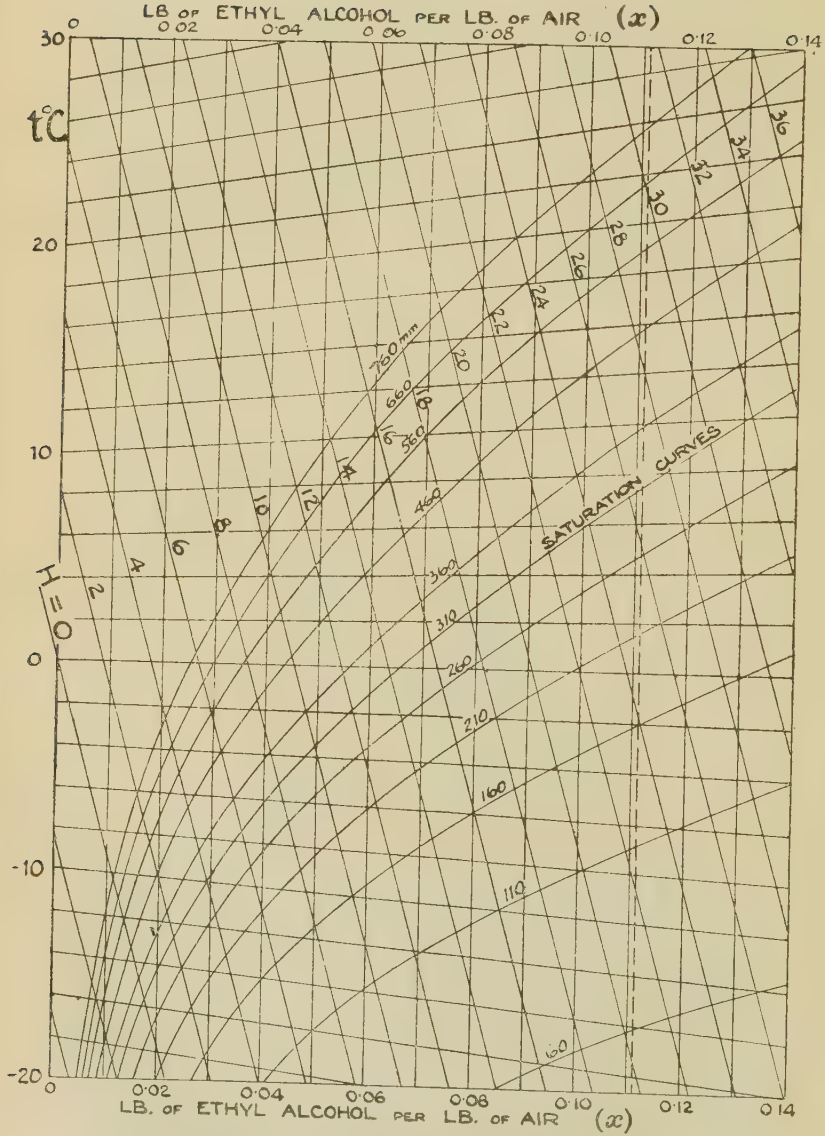

CARBURATION CHART FOR ETHYL ALCOHOL

Factors controlling the Rate of Evaporation.

Heat flows from the air towards the liquid particles as it leaves the jet to provide the latent heat of vaporization, and the vapour formed diffuses outwards into the surrounding air in the induction pipe. The double action is represented by fig. 5. In steady flow the well-known equations for diffusion and for heat-transference are of the same form. While the vapour diffusion depends upon a partial-pressure gradient, the heat-flow depends upon a temperature gradient ; hence, so long as evaporation is taking place, there must be a temperature-difference θ between the liquid particle and the surrounding air.

Fig. 5.

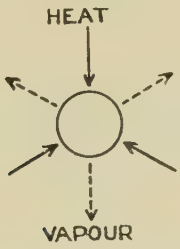

Let E lb. per ft.^{2} per sec. be the rate of evaporation from the surface of particle when the air blows past it at a velocity of V ft./sec. Let L_e C.H.U./lb. be the latent heat of vaporization at the temperature of the liquid and let l ft. be a linear dimension of the surface. E is likely to depend upon V, L_e, θ, and l, together with

k, the thermal conductivity of the mixture of vapour and air ;

c, the specific heat per unit volume of vapour and air ;

ρ, the difference in concentration of vapour and air ;

K, the coefficient of diffusion of the vapour ;

ν, the kinematic viscosity of the mixture of vapour and air.

E is expressible, therefore, in terms of $l^m L_e^x \theta^y V^z k^p K^q c^r \nu^s \rho^t$. Dimensionally

$$\frac{M}{L^2T} = L^m \left(\frac{\text{Heat}}{M\theta}\right)^x \theta^y \left(\frac{L}{T}\right)^z \left(\frac{\text{Heat}}{LT\theta}\right)^p \left(\frac{L^2}{T^2}\right)^q \left(\frac{\text{Heat}}{L^3\theta}\right)^r \left(\frac{L^2}{T^2}\right)^s \left(\frac{M}{L^3}\right)^t.$$

From which E is a function of

$$\frac{k\theta}{lL_e}\left(\frac{Vcl}{k}\right)^{r+t-q-s}\left(\frac{c\nu}{k}\right)^{-t+q+s}\left(\frac{\nu}{K}\right)^t - \left(\frac{K\rho L_e}{k\theta}\right)^t,$$

or $\dfrac{lL_eE}{k\theta}$ is a function of

$$\frac{Vcl}{k}, \quad \frac{c\nu}{k}, \quad \frac{\nu}{K}, \quad \frac{K\rho L_e}{k\theta}.$$

In practice $\dfrac{c\nu}{k}$ may be regarded as constant, and, if the total pressure is kept constant, so also may $\dfrac{\nu}{K}$. This, with a rearrangement of the non-dimensional groups, enables us to express $\dfrac{lE}{K\rho}$ as a function of $\dfrac{Vcl}{k}$ and $\dfrac{K\rho L_e}{k\theta}$.

This affords a basis for experimental observations, and is being used as such in work which the writer has in progress.

Behaviour of the Mixture during Compression.

It may be asked why complete evaporation of the fuel in the induction manifold should be aimed at, since the work of compression will in any case cause the evaporation of the normal proportion of fuel required. This is true, with the proviso that the necessary amount of fuel, liquid and vapour, is introduced into the cylinder. But a wet mixture, formed when insufficient heat is available, tends to leave the liquid particles behind at the bends and pockets of the induction passages, so that in starting the engine only a weak mixture will enter the cylinder, unless the induction system is simply flooded with fuel in order that a quantity of the liquid finds its way in.

The advantage of completely vaporizing the fuel in the induction on multicylinder engines is, it need hardly be mentioned, to have an even distribution to the cylinders.

Given different thermal conditions of the fuel and air entering the engine, the obvious tool for studying relative characteristics is a *total-heat–entropy* chart of the mixture.

Such a chart can be constructed for only one strength of mixture at a time. It has been assumed that the mixture contains 0·111 lb. of ethyl alcohol to 1 lb. of air (the chemically correct mixture), and a *total heat–entropy* chart has been prepared and is presented in fig. 6.

Construction of the Chart.—The total heat (enthalpy) of the mixture is taken as the sum of the total heats of the constituents reckoned at their partial pressures from 0° C. In constructing the chart the entropy of the fuel was reckoned from liquid at 0° C., but the entropy of the air was reckoned from an imaginary-state point at 1 lb./in.^{2} abs. and 1° C. abs. This latter, if the temperature is T and the partial air pressure is p_a, is expressible for unit mass by

$$=c_p \log_e \mathrm{T} - \frac{\mathrm{R}}{\mathrm{J}} \log_e p_a.$$

This introduces an imaginary datum for the entropy of the mixture, which is the sum of the entropies of the fuel and air in the mixture, but no disadvantage arises, since the difference between the entropy reckoned in this way and that reckoned with any other datum-point for the air is constant.

It is assumed that the characteristic law $\mathrm{PV} = \overline{\mathrm{R}}\mathrm{T}$ applies to the dry vapour where V is the volume of the vapour, P its partial pressure, T the mixture temperature, and $\overline{\mathrm{R}}$ the universal gas constant.

The chart includes lines of constant dryness (by "dryness" being meant that portion of the alcohol present which is in the vapour form), lines of constant temperature, and lines of constant total pressure.

When the air and alcohol enter the engine, each at 15° C., it has already been noted that the total heat available is of the order of 4·5 C.H.U. Assuming the total pressure to be 15 lb./in.^{2} abs., it is seen that the initial dryness would be only 0·2, *i. e.*, only a fifth of the alcohol supplied in the theoretical mixture would be vaporized. But if all the alcohol, liquid and vapour, is compressed along with the air adiabatically, then at the normal pressure at the end of compression there is a sufficiency of vaporized fuel to afford an ignitable mixture.

But again it is to be noted that this applies to conditions of thermal equilibrium and to a mixture containing at first small liquid particles equally distributed through-

Fig. 6.

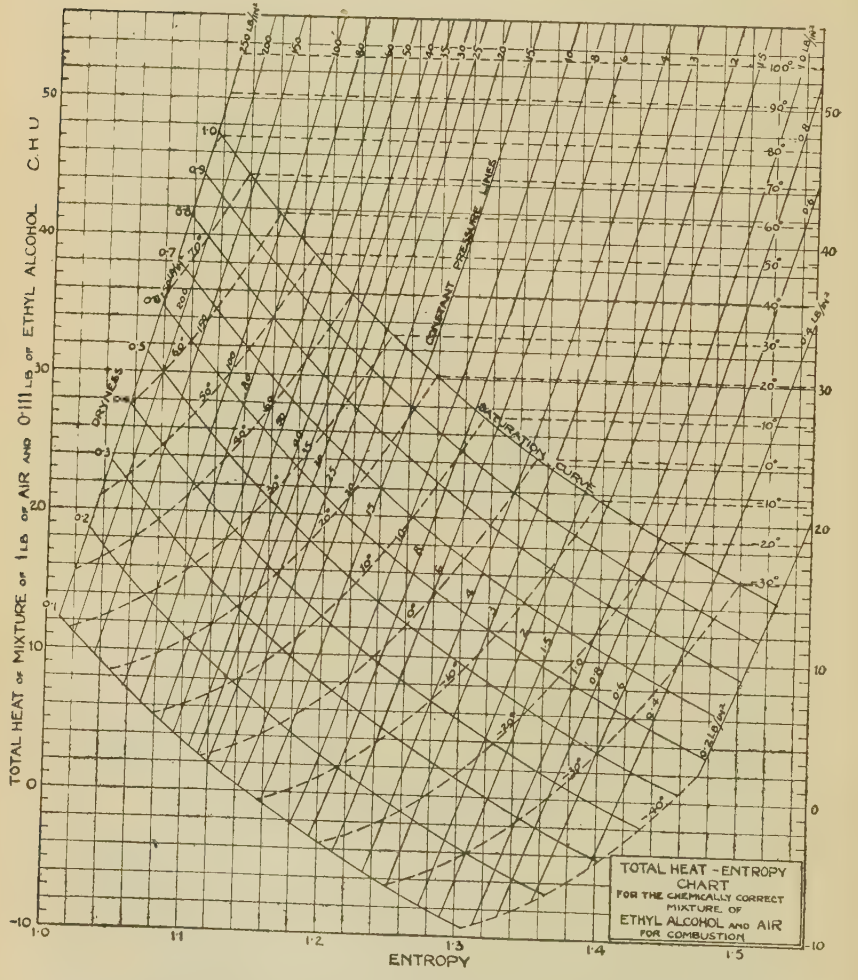

out the gaseous mass. If the liquid is concentrated in pools either above the piston or in some pocket of the combustion chamber, the speed of compression may be too high to allow sufficient time for evaporation to be completed before the igniting spark passes.

LVI. *A Correlation of some Thermoelectric and Thermomagnetic Data.* *By* L. F. Bates, *Ph.D., D.Sc., Reader in Physics, University College, London* *.

Introduction.

A SHORT time ago an account † was given of some measurements of the thermoelectric powers of rods of manganese arsenide. This substance possesses pronounced ferromagnetic properties and has a ferromagnetic Curie point in the neighbourhood of 45° C. In earlier work the magnetic properties of specimens of manganese arsenide had always been investigated when the substance was in the form of a powder.

The preparation consisted in heating black metallic manganese with excess arsenic in a moderately wide quartz tube, which was evacuated and sealed. The tube and its contents were maintained at about 750° C. for several hours, and were then allowed to cool slowly to air temperature. The tube, with the exception of one end, was well lagged, so that on cooling the excess arsenic collected at the cooler end. After removal the arsenide was broken up into a moderately fine powder, digested in concentrated hydrochloric acid for some days, washed several times in water and then in alcohol, and finally dried.

In driving off the last traces of the alcohol the powder was usually heated to about 60° C. in a crucible over a small Bunsen flame; consequently the temperature of the powder was raised at least once in this process. Actually it was allowed to cool and was heated several times in this manner, so that before its magnetic properties were determined the substance had been made to change from the ferromagnetic to the paramagnetic state several times. It will now be shown that owing to this thermal treatment an important property of freshly prepared manganese arsenide was not recorded.

To make a rod of manganese arsenide some of the purified powder was packed into a long narrow quartz tube sealed at one end. Usually a little free arsenic

* Communicated by the Author.

† L. F. Bates, Phil. Mag. xiii. p. 393 (1932).

was placed on the top of the powder, and the tube was evacuated and sealed. The tube was then placed vertically inside a furnace and heated as described in a previous paper *. When the rod so formed was removed from the tube it was not possible to purify it further, and the heating process described above was not carried out. Some of the rods used in the thermoelectric experiments were, however, heated during the attachment of terminals or clips, to which wires had to be soldered, and so forth. This accounts for many of the points of difference between the results obtained with the several specimens.

The magnetic properties of these rods have now been investigated, using a new magnet † designed to give a high uniform field over a moderately wide gap between flat pole-pieces.

Magnetic Measurements.

The rod whose magnetic properties were to be investigated was placed inside a copper tube, in which it fitted loosely. A small quantity of loosely packed cotton wool or spongy rubber was placed at each end of the tube, in order to permit the free expansion of the rod when its temperature was raised. One end of the tube was closed by a soldered copper plate, whilst the other end was fitted with a screw-plug, with a suitable washer, so that the tube could be made liquid-tight. This was necessary in case the rods were porous. A small induction solenoid was wound upon the middle portions of the tube.

An identical solenoid was wound on a similar but empty copper tube. The two tubes were then mounted parallel and close together between mica strips in a brass clamp. The latter was attached to the lower end of a vertical brass rod supported in a brass guide, so that the tubes were symmetrically placed between the pole-pieces of the magnet. The brass rod could be turned about its axis through exactly 180° by means of a special handle provided with stops. The tubes were immersed in a bath of oil which was electrically heated and stirred,

* L. F. Bates, *loc. cit.*

† L. F. Bates & B. Lloyd-Evans, Proc. Phys. Soc. xlv. p. 425 (1933).

the temperature of the bath being recorded by a mercury thermometer.

The two solenoids were joined in opposition and connected to the terminals of a sensitive ballistic galvanometer of long period. On turning the brass rod through 180° the magnetization of the specimen was reversed, and the deflexion of the ballistic galvanometer measured the magnetization in a known field. The deflexion was only a correct measure of the magnetization when the two solenoids were very accurately wound and placed exactly parallel. A correction in the case of imperfect mounting was obtained by noting the deflexion when the specimen was removed. In practice it was easier and sufficiently accurate to note the deflexion when the specimen was at a temperature some ten degrees above the Curie point, and to take this as a measure of the necessary correction.

As specimens of different lengths and diameters were used in these experiments it was considered desirable to calibrate the galvanometer for each of set experiments by using a specimen of pure nickel of approximately the same dimensions as the arsenide in the tube. For this purpose the saturation intensity of magnetization of pure nickel * was taken to be 500 c.g.s. units. An exact knowledge of the saturation intensity of magnetization of nickel was not of importance, for the arsenide specimens were cast, and therefore not of strictly uniform section, and some of them were porous ; the value 500 was taken to give a satisfactory guide.

The experiments on the arsenide rods were divided into two main groups, viz., the determination of the initial I, H curve for the specimen at room temperature and the determination of the variation of the intensity of magnetization for the specimen with temperature in fields of 5810 and 6360 gauss, corresponding to currents of 15 and 20 amperes respectively in the magnet coils. Actually little error appeared likely to arise from taking the deflexions with the higher field to be directly proportional to the intrinsic magnetization of the specimen, which, strictly, should be obtained by extrapolation to zero field.

* H. H. Potter, Phil. Mag. xii. p. 255 (1931), assumes this value ; R. Becker, *Zeit. für Phys.* lxiv. p. 673 (1930), assumes 483, the value given by P. Weiss.

In taking measurements in the immediate neighbourhood of the ferromagnetic Curie point a disturbance attributed to magneto-caloric effects, and described elsewhere *, was encountered to some small extent. It was then necessary to obtain a series of deflexions corresponding to successive rotations of the tubes through 180°. These deflexions were plotted in the same manner as a set of the successive amplitudes of a damped galvanometer could be plotted, and the deflexion in the absence of magneto-caloric effects was obtained by extrapolation in the same manner in which the amplitude of the first swing of the galvanometer in the absence of damping could be obtained graphically.

Except where otherwise stated the specimen was always cooled to 0° C. before a set of observations was commenced.

Results.

The most instructive set of curves was obtained with a specimen prepared in the same tube as specimen B*d* 2, referred to in the paper on thermoelectric measurements. This was made by introducing the tube containing the powdered arsenide into a furnace at 1000° C., after a certain amount of preliminary heating. The furnace was maintained at this temperature for about ten minutes, the furnace current was then reduced and the tube allowed to cool slowly *in situ*. As a small hole was open in the lower end of the furnace the lower end of the tube was somewhat cooler than the upper end. On opening the cold tube a series of short and polished rods coated with black powder was obtained, *i. e.*, some of the manganese had apparently volatilized.

The results of the magnetization measurements are reproduced in fig. 1. In this figure Curve I. was the curve obtained when the temperature of the specimen was raised for the first time after its preliminary cooling at 0° C. It shows that the intrinsic magnetization decreased more or less steadily until a temperature of nearly 44° C. was reached, when a very rapid decrease in the intrinsic magnetization occurred. After reaching the temperature 50° C. the specimen was allowed to

* L. F. Bates, Proc. Phys. Soc. xlii. p. 441 (1930).

cool slowly to room temperature; later it was cooled to 0° C.

The results which were obtained when next the temperature of this specimen was raised are shown on Curve II. This shows that a considerable increase in the intrinsic magnetization at low temperatures had occurred, and that the ferromagnetic Curie point, obtained by extra-

Fig. 1.

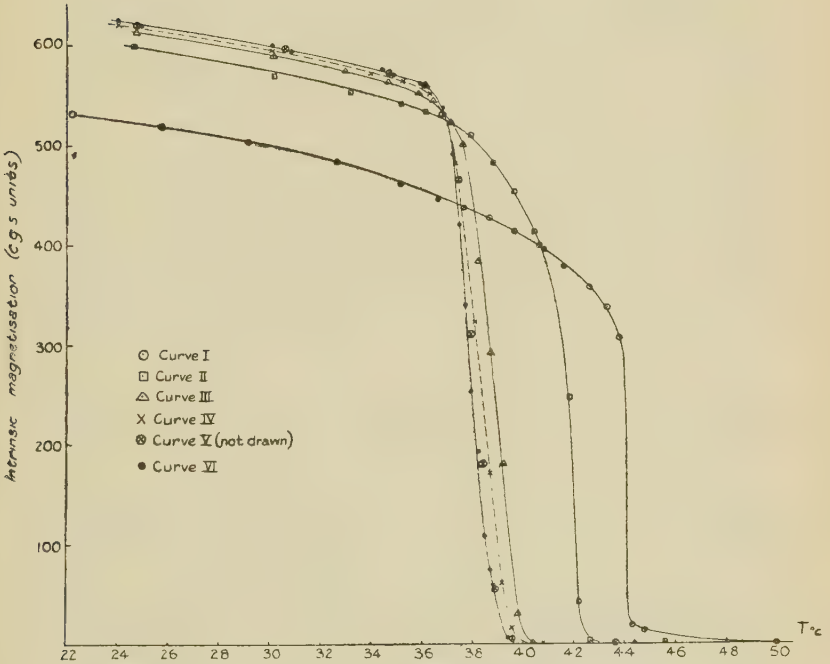

polation from the descending portion of the curve, had been lowered by about 2° C.

Once more the specimen was cooled slowly to 0° C., its temperature was then raised for a third time, and the results of Curve III. were obtained. In this case the intrinsic magnetization at low temperatures had only slightly increased over that of Curve II., but the loss of ferromagnetism commenced more abruptly, though it continued somewhat less rapidly, to become complete at a temperature some 2° C. lower than in Curve II.

In like manner the results of Curves IV. and V. were successively obtained. Again the intrinsic magnetization was slightly increased and the ferromagnetic Curie point was again lowered, but the changes were smaller. Curves IV. and V. were so nearly alike that it was obvious that some limiting curve was being approached. This limiting curve appears to be that obtained by quenching the specimen after the above changes have taken place.

Thus after the observations of Curve V. had been completed the specimen was cooled as quickly as possible from 50° to 0° C. When the temperature of the specimen was raised once more one set of points shown on Curve VI. was obtained. Here, again, the intrinsic magnetization at low temperatures was increased, but only very slightly increased, and the ferromagnetic Curie point was also very slightly lowered. Curve VI. was the final curve obtained ; slow cooling or rapid cooling from high to low temperature produced no further changes within the limits of experimental error ; in fact, two sets of results, obtained on successive days, are plotted on Curve VI.

Other specimens prepared in the same tube gave similar sets of curves, any appreciable differences being confined mainly to the first curve.

It should be recorded that the necessity for extrapolation to allow for the presence of magneto-caloric effects was always less in the case of Curve I. than in the cases of the remaining curves ; indeed, the need for extrapolation appeared steadily to increase with successive curves.

The I, H curves for the initial magnetization at room temperature (17° C.) for the specimen used for fig. 1 are shown in fig. 2. Here Curve A was obtained before Curve I. was recorded. Curve B was obtained after Curve I. and before Curve II. was taken. Curve III. was obtained after the two sets of results of Curve VI. had been obtained. The experimental arrangements were not suitable for the accurate measurement of the retentivity and of the coercive force. The retentivity was only about 5 per cent. of the saturation magnetization, whilst the coercive force was about 7·5 gauss. The main interest in these curves lies in the large fields required to cause the substance to show marked signs

of approaching saturation. It must, however, be recorded that the allowance for the demagnetization factor of the small specimen used was subject to some error, and the initial susceptibility cannot be obtained with great accuracy from such graphs.

A further series of experiments was made with another rod specimen of the same yield as specimen B*d* 2, which also had not been subjected to thermal treatment since its manufacture, in order to obtain information concerning the effect of cooling the substance to very low temperatures. It was first cooled to 0° C., and its

Fig. 2.

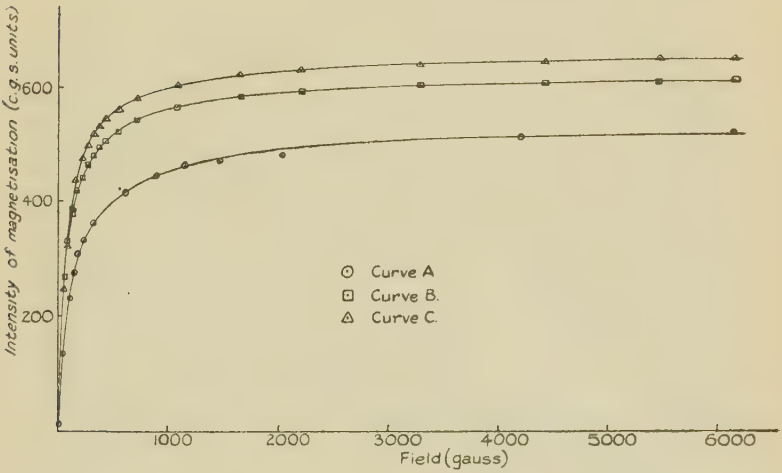

temperature was then raised to 18° C. At the latter temperature the specimen gave an intensity of magnetization of approximately 535 c.g.s. units in a field of 6360 gauss. It was then placed in liquid air, when it was found that the same field produced an intensity of magnetization of 803 c.g.s. units. The temperature was now raised to 18·0° C., when the intensity of magnetization was 611 units.

It was now heated to a temperature of 50·1° C., then rapidly cooled to 0° C. and again placed in liquid air. The intensity of magnetization was now 833 units. The difference between the two values at liquid-air temperature was therefore 30 units. Again the temperature was raised to 18° C., the new value of the

magnetization being 641 units; the difference between the last two values at 18° C., is 30 units. This meant that after the substance had undergone a transition from the ferromagnetic to the paramagnetic state the magnetizations at room temperature and at liquid-air temperature were increased by about the same amounts.

Finally, the temperature was raised to 50·1° C., the specimen was again rapidly cooled to 0° C., and then allowed to reach 18° C., when intensity of magnetization was 643 units. This meant that the second cooling to liquid-air temperature had produced but little additional change in the magnetic properties.

Comparison of Thermoelectric and Thermomagnetic Data.

In order to permit direct comparison of the thermoelectric and magnetic data the curves of fig. 3 are reproduced; most of them were previously published in the earlier communication. These curves are numbered in exactly the same manner as those of fig. 1; this means that, for example, Curve III. of each figure was obtained after the two specimens had received the same thermal treatment. It should be recalled that the curves of fig. 3 were obtained by measuring the thermoelectromotive force with respect to copper between two ends of the arsenide rod when the ends were maintained at specified temperatures differing by 2° C. In fig. 3 the thermoelectric power, obtained by dividing the thermoelectromotive force by the above temperature difference, viz., 2° C., is plotted against the temperature of the hotter arsenide-copper junction.

From a scrutiny of figs. 1 and 3 it is obvious that all the changes in thermoelectric power are intimately connected with the changes in intrinsic magnetization. It is most striking that whilst the intrinsic magnetization steadily increases to a maximum after successive transitions from the ferromagnetic to the paramagnetic state the difference between the thermoelectric powers in these two states steadily approaches a minimum.

By continuing the straight portions of the rapidly descending branches of the curves of fig. 3 to meet the more or less horizontal branches, representing the thermoelectric powers in the paramagnetic state, as shown

by the dotted lines of Curve VII., the temperatures at which the thermoelectric effects associated with ferromagnetism may be considered to have disappeared are obtained. These temperatures may be compared with the ferromagnetic Curie points obtained from the

Fig. 3.

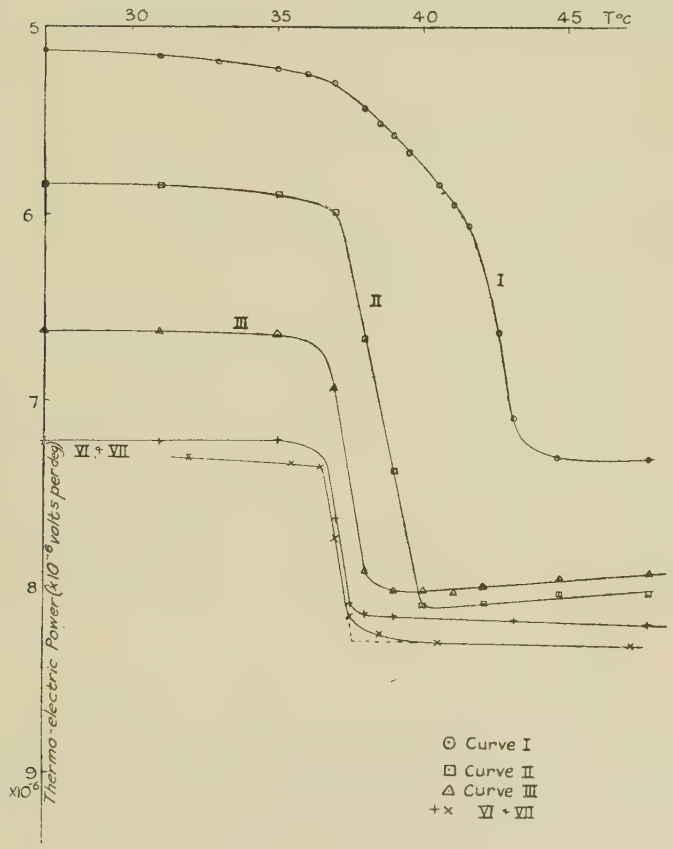

curves of fig. 1. Actually the latter temperatures are about 1° to 2° higher than the corresponding temperatures deduced from the curves of fig. 3.

It must be remembered that the thermoelectric and the magnetic measurements were made on different specimens, even though they were taken from the same

sample. There appears to be no doubt, however, that if it had been possible to make the two sets of measurements simultaneously with the same specimen, the two sets of curves would have been still more closely connected.

This view is substantially supported by the fact that the intrinsic magnetization curve of the specimen B*d* 2 itself gave a ferromagnetic Curie point at 37·4° C. This curve is reproduced in fig. 4; it was obtained after the specimen had been cooled suddenly from 50° to 0° C.

Fig. 4.

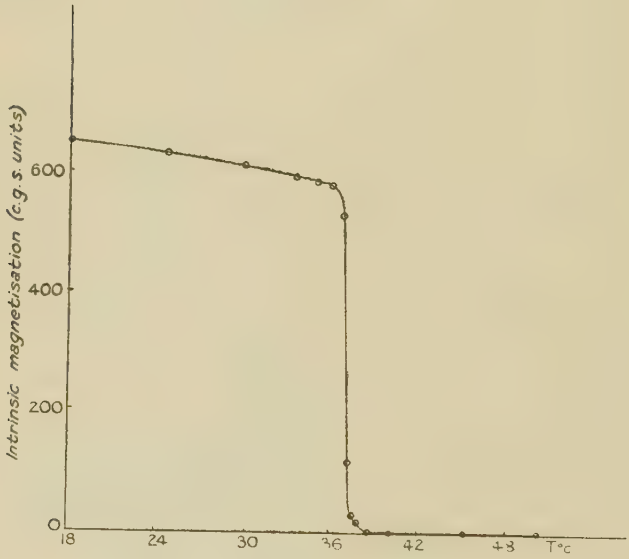

The corresponding temperature obtained by extrapolation from curves V. and VI. of fig. 3 is 37·6° C. The agreement here is as close as could be expected.

This view is further supported by the experiments with the rod A*a* described in the earlier paper. After the latter specimen had been suddenly cooled from 50° to 0° C. the ferromagnetic Curie point was found at 38·6° C.; the corresponding temperature deduced from the thermoelectric measurements was 38·3° C. Again, the ferromagnetic Curie point for another specimen,

AB*a* 1, which had been similarly treated was 39·6°, whilst the corresponding temperature derived from the thermoelectric measurements was 39·7° C.

Another specimen, AB*a* 2, gave a ferromagnetic Curie point at 38·4° C., whilst the temperature obtained from the thermoelectric measurements was 38·8° C. In this case the second temperature would be expected, on the above view, to be a little higher than the first, because this specimen was never rapidly cooled, and the curve of intrinsic magnetization was similar to Curve IV. of fig. 1.

In all the cases quoted the agreement is as good as could be expected, in view of the finite difference of temperature between the two junctions in the thermoelectric experiments, and particularly so when it is remembered within how small a temperature range the transition from the ferromagnetic to the paramagnetic state occurred.

In the earlier paper the thermoelectric power curves for a rod B*d* 1, also taken from the same yield as B*d* 2, were not well defined like those for B*d* 2. There is now little doubt that this divergence arose because of the presence of fissures in B*d* 1. This has been made clear by work on the resistance of such specimens, which, it is hoped, will shortly be published. The effect of fissures is to disturb the uniform fall of temperature along the rod, and thus give rise to incorrect values of the thermoelectric power calculated from the observations.

Discussion.

As a result of these experiments on manganese arsenide certain definite conclusions can be drawn.

There is no doubt that all freshly prepared specimens of the arsenide would exhibit a series of changes, consisting of a progressive increase in the intrinsic magnetization at low temperatures and a progressive lowering of the ferromagnetic Curie point, after successive transitions from the ferromagnetic to the paramagnetic state have occurred. Many freshly prepared specimens in addition to those described here were investigated, and in all cases a similar sequence of magnetic changes was observed. Similar changes were observed when

the freshly prepared specimen was powdered or was left in the form of a rod. It was possible that powdering a specimen lowered its ferromagnetic Curie point by a fraction of a degree, but this phenomenon was not fully investigated. Similar changes in magnetization occur when a freshly prepared specimen is cooled to a very low temperature.

The intrinsic magnetization curve obtained during the first transition of a specimen is much more like that for an ideal ferromagnetic than any subsequently obtained. Subsequent curves are characterized by much more abrupt changes from a state of high intrinsic magnetization to a state of low magnetization. In this connexion, too, it must be recorded that less extrapolation to allow for magnetic-caloric effects is necessary in the case of the first curve than in the cases of curves subsequently obtained.

Every change in the ferromagnetic properties is accompanied by a change in the thermoelectric properties. Incidentally the curve of thermoelectric power with temperature obtained when a freshly prepared specimen is first heated is much more like the curves obtained for nickel * than the curves subsequently obtained. In all cases the difference between the thermoelectric powers in the ferromagnetic and paramagnetic states decreases to a minimum with successive transitions, the thermoelectric power for the paramagnetic state often remaining more or less constant, although the intrinsic magnetization at low temperatures steadily increases to a maximum.

The greatest resemblance exists between the curves of thermoelectric power and those of intrinsic magnetization with temperature, when in the former the temperature of the hotter junction, and not the average temperature of the junctions, is plotted. This means that the abrupt changes in thermoelectric power cease when the temperature of the hotter junction reaches the ferromagnetic Curie point. On the whole the changes of thermoelectric power are more abrupt than the changes in magnetization, possibly owing to the finite temperature difference between the junctions.

* K. F. Grew, Phys. Rev. xli. p. 356 (1932).

It would appear that the irreversibility of the processes involved is responsible for these features, for with the passage of heat from the hot junction to the cold permanent changes in the magnetic condition arise in the neighbourhood of the ferromagnetic Curie point.

The maximum rate of change of the thermoelectric power with temperature occurs at the same temperature as the maximum rate of change of the square of the intrinsic magnetization with temperature within the limits of experimental error. It has been shown * that this is the temperature at which the specific heat of a ferromagnetic body is a maximum, as it should be in accordance with the Weiss hypothesis of an internal molecular field and the Heisenberg theory of ferromagnetism. Incidentally the powder used in the specific heat determination was in its final state, *i. e.*, the state reached after being rapidly cooled many times from 50° to 0° C., and the ferromagnetic Curie point was higher than the values recorded in this paper.

Several observers, in particular Smits, Gerding, and Vermast †, have noted a volume change as the arsenide is changed from the ferromagnetic to the paramagnetic state. No attention, however, has been paid to the volume changes exhibited by freshly prepared specimens during the first transition ; it would be most interesting to know whether the increase in intrinsic magnetization at low temperatures described above is accompanied by a permanent increase or decrease in volume of the arsenide. Dr. R. E. Gibbs has kindly informed me that his experiments with a single crystal show that there is no change in crystal structure as the substance passes through the ferromagnetic Curie point.

Finally, it is impossible to give any further explanation of the fact that some rod specimens of the arsenide exhibit a positive Thomson coefficient whilst others exhibit a negative one than that based on the assumption that the manganese atom can exist in different states in these specimens. It has been suggested that in one case the ferromagnetism is associated with "missing spins," and in the other with spinning electrons which

* L. F. Bates, Proc. Phys. Soc. xlii. p. 441 (1930).

† A. Smits, H. Gerding, & F. Vermast, *Zeit. für phys. chem.*, Bodenstein-Festschrift, p. 357 (1931).

are supposed present in each molecule of the arsenide; for if each molecule of a substance possesses an electron with an unbalanced spin moment, or if each molecule possesses an unbalanced spin moment due to a missing electron, ferromagnetisn will arise, but the thermo-electric effects will be different in the two cases. The data given in this paper require that each molecule shall possess three such electrons.

It is now generally accepted that ferromagnetic phenomena are due to the interactions (ss') of spinning electrons in neighbouring atoms. The Heisenberg theory based on this hypothesis has had a considerable amount of success, although it is well-known that it does not completely explain the behaviour of ferromagnetic materials in the immediate neighbourhood of their ferromagnetic Curie points.

A very careful survey of the theoretical aspects of the temperature variation of intrinsic magnetization and its associated properties has been made by Stoner *. He emphasizes the fact that in the case of nickel, for which accurate data exist, the intrinsic magnetization in the neighbourhood of the ferromagnetic Curie point is considerably greater than that postulated for an ideal ferromagnetic with three effective spins per five atoms, as required by low temperature measurements on nickel. He emphasizes, too, that the magneton numbers derived from low temperature saturation measurements with nickel are considerably less than those calculated from susceptibility measurements on nickel in the paramagnetic state.

To account for these facts Stoner supposes that the interaction (ls) between the spin s and the orbital moment l of the atom as a whole becomes more important as the temperature rises. He pictures the process as one corresponding to a change in a paramagnetic substance from a state in which the Weiss magneton number is

$$5\sqrt{4s.(s+1)} \quad \text{to} \quad 5\sqrt{4s.(s+1)+l.(l+1)}.$$

Such an interaction would, of course, be negligible in the case of an ideal ferromagnetic.

In addition the interactions (ls') between the orbital moment of one atom and the spin of another must also

* E. C. Stoner, Phil. Mag. xii. p. 737 (1931).

be taken into account. These, of course, become very small as the ferromagnetic Curie point is approached. It is this type of interaction which is held responsible for the fact that the intrinsic magnetization of nickel is rather greater than that attributed to an ideal ferromagnetic in the region of the Curie point.

It is now suggested that such *ls* and *ls'* interactions are responsible for the magnetic changes which are observed when freshly prepared specimens of manganese arsenide are taken through successive transitions as described above. It is suggested that during the large volume changes which occur during the transition from the ferromagnetic to the paramagnetic state a rearrangement of the electronic configuration takes place, so that when the specimen is cooled the *ss'*, *ls*, and *ls'* interactions are all increased. Consequently there is an increase in the intrinsic magnetization of the arsenide, and presumably it is the increase in the *ls'* interactions which gives successive magnetization and thermoelectric power curves their peculiar forms.

When the arsenide passes from the ferromagnetic to the paramagnetic state a large decrease in volume occurs. Obviously the substance is subjected to considerable internal strain, otherwise the observed temperature hysteresis of magnetization would not occur. Now it is noteworthy that permanent increases in the magnetization also occur when the freshly prepared substance is cooled from room temperature to the temperature of liquid air. In this case too a considerable contraction of the substance must take place and strains be set up. Consequently the changes in intrinsic magnetization occur as a result of the contractions, either on cooling to low temperatures or on passing from the ferromagnetic to the paramagnetic state. This explains why Curve I. of fig. 1 is more like that for an ideal ferromagnetic than the succeeding curves, for on the first cooling to 0° C. after its preparation at high temperature the arsenide is not suddenly subjected to the large contraction which occurs when the substance is later raised through the ferromagnetic Curie point.

Consequently it would seem that the ferromagnetism of manganese arsenide depends on the distance of closest approach of the atoms of manganese. Such an effect does not appear to have been fully considered

in recent theories of ferromagnetism. It suggests that the constant of the internal field postulated by Weiss must vary with the volume, and therefore with temperature, particularly in regions where the volume changes are considerable. Moreover, if these suggestions are correct then the value of the gyromagnetic ratio for the arsenide at room temperature should depend upon the thermal treatment to which it has been subjected. For the freshly prepared substance a value of the splitting factor $g=2$ would be expected; for the substance after sudden cooling from the paramagnetic to the ferromagnetic state a value of g somewhat less than 2 would be expected. It would be most interesting to have measurements of the gyromagnetic ratio for the arsenide in the two conditions, particularly in view of the fact that the extraordinary value of $g=0{\cdot}5$ has recently been found in the case of pyrrhotite *.

Summary.

The magnetic properties of some rods of manganese arsenide, prepared for the investigation of the thermoelectric properties of the substance, have been examined. It is found that each specimen which has not been heated since its preparation is ferromagnetic up to a temperature of about 45° C. Such a specimen exhibits a series of changes in its magnetic properties following each transition from the ferromagnetic to the paramagnetic state, until a steady condition is reached.

The changes consist of a progressive increase in the intrinsic magnetization and a progressive lowering of the ferromagnetic Curie point. They are intimately connected with corresponding changes in the thermoelectric power of the substance previously recorded. They are interpreted on the basis of an interaction between the spin moment of one atom and an orbital moment of another.

I am much indebted to the Government Grants Committee of the Royal Society for a grant which entirely covered the cost of the magnet used in these investigations. I also record my thanks to Professor E. N. da C. Andrade for the many facilities afforded me.

* Ludloff & Reymann, *Phys. Zeit.* xxxiv. p. 233 (1933).

LVII. *The Clean-up of Hydrogen by Magnesium.* By A. L. Reimann, *B.Sc.*, *Ph.D.*, *F.Inst.P.* (Communication from the Research Staff of the M.O.Valve Company, Limited *.)

Abstract.

1. A clean surface of magnesium will absorb at room-temperature something like one out of every one and a half million molecules of hydrogen incident on it. The hydrogen thus absorbed ("contact-gettered") only temporarily contaminates the surface, diffusing inwards at an appreciable rate. While the contamination lasts, however, it retards the absorption of further hydrogen.

2. Hydrogen is also cleaned up during slow dispersal of magnesium from a heated source within the vacuum vessel. There is no evidence that this is anything other than contact-gettering by a series of freshly formed surfaces.

3. Magnesium contact-getters atomic hydrogen enormously faster than ordinary molecular hydrogen.

4. The clean-up of hydrogen on to a magnesium film may be greatly accelerated by passing an ionizing electric discharge through the gas. This effect is due to the formation of atomic hydrogen from the H_2^+ ions when they are neutralized and to the relatively high rate at which atomic hydrogen is contact-gettered.

5. The quantity of hydrogen that may be taken up by magnesium is very great. At the end of a series of experiments carried out with one getter deposit it contained about one-sixth or one-seventh as many hydrogen atoms as magnesium atoms.

6. Gettered hydrogen may be re evolved from magnesium owing to a "vapour pressure" exerted by the cleaned-up gas. This vapour pressure varies rapidly with concentration and temperature.

7. Gettered hydrogen is also reliberated when the magnesium is bombarded by electrons or by CO^+ ions. In the case of electron bombardment, the effect has been observed with velocities of impact as low as 4 volts.

---

* Communicated by C. C. Paterson, M.I.E.E.

Introduction.

AN important process in high-vacuum technique is the "clean-up" of residual gases by various solid substances known as "getters." Of these, such electropositive metals as magnesium, calcium, barium, and sodium are among the most efficient.

There are several distinct ways in which a getter may clean up a gas. The getter is usually volatilized or "dispersed" from a small piece, welded or otherwise attached to a suitable carrier, whereupon it condenses upon the colder parts of the vacuum vessel, such as the glass walls. A gas may be cleaned up either during the dispersal of the getter ("dispersal-gettering"), or subsequently. Clean-up after dispersal may occur through mere contact of the getter deposit with the gas ("contact-gettering"), but in general it takes place much more rapidly when a suitable electric discharge is passed through the gas ("electric-discharge gettering").

A gas may in certain circumstances be reliberated from a getter deposit after having been cleaned up by it. This may occur either (*a*) on account of a "vapour pressure" of the gas if dissolved or of a dissociation pressure if chemically combined, or (*b*) in consequence of electron or ion bombardment.

Preliminary experiments having indicated that hydrogen may be gettered by and reliberated from magnesium in at least most of the ways enumerated above, it was decided to undertake a more detailed study of the phenomena with this getter-gas pair.

The Apparatus.

A small bulb B (fig. 1), containing the magnesium, and a sensitive Pirani manometer M were joined together by wide tubing. To this was joined a short piece of narrower tubing, ending in a palladium tube Pd. The volume of the whole was 145 c.c.

Within the bulb B was mounted an oxide-coated filament F close to a nickel mesh anode A and a nickel disk D (previously outgassed), to whose surface was welded a small piece of magnesium (also previously outgassed). The magnesium was cut from a ribbon found by spectroscopic analysis to contain not more than about 0·1 per cent. of

impurity, this being mainly calcium. The disk was so arranged that by suitably tilting the apparatus it could be made to take up either of the positions 1 or 2. This made it possible to heat the anode by high-frequency induction without at the same time dispersing the magnesium from the disc (in the position 2).

Fig. 1.

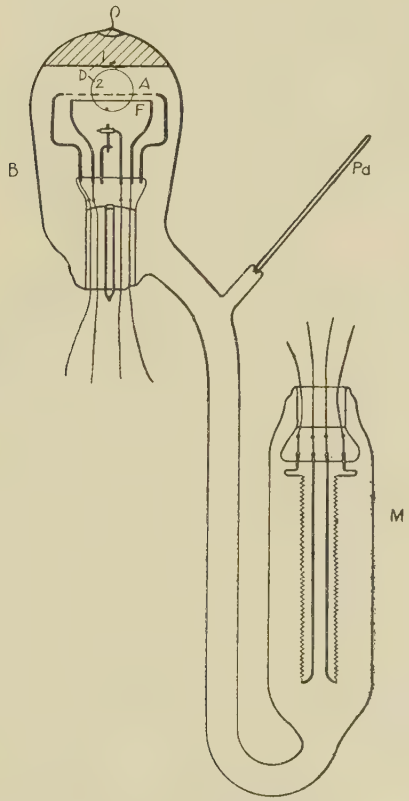

Apparatus used for the study of the gettering of hydrogen by magnesium.

The Pirani manometer consisted of a tubular bulb containing two independent stabilized tungsten spiral filaments, each of 0·047 mm. diameter wire, of 28 cm. length, wound into a spiral 0·9 mm. in diameter and 6 cm. in length. Each filament was flashed in a vacuum at 20 volts

for ten minutes prior to use. The tube M was clamped to a similar evacuated and sealed-off tube (not shown), and both were immersed in a water-bath at room-temperature. The filaments in each bulb were connected up to form opposite arms of a Wheatstone bridge, across whose ends a P.D. of 2 volts was maintained. The bridge was balanced with a good vacuum in the tube M by adjusting a very small variable resistance inserted in one arm, and the " out-of-balance " current in a microammeter was then taken as a measure of pressure. By inserting a resistance in series with the microammeter the manometer could be made less sensitive. The manometer was calibrated for each of two sensitivities by means of a McLeod. When set at the higher sensitivity, pressures as low as 2×10^{-6} mm. of Hg could be read with it. This form of Pirani manometer was developed by Mr. LeRossignol, of these Laboratories.

After the apparatus had been pumped and baked, and the electrodes and palladium tube outgassed, the tube connecting it to the pump was bent by carefully heating it in a flame until the getter-disc was brought into the position 1, whereupon it was gently heated by high-frequency induction and a film of magnesium caused to cover the top of the bulb. The area covered was about 15 cm.^{2} The apparatus was then sealed off.

In the centre of the patch of magnesium it made contact with a wire sealed into the wall of the bulb. This wire, which was of copper-clad nickel-iron, originally came right through the glass, the latter projecting inwards a little where it did so. The projection (glass and wire) was then ground down and polished. In this way the end surface of the wire was made continuous with the surface of the glass and good contact with the magnesium thus provided for.

Contact-gettering.

Upon now admitting a little hydrogen (from the reducing part of a coal-gas flame) through the palladium tube, the absorption curve 1 in fig. 2 was obtained. The disc was now bombarded with electrons from the coated filament until the old deposit of magnesium was covered over by a fresh one. Successive further doses of hydrogen admitted to the apparatus were now absorbed, as shown

by curves 2, 3, and 4. The phenomenal increase in the rate of absorption of the later doses can only be attributed to the fact that the first magnesium surface had been exposed to seal-off gas, whereas the second, formed under

Fig. 2.

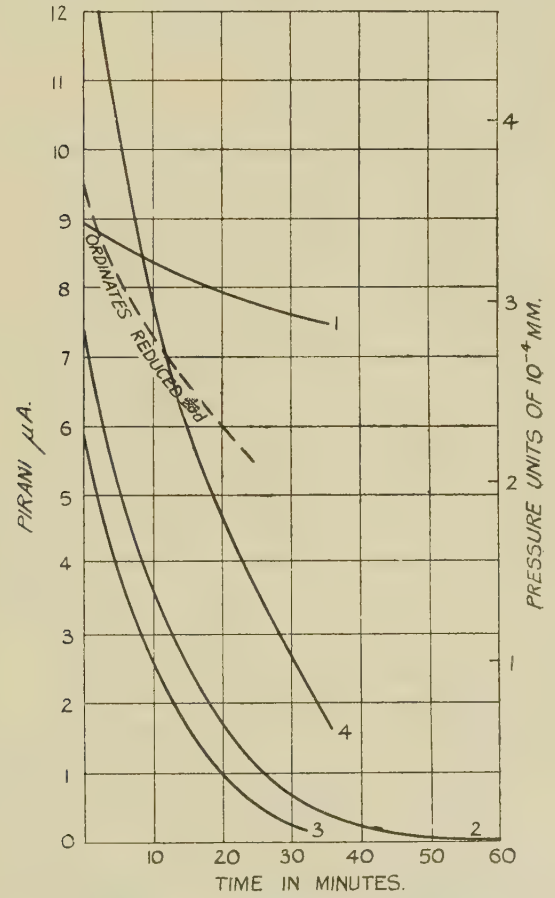

Dependence of absorption of hydrogen by Mg on state of surface.

ideally clean conditions, had not. The effect of glass-gas contamination in slowing down the rate of absorption of hydrogen was clearly demonstrated in a separate series of experiments.

A closer examination of the curves 2, 3 and 4 reveals the fact that the *relative* rate of fall of pressure, $-\frac{1}{p}\frac{dp}{dt}$, increases as the pressure diminishes. This must be due to the limited rate at which diffusion into the interior occurs. We have a plausible picture of a mechanism if we think of the observed rate of pressure fall as the rate of *adsorption* of hydrogen by the surface and imagine the adsorbed gas to be thereupon *absorbed*, *i.e.*, to diffuse into the interior of the getter-film. The rate of adsorption must depend on the state of the surface at the moment, *i. e.*, upon the instantaneous surface-concentration of adsorbed gas. This will be least (and the relative rate of further adsorption therefore greatest) when diffusion is best able to cope with the gas condensed, thus maintaining a nearly clean state of the surface.

A further illustration of the dependence of the relative rate of pressure decrease upon the pressure is given by the dashed curve in fig. 2, whose ordinates are reduced 1/20. The relative rate of pressure decrease is here markedly less than in curves 2, 3, and 4. This is not due to its having been taken after the last-named curves, for curves taken still later with smaller pressures again fell as steeply as 2, 3, and 4. It is interesting to note that immediately after admission of the hydrogen at the higher pressure the steepness compared with that of curves 2, 3, and 4, but soon fell away. Perhaps the most striking manifestation of such "fatigue" is that which may be observed immediately after a period in which the gas has been made to clean up at an abnormally rapid rate, *e. g.*, after an ionizing electric discharge. This is illustrated by the curve of fig. 3. The parts C of this curve represent simple contact absorption and the parts D electric-discharge clean-up. It will be observed how the parts C, after the first one, are convex upward, indicating gradual recovery from fatigue.

The magnesium exhibited no appreciable *permanent* fatigue as regards the speed with which it contact-gettered hydrogen after about 25 times as many hydrogen molecules had been absorbed as there were magnesium atoms on the surface. This, apart from any other evidence, shows what an important rôle diffusion into the interior of the getter-film must play.

The relative rates of pressure diminution given by the

lower parts of the curves 2, 3, and 4 of fig. 2 correspond to an absorption of about one hydrogen molecule out of every $1{\cdot}5\times10^6$ impinging on the getter-surface.

Dispersal-gettering.

This is not easy to observe. When the dispersal is fairly rapid, the pressure immediately after dispersal is

Fig. 3.

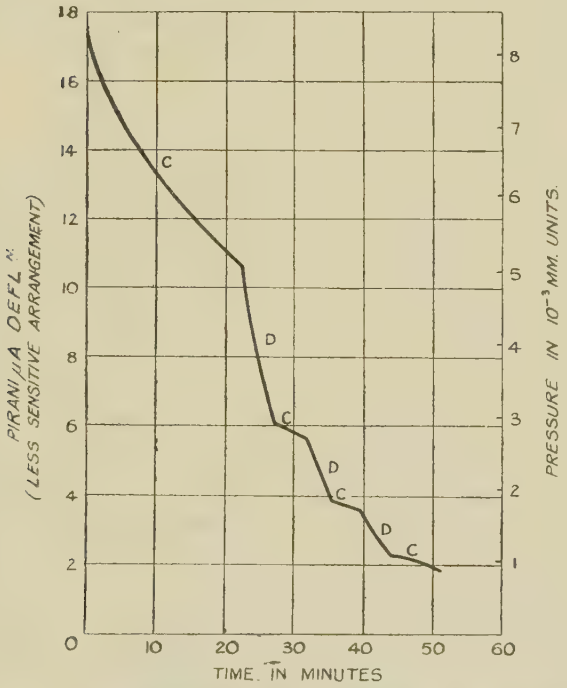

Fatigue in hydrogen absorption following electrical clean-up.

generally found to be greater, not less, than before. This is due to the fact that, even after the most careful outgassing, magnesium still contains *some* gas (mainly hydrogen), more of which is liberated during dispersal than is gettered. By carrying out the dispersal with extreme slowness, however, several minutes being taken over it, a diminution of pressure may be observed, in

spite of the gas-content of the magnesium. This is best done by welding the magnesium to a wire which is carefully heated by a current to disperse the magnesium. If the wire is fairly stout, dispersal occurs long before it reaches a visible red heat.

One would naturally expect any gas which is absorbed when in contact with a particular getter also to be cleaned up by it during slow dispersal, for in this the surface of the getter is being continually renewed, and can contact-getter at the maximum rate. There is no evidence that the dispersal-gettering of hydrogen by magnesium is anything other than contact-gettering by a series of freshly formed surfaces.

Contact-gettering of Atomic Hydrogen.

It is well known that hydrogen can exist in two forms—the ordinary molecular and the atomic. It has been shown by Langmuir and Mackay * and by Langmuir † that a convenient method of atomizing molecular hydrogen is to allow it to come into contact with an incandescent tungsten or other metal filament.

With an apparatus similar to that of fig. 1, except that the bulb B contained only a magnesium getter-disc and a tungsten filament, it was found, after the magnesium had been dispersed, that the rate of diminution of hydrogen pressure was enormously faster when the tungsten filament was alight than when it was not. From this it must be concluded that the contact-gettering of atomic hydrogen by magnesium is very much more rapid than that of ordinary molecular hydrogen.

Similarly, with the apparatus of fig. 1, it was at first found that the rate of contact-gettering was considerably higher when the coated filament was alight, even at only a dull red heat, and without any voltage being applied to the anode or getter, than when the filament was cold. The effect was observed to increase with the temperature of the filament. It could not have been due to a chemical combination between the hydrogen and anything on the filament, for the magnesium was obviously affected, exhibiting marked fatigue. It might still be imagined that

* I. Langmuir and G. M. J. Mackay, J. Am. Chem. Soc. xxxvi. p. 1708 (1914).

† I. Langmuir, *ibid.* xxxvii. p. 417 (1915); xxxviii. p. 1145 (1916).

the hydrogen became oxidized through contact with the filament, and that the resulting water-vapour simply "poisoned" the getter. That this was not the case, however, was shown by the fact that after a period of rest the magnesium was found to have completely recovered its original gettering power, whereas recovery after water-vapour poisoning has never been observed to occur. The only plausible explanation of the effect would appear to be that a glowing oxide-coated filament, like a hot tungsten filament, may, at least in certain circumstances, convert molecular into atomic hydrogen.

It was at first feared that this effect might seriously mask the discharge clean-up and render quantitative observations of the latter difficult or impossible. Fortunately, however, with progressive use of the filament it became a less and less efficient hydrogen atomizer at any given temperature, and at the same time it became thermionically more and more active—it started off rather badly in this respect. By taking advantage of the increased thermionic activity, and drawing electrons at progressively lower temperatures, it was presently found possible to eliminate altogether the atomization of the hydrogen by the filament.

Electric-discharge Gettering.

After the filament had been brought into a sufficiently active condition, a fresh film of magnesium was deposited on top of the old, by bombarding the disc.

Curves similar to that of fig. 3 were then obtained. In the parts C the filament was burnt at a very dull red heat and the anode and getter left floating, whilst in the parts D, in addition to the filament being alight, the anode was raised to a sufficiently high potential to cause ionization (*e. g.*, in the actual case of fig. 3, 23 V.), and the getter was held at a slightly negative potential (-5 V.) to prevent electrons from reaching it.

It was found that the parts D of such curves were steeper than the parts C only when the anode potential exceeded 16 volts, which is the ionization potential of hydrogen. Below this potential switching on the anode had no effect on the rate of absorption of gas. This shows that for the discharge to accelerate the clean-up it is necessary for it to ionize the gas.

Considering these phenomena qualitatively, one would naturally suppose that the particles (ions) it is necessary to form in order that discharge-gettering shall occur must reach the getter-surface, *i. e.*, that the discharge cleans up the gas simply by virtue of the absorption of positive ions by the getter. A few simple measurements at once show, however, that this cannot be the case. By inserting a galvanometer in the getter-film circuit the rate of collection of positive charge by the getter can be measured, and from this it is easy to calculate the number of positive ions arriving at the getter-surface per second; and from the increase in the rate of fall of pressure due to the discharge the number of hydrogen molecules cleaned up per second by the discharge may also be calculated. If the discharge-gettering of hydrogen were simply due to the absorption of positive ions by the magnesium, the two numbers should be equal. It is actually found, however, that the number of molecules cleaned up by virtue of the discharge always exceeds the number of positive ions collected by the getter, and sometimes by a large factor. By changing the anode potential from 102 to 23 volts, the number of molecules cleaned up by the discharge per ion collected by the magnesium was found to increase from about 2 to 70. The geometry of the tube was such that as the anode potential was decreased the fraction of the total number of ions formed that was collected by the getter must necessarily also have decreased. It would appear, then, that the thing that really matters in the discharge-gettering of hydrogen is the total number of ions *formed*, not where they are neutralized.

If neutralization consisted in merely converting H_2^+ back into H_2 this conclusion would obviously be absurd. It can be upheld only by supposing that what is gettered as a result of the discharge, while electrically neutral, is different from H_2, and that it is formed as a by-product of ionization. There seems only one thing that this can possibly be, and that is atomic H.

We are confirmed in this conclusion not only by the already established fact that magnesium contact-getters atomic hydrogen enormously faster than it does molecular, but also by published work on the ionization of hydrogen*.

* H. D. Smythe, Phys. Rev. xxv. p. 452 (1925).

Accordiug to this, the H_2^+, which is the only primary product of ionization, and which is formed at about 16 volts, is nearly unstable. When it collides with another molecule either of two things may happen, The $H_2^+ + H_2$ may form $H_3^+ + H$, or—and this happens much more frequently—the H_2^+ simply breaks up into $H^+ + H$. In the present case the only collisions with which we are concerned are those with either the emitting filament or the magnesium film, the free paths being much too long for an important number of collisions with hydrogen molecules to occur. We have, therefore, only to assume that *any* collision, *i. e.*, not only one with a hydrogen molecule, will break up the nearly unstable H_2^+, to have a completely satisfactory theory of hydrogen discharge-gettering. The H^+ formed will, of course, be immediately neutralized at the electrode where the collision occurs, so that as the final product formed from our H_2^+ we have two neutral hydrogen atoms.

Non-electrical Re-evolution of Gettered Hydrogen.

After a sufficiently prolonged and rapid discharge clean-up, resulting in a high concentration of dissolved hydrogen in the region of the surface of the getter-deposit, a re-evolution of gas may be observed when the discharge is stopped. A pressure-time curve for such a case is shown in fig. 4. The curve AB represents the last part of a prolonged discharge clean-up, the anode potential being 100 volts and the space-current 3 mA. On the discharge now being stopped, the pressure rose as shown by the curve BC. The discharge was then switched on again, the anode potential and space-current being the same as before. This gave rise to the clean-up represented by the curve CD. On the filament now being dimmed, so as to pass only 0·5 mA. instead of 3 mA., with the anode potential still equal to 100 volts, the pressure rose again, as shown by DE. Finally, the discharge was stopped again, and this resulted in the further rise of pressure represented by EF. The flattening out of the curve EF occurs at a lower pressure than that of BC, presumably owing to the diffusion of hydrogen to more deep-seated parts of the getter-deposit which had taken place in the interval.

The rate of re-evolution of gettered hydrogen varies strongly with temperature as well as with concentration. This is shown in fig. 5, where the hydrogen pressure of

Fig. 4.

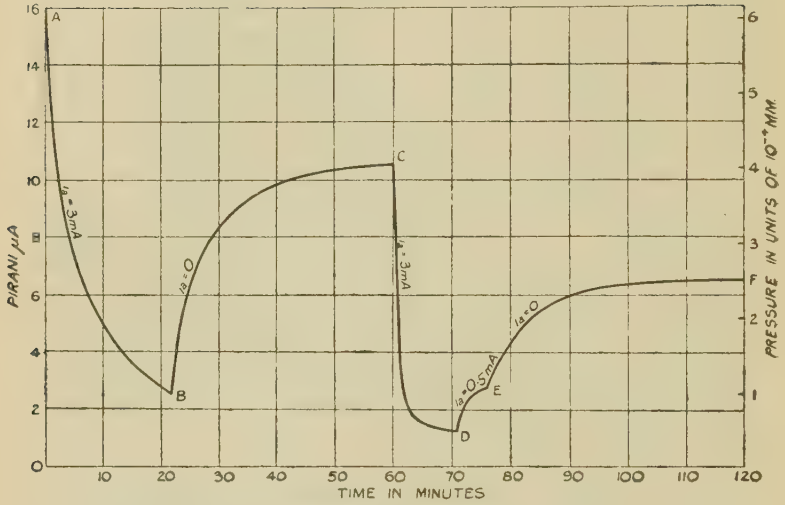

Re-evolution of gettered hydrogen at room-temperature.

Fig. 5.

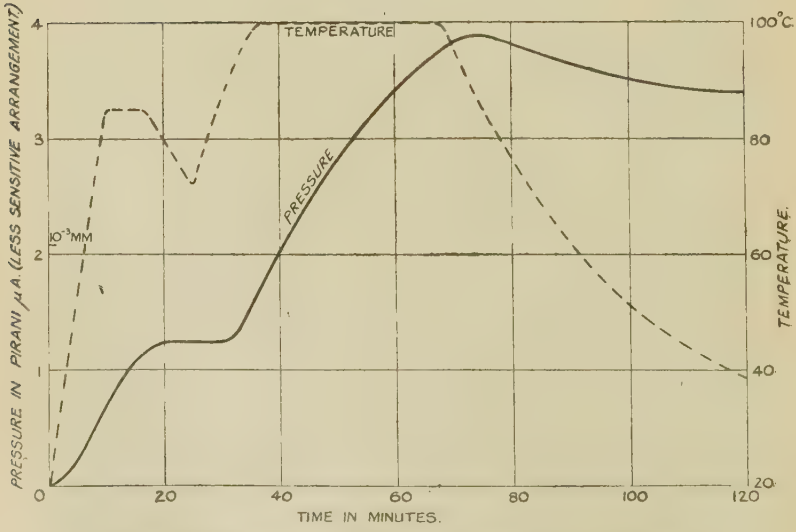

Temperature-dependence of "vapour pressure" of hydrogen in magnesium.

a magnesium film which had cleaned up a total of something like one hydrogen atom for every six or seven magnesium atoms in the film is plotted as a function of temperature and time. It will be observed that a state of true equilibrium was not at any time reached, owing, no doubt, to the slowness of diffusion.

Liberation of Gettered Hydrogen by Electron and Ion Bombardment.

After a considerable quantity of hydrogen had been cleaned up by the magnesium, a discharge was passed with the anode and getter-film both held at 10 volts positive to the filament. This gave rise to a rapid increase of pressure.

It should be noted that this liberation of hydrogen by bombardment could not have been due to mere heating of the getter-film. The energy dissipated by bombardment over the whole surface area of the film ($\sim$15 cm.^{2}) was only of the order of a milliwatt, and this could not have brought about a perceptible increase in the temperature.

Upon the bombardment being continued, and successive accumulations of hydrogen diffused out through the palladium tube, the rate of evolution showed a marked falling off. After allowing the apparatus to rest for two days, however, and then repeating the bombardment under the same conditions, the rate of liberation was found to have increased somewhat. These "fatigue" and "recovery" phenomena have an obvious explanation in terms of diffusion of hydrogen from deep-seated parts of the magnesium film to the surface.

With the apparatus used, the presence of the anode between the filament and getter-film prevented appreciable getter-currents from being passed with electron velocities below about 4 volts. It was possible to detect a liberation of hydrogen down to bombarding velocities as low as this, however.

Not only electrons, but apparently also positive ions, may dislodge hydrogen from magnesium. A small vessel containing CO was attached to an apparatus similar to that of fig. 1, but actual communication prevented by a thin-walled glass partition, and an iron armature was

mounted inside the vessel in such a way that it could be made to break the partition by means of an electro-magnet. After the magnesium film had cleaned up a considerable quantity of hydrogen the partition was broken and CO thus admitted to the discharge vessel. On now passing a discharge in the CO with the anode at +24 volts and the getter-film at −5 volts with respect to the filament, the CO began to be cleaned up, but at the same time a rapid evolution of hydrogen from the magnesium occurred. In one such experiment the liberation of hydrogen from the magnesium was so rapid that, in spite of the clean-up of the CO, the total gas-pressure actually increased. It cannot, perhaps, be definitely asserted that the hydrogen was not merely displaced from solution in the magnesium as the CO was gettered. In view, however, of the relative slowness with which the clean-up of CO occurred, it would appear much more likely that the hydrogen was actually dislodged by the impacts of the CO^+ ions.

The author desires to tender his acknowledgement to the General Electric Company and the Marconiphone Company, on whose behalf the work was done which has led to this publication.

LVIII. *Experiments on the Photographic Effect of X-Rays.* *By* G. W. Brindley, *M.Sc.*, *and* F. W. Spiers, *Ph.D.*, *Physics Department, University of Leeds* *.

1. *Introduction.*

In measuring the intensity of reflexion of X-rays by photographic methods it is of fundamental importance to know exactly how the density of photographic blackening varies with the intensity of the radiation. It has generally been assumed that when the density is not too great there is a linear relation between the intensity and the density, but for greater densities this linear law no longer holds good. Since there are obvious advantages in working in the region where the linear relation is satisfied, we have carried

* Communicated by Prof. R. Whiddington, F.R.S.

out a series of experiments to determine how exactly the linear relation holds and also at what point the relation ceases to be linear.

The density D of photographic blackening is defined by the equation

$$D = \log_{10} (L_0/L),$$

where L_0 and L are respectively the intensities of light passing through the unblackened and through the blackened part of the photographic film or plate. For visible radiation the density D varies with the intensity I and the exposure time t according to the Schwarzschild law,

$$D = f(It^p),$$

where the index p is less than unity. For X-radiation Bouwers *, Glocker and Traube †, and others have shown that p is practically equal to unity; Bouwers, for example, gives $p = 0{\cdot}99 \pm 0{\cdot}02$. For X-radiation, therefore, we have

$$D = f(It).$$

The form of the function $f(It)$ has been examined in particular by Bouwers for a wide range of values of D, I, and t, and he finds that the equation

$$D = C \log (It/a + 1)$$

holds with considerable exactness up to densities as great as 3. In this equation C and a are constants; C is independent of the wave-length, but increases asymptotically with the time of development. For small densities, however, $D < 1$, the results given by Bouwers do not agree, even approximately, with a linear relation either between D and I or between D and t. It is, therefore, a matter of some importance to investigate whether the assumption of a linear relation between D and I has any real justification.

2. *Experimental.*

We have carried out two kinds of experiments: one in which the time of exposure has been varied and the intensity kept constant, and one in which the intensity

* A. Bouwers, *Zeit. f. Phys.* vol. xiv. p. 374 (1923).

† Glocker and Traube, *Phys. Zeit.* vol. xxii. p. 345 (1921). See also 'Photographic Photometry,' by Dobson, Griffith, and Harrison, ch. i. sect. 5, p. 25. Oxford (1926).

has been varied and the time of exposure kept constant. In both experiments MoKα radiation was used. This was obtained from a tube of the Shearer type fitted with a needle-valve pressure control. Monochromatic radiation was obtained by reflecting from a cleaved calcite crystal. The films (Ilford duplitized X-ray films) were developed under standard conditions in a vertical bath, and the densities were measured with a Cambridge recording microphotometer *. The films were mounted in a holder so that they were screened from all radiation except the reflected radiation, which was passed through a narrow slit.

For experiments of the first type the voltage and tube current were maintained constant while a series of exposures, varying from $\frac{1}{4}$ minute to about 6 minutes, were made on a strip of film. The exposed areas of the film, each about 5 mm. long and 1 mm. wide, were separated by small areas of unexposed film, so that the density of the exposed film could be measured with respect to that of the unexposed film. Typical results for a strip of Ilford film are shown in fig. 1. The curve between D and t passes through the origin and is linear up to a density of about 1·4 ; for higher densities the curve bends over and is in general agreement with the curves given by Bouwers.

In the second set of experiments the intensity of the radiation has been varied and the time of exposure kept constant. This has been done by previous workers by placing the film at different distances from the source of radiation, and calculating the relative intensities by means of the inverse square law. In the present experiments an absorption method has been used. This was made possible by the use of strictly monochromatic radiation. A number of films, each about 3 cm. by 2 cm., separated by pieces of thin black paper, were placed together in a holder normal to the path of the reflected X-ray beam, *and the films themselves provided the absorbing medium.* This method has the important advantage of making the results independent of variations in the intensity of the incident radiation, because all the films are exposed simultaneously. The linear absorption of the films was found to be of a very convenient magnitude for these experiments ; for example, in one

* This instrument was purchased out of a grant made to Professor Whiddington by the Royal Society.

experiment the photographic density of the first film was 1·50 and of the tenth film 0·27. After being exposed, the films were mounted vertically in a frame and were all developed together under standard conditions. The lines on the films were sharp and narrow and were photometered by a null method which gave the densities in terms of positions on a calibrated photographic wedge.

The following considerations show how such measure-

Fig. 1.

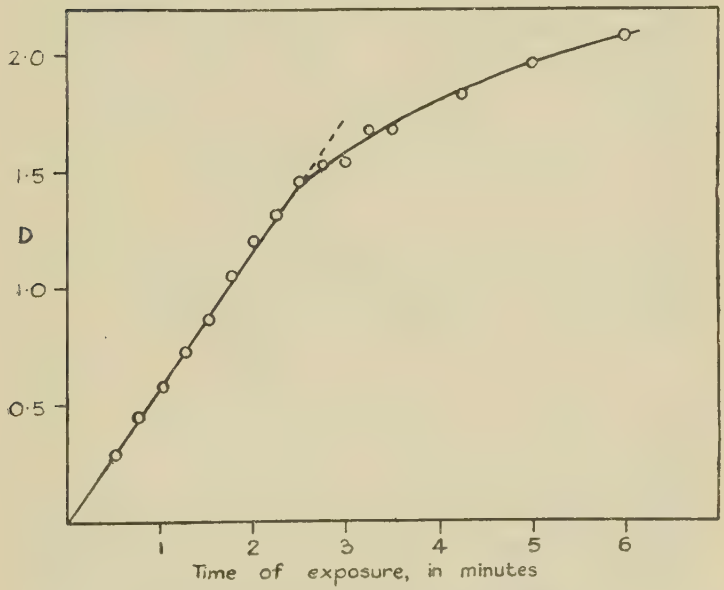

The variation of the density of photographic blackening with time of exposure.

ments determine the nature of the relationship between D and I. Let I_1 be the intensity falling on the first film and I_n that on the nth film. Then, assuming that absorption in the material of the film follows the usual exponential law, the radiation I_n, which has passed through $(n-1)$ films, is related to I_1 by the equation

$$I_n = I_1 e^{-\mu(n-1)x},$$

where x is the thickness of the films and μ the linear absorption coefficient for MoKα radiation. Then

$$\log I_n = \log I_1 - \mu(n-1)x.$$

It follows, therefore, that $\log I_n$ is a linear function of n.

Two special cases may be considered. Firstly, if D is proportional to I, then $\log D_n$ plotted against n should be a straight line. Secondly, if D is a linear function of $\log I_n$, then the graph D_n against n should be straight.

Fig. 2.

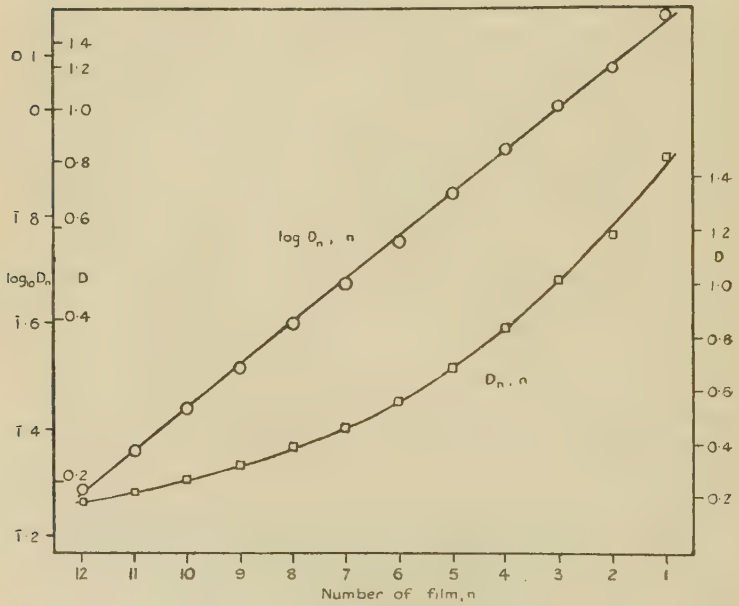

The variation of the density of photographic blackening with intensity of radiation.

In fig. 2 these graphs are plotted for a typical set of experimental results. The graph of $\log D_n$ against n is obviously linear, *showing that* D *is proportional to* I. The graph of D_n against n is a well-defined curve, showing that D is not a linear function of log I at small densities.

Further experiments have been made in which thin sheets of aluminium were interposed between photographic films, the sheets being approximately equal in absorbing power to two films. The graph of $\log D_n$

against n was again found to be straight and, taking into account the absorption of the photographic film, already measured, a reasonable value was obtained for the absorption coefficient of aluminium. These results showed that absorption in the photographic film follows the usual absorption law, and thereby justified the main assumption in the second part of the investigation.

3. *Summary.*

Experiments on the change of photographic density, due to monochromatic X-rays, show that the density is directly proportional to the intensity of the radiation and to the time of exposure, provided the density is not greater than about 1·4. The variation of D with I has been tested by an absorption method, in which the films themselves provide the absorbing medium; this method does not appear to have been used previously.

Finally, we would like to express our thanks to Professor Whiddington for his interest in these experiments and for providing the necessary facilities, and also to Mr. F. H. Partridge for assistance in photometering the films.

LIX. *On the Scattering of Gamma-Rays in Air and Water.*

By W. J. Rees, *M.Sc., and* L. H. Clark, *Ph.D., Surgical Unit, University College Hospital Medical School and Barnato Joel Laboratories, Middlesex Hospital*.*

IT is well known that the absorption of gamma-rays in matter is accompanied by the emission of corpuscular and scattered radiation from the substance irradiated. The radiations scattered in different directions from an irradiated medium have been investigated very fully, notably by Florance [1], Gray [2], and Compton[3]. It has been shown that the penetrating power of the scattered radiation diminishes as the scattering angle—that is, the

* Communicated by Prof. Sidney Russ, C.B.E., D.Sc.

angle between the primary and scattered ray—is increased. A question which has not been so fully dealt with, however, is the significance and quality of the scattered radiation reaching a point in a light and more or less extensive medium irradiated with gamma-rays. This physical problem has an important bearing on the subject of dosage in radium therapy, and is the one with which we are concerned in this paper. It is to be expected from Compton's theory of scattering [4] that the scattered radiation reaching any point in the medium would be heterogeneous. Evidence has been put forward by Bruzau [5] and by us [6] indicating that the scattered radiation traversing a small electroscope immersed in a tank full of water is definitely less penetrating than the primary gamma-rays. Ionization measurements of heterogeneous radiations may be complicated by the fact that the ionization chamber may be more sensitive to some wave-lengths than to others. If the walls of the chamber are made of aluminium, however, this effect is minimized. This paper describes an experimental investigation of radiations scattered from air and water made with an electroscope having thin walls of aluminium.

Apparatus.

Fig. 1 shows the arrangement of the apparatus. The electroscope was mounted at the centre of a large iron tank lined with asbestos sheets 0·75 cm. thick, which absorbed any soft radiation scattered from the metal walls. The source of gamma-rays, S, was mounted vertically above and at a considerable distance from the electroscope, E. The latter consisted of an aluminium cylinder 4 cm. long and 4 cm. in diameter, mounted at the end of a horizontal cylindrical aluminium casting, A. The wall of the electroscope was of aluminium 0·006 cm. thick, covered on the outside with a sheath of celluloid 0·025 cm. thick, whilst the wall of the aluminium casting was 0·3 cm. in thickness. Ionization readings were taken with a telemicroscope provided with an eye-piece scale, which was inserted into the aluminium casting, a small pea-lamp in the latter illuminating the gold-leaf system of the electroscope.

The source of gamma-rays, S, consisted of a number of radon seeds completely enclosed in a lead cylinder

1·9 cm. long and 1·2 cm. in diameter, having a wall of 0·3 cm. The lead cylinder was slipped into a brass cup which was suspended from the ceiling vertically above the centre of the electroscope and about 93 cm. from it. It was necessary to use powerful radon sources containing up to 0·5 Curie, as the ionization readings generally were small. The natural leak of the electroscope, however, was never more than 0·1 division per minute.

In some of the experiments the lead cylinder, L (fig. 1),

Fig. 1.

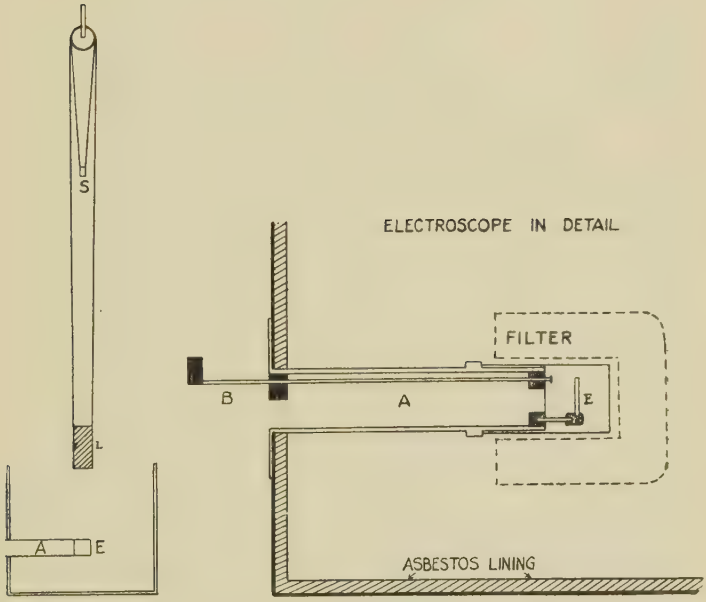

10 cm. in thickness, was placed between the source, S, and the electroscope, E. This lead filter practically eliminated the effect of the primary rays on the latter without intercepting the primary rays to the main volume of the medium in the tank.

Scattered Radiation from Air.

When the tank was empty the amount of radiation scattered into the electroscope from the air and its surroundings was considerable. Using a radon source

of 0·26 Curie it was found that the insertion of the lead filter, L, only reduced the ionization to 45 per cent. of the value obtained without it. Had the ionization been due entirely to the primary gamma radiation, absorption of these rays in 10 cm. of lead would have reduced their ionization effect to 0·67 per cent., that is, only one-seventieth of that actually found.

When the lead cylinder screened the electroscope from the primary rays the radiation entering the instrument was much less penetrating than when the cylinder was removed. This could be seen by comparing the reduction in ionization caused in each case by covering the electroscope with a cylindrical filter, with a closed end, of aluminium 0·16 cm. thick. With the lead cylinder in position—that is, when scattered radiation alone was operating—this aluminium filter reduced the ionization to 18·2 per cent., whereas without the lead cylinder the reduction amounted to less than 2 per cent. A test was made to determine whether the soft scattered radiations observed with the lead cylinder in position came from the latter. This consisted in measuring the penetrating power of the radiation entering the electroscope under two conditions. In the first any soft scattered radiation from the cylinder was allowed to operate, but in the second the cylinder was enclosed in a box of aluminium of thickness 0·5 cm., which would absorb any soft radiation from the lead. The test showed that neither the amount nor the penetrating power of the radiation entering the electroscope was affected by covering the lead cylinder in this way. It may be concluded then that this radiation is not scattered from the lead cylinder, but from the air.

Water was poured into the tank, and measurements were taken at various stages in the filling. The primary beam to the electroscope was eliminated by the 10 cm. lead cylinder, and the curve A in fig. 2 shows how the ionization in the electroscope varies as the tank is filled with water. The vertical lines P 1, P 2 show the levels of the top and bottom of the electroscope. It is seen that the ionization recorded is much greater when the electroscope is out of water than when it is immersed, and as the chamber is gradually covered with water the ionization rapidly falls to a minimum value. The position of the minimum value was found by adding only small quantities of water at a time, and occurs when 700 c.c. have

been added after the chamber has been covered, *i. e.*, when the chamber has been covered by a layer of water 0·51 cm. thick. As the water rises above this level the ionization increases to another maximum value, which occurs when the tank is very nearly full.

The above experiment was then carried out with various filters over the electroscope, and the curve B in fig. 2

Fig. 2.

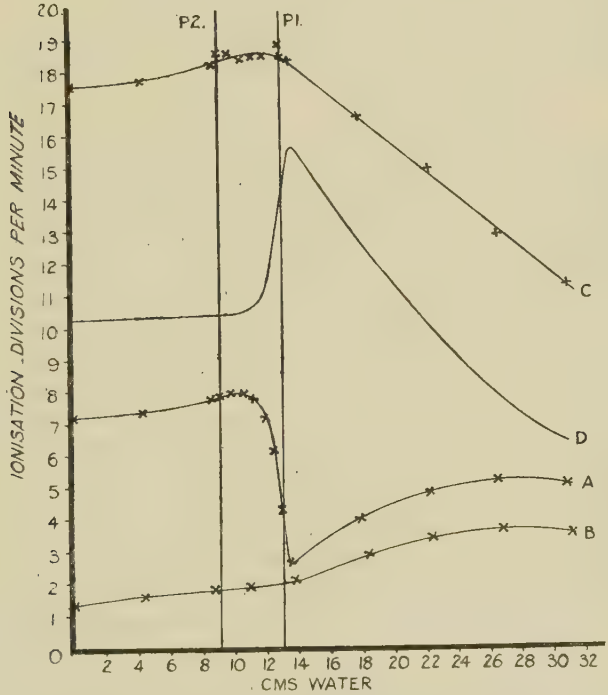

is for a filter of aluminium 0·34 cm. in thickness. It will be observed that the preliminary large ionization effect is entirely cut out by this filter, showing that the radiation scattered from air contains quite a large component of very soft radiations.

The initial experiment was repeated with the lead cylinder removed, and the curve C in fig. 2 was obtained. In this curve there is no sudden fall in the ionization when the electroscope is covered with water, although there is no filter round the electroscope and although

the case exactly corresponds to curve A except that the 10 cm. lead cylinder is removed from the primary beam. The introduction of the primary beam to the electroscope and its more immediate surrounding of water increases the ionization. The curve D was obtained by subtracting the values of curve A from those of curve C. Since the latter corresponds to the ionization effect of primary plus scattered radiation, and curve A to that of scattered radiation alone, the new curve D, which is the difference between the two, must give the ionization effect due to the primary rays and rays scattered from the cone of water which would lie within the shadow of the lead cylinder.

The new curve shows the following features :—Until the water reaches the electroscope the curve is practically horizontal, as would be expected, since the introduction of water under the electroscope cannot affect the primary radiation reaching the latter from above. As the water covers the chamber the ionization effect increases to a sharp maximum when the electroscope is covered by 5 mm. of water. This increase in ionization must be due to a soft radiation similar in penetrating power to that observed from air, and its presence has been previously masked by the fact that when the primary beam is cut out, the soft radiation produced is absorbed in the layers of water within the shadow of the lead cylinder and is entirely cut off from the electroscope. When, however, the lead cylinder is removed, the water in immediate contact with the electroscope is radiated by the primary rays, and the effect of the soft scattered radiation is observed. What a very considerable part these soft radiations play is judged from the fact that their effect is to increase the ionization by approximately 49 per cent. above that due to the unfiltered primary rays alone. This radiation will be present in all under-water measurements in which both the primary and scattered rays are operating.

A further consideration of curve D shows that after the maximum is passed—that is, after the chamber is covered by more than 0·5 cm. of water—the curve falls steeply as the depth of water increases, and over this region the absorption of the radiation is truly exponential. The coefficient of absorption of the radiation in water found from this part of the curve is 0·052 cm.$^{-1}$ The

value given by Bruzau [5] for the gamma-rays of radium, filtered by 0·5 mm. of platinum was 0·055 cm.$^{-1}$.

The Penetrating Power of the Scattered Radiations.

(A) *Radiations Scattered from Air.*

Measurements were made of the quality of the radiation entering the electroscope when the tank was empty and the primary beam to the electroscope intercepted by 10 cm. of lead. For this purpose cylindrical filters of aluminium and of copper, each provided with a closed end, were used, and these could be slipped over the electroscope. These filters ranged in thickness from 0·006 cm. to 2·9 cm.

It was necessary to replace the lead cylinder, L, by a filter of the same thickness but bigger lateral dimensions, to ensure that none of these new filters were struck by primary gamma-rays which had not first been filtered by 10 cm. of lead. The filter used consisted of a truncated lead pyramid having its apex at the source of radiation. The section of the filter was rectangular, measuring 8·5 by 7·8 cm. at the top and 10 by 9·1 cm. at the bottom. The cross-section of the shadow thrown by this filter around the electroscope was greater than that of the largest filter used. Experiments corresponding to those already described were carried out with the new lead filter, and results similar to those given were obtained. As the volume of the irradiated medium in the tank was reduced by replacing the lead cylinder L by the truncated lead pyramid, the ionization caused by the scattered radiation was less. To compensate for this loss more powerful radon sources amounting to 0·53 Curie were used.

In the first instance the penetrating power of the softer components of the radiation scattered from air was measured in aluminium and in copper. The thickest filter used in this experiment was one of aluminium 0·34 cm. thick. The values obtained are plotted on the curve in fig. 3, where the crosses refer to aluminium and the circles to copper filters. The density relation between these two metals has been used to convert each thickness of aluminium to the equivalent thickness of copper. The fact that all the points lie approximately on a single curve indicates that these softer scattered rays are

absorbed to the same extent by equivalent thicknesses of aluminium and copper. The following mass absorption coefficients were obtained for these rays :—

Copper. cm.	Range of thickness. μ/ρ.
0 –0·012	9·45
0·012–0·03	2·57
0·03 –0·052	1·31
0·052–0·103	0·147

Fig. 3.

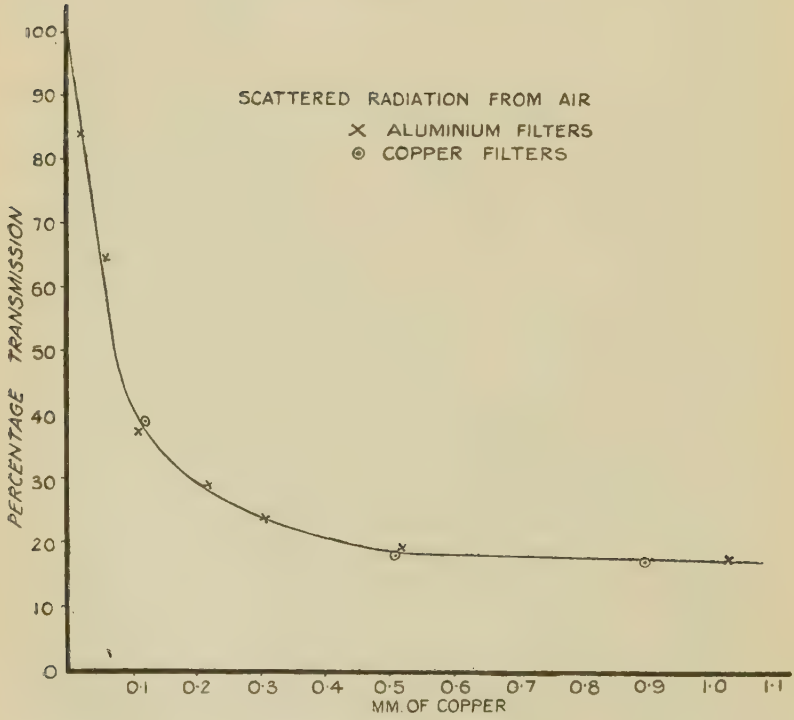

Much of this radiation is of the same order of penetrating power as the beta-rays of radium B+C.

The penetrating power of the harder constituents of the radiation scattered from air was then measured in aluminium and in copper. A cylindrical aluminium filter, 0·34 cm. in thickness, was slipped over the electroscope, and the ionization recorded under these conditions

was taken as 100 per cent. These absorption measurements therefore were made in what corresponds to an electroscope having walls of aluminium (0·34 +0·006) cm. thick. Aluminium of this thickness would be much more than sufficient to absorb any characteristic radiation from the copper filters for which μ/ρ in aluminium is 36 gm.$^{-1}$ cm.^{2} [7]. Curves A and B in fig. 4 show the apparent absorption of the harder scattered rays from air

Fig. 4.

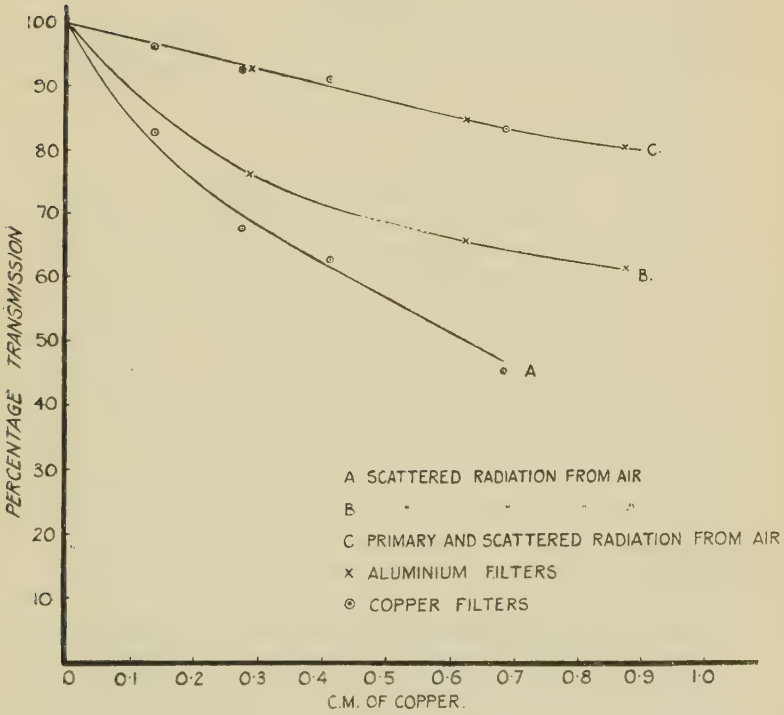

in copper and aluminium respectively. In curve B each thickness of aluminium has been reduced by the density relation to the equivalent thickness of copper. Radon sources of 0·53 Curie were used for these measurements. The values plotted were those obtained after allowance had been made for radiation entering the electroscope through the open end of the filter facing the telemicroscope (*vide* fig. 1). The fraction of the total radiation entering this end was calculated for the case when the electroscope

was surrounded by the cylindrical aluminium filter, 0·34 cm. thick, and amounted to 18 per cent. These more penetrating scattered radiations from air, unlike the softer components (*vide* fig. 3) are more easily absorbed in copper than in aluminium.

Absorption measurements in aluminium and copper were also made with no lead filter in the primary beam to the electroscope. Curve C in fig. 4 refers to this radiation, which consists of primary rays associated with scattered rays from air. In this instance primary gamma-rays predominate, and aluminium and copper appear to be equally absorbent to these rays. This finding is in agreement with the results of Ahmad [8] and Soddy & Russell [9].

(B) *Radiations Scattered from Water.*

The tank was then filled with water to within 4·5 cm. of the top. Under these conditions the ionization due to the scattered radiation from the water is a maximum. Absorption measurements were then made in aluminium and in copper for the condition in which the primary beam to the electroscope was filtered by the truncated lead pyramid. The effective thickness of the walls of the electroscope throughout these measurements was 0·346 cm. of aluminium. This experiments is therefore identical with the preceding one, except that the tank is now practically full of water. The scattered radiations from water were found to be absorbed to a greater extent in copper than in an equivalent thickness of aluminium. The apparent mass-absorption coefficients obtained from this and the preceding experiment when the tank was empty are given in the table on the following page.

The values for scattered radiations in columns 2 and 3, when compared with those in column 4 for primary and scattered radiation, serve to show the change in penetrating power of the radiation on scattering, as measured under our experimental conditions. We have been obliged to use cylindrical filters fitting closely to the electroscope, as scattered radiation entered the latter on all sides. The amount of scattered radiation from the filters under these conditions is considerable, as may be judged from the fact that our apparent absorption values for primary + scattered radiation are roughly one-half those of Ahmad [8]. As this is the case for both copper and aluminium filters

it suggests that the effect of scattered radiation from the filters on the mass-absorption coefficients is the same for these two metals.

Compton[10] and Ahmad[8] have suggested a method for estimating the effective wave-length of gamma-rays from absorption measurements of the radiation in two elements differing widely in atomic number. The effective wave-length is given by the expression

$$\lambda = \left\{ \frac{(\mu_{e.\mathrm{Cu}} - \mu_{e.\mathrm{Al}})}{\mathrm{K}(\mathrm{Z}_{\mathrm{Cu}}^3 - \mathrm{Z}_{\mathrm{Al}})} \right\}^{\frac{1}{3}},$$

Apparent Mass-absorption Coefficients of Scattered and Primary Rays.

Filter.	Scattered radiation from air.	Scattered radiation from water.	Primary + scattered radiation from air.
cm.	μ/ρ.	μ/ρ.	μ/ρ.
Aluminium :			
0 –0·96	0·11	0·14	0·027
0·96 –2·9	0·045	0·036	
Copper :			
0 –0·138	—	0·29	
0·138–0·4	—	0·14	
0 –0·276	0·15	—	0·026
0·276–0·69	0·11	—	
0·4 –0·69	—	0·049	

where λ is the wave-length of the radiation, $\mu_{e.\mathrm{Cu}}$ and $\mu_{e.\mathrm{Al}}$ are respectively the absorption per electron in copper and aluminium, K is a constant, and $\mathrm{Z_{Cu}}$ and $\mathrm{Z_{Al}}$ the atomic numbers of copper and aluminium respectively. This formula may, with certain reservations, be applied to our results. Considering first the scattered radiation from air, it is seen that there are two components (*vide* table). The softer is absorbed very nearly to the same extent in aluminium as in copper. This may be due to beta-rays, as the wall-thickness of the electroscope was insufficient to exclude them entirely. Over the range of filters equivalent to 0·3 to 0·9 cm. of copper, however, aluminium is much less absorbent than copper, and the

effective wave-length calculated for this range is 0·079 Å.U. In the case of the radiations scattered from water, calculations over the same range give an effective wave-length of 0·078 Å.U. The reservation on these values is that they represent a minimum wave-length for the scattered radiations we have measured. Correction for radiation scattered from the filters themselves may make the factor ($\mu_{e.Cu} - \mu_{e.Al}$) even as much as twice that obtained from our actual measurements. It is probable, therefore, that the effective wave-length of the harder scattered radiations from air and water lies between 0·08 and 0·10 Ångström units.

Conclusion.

It has been shown that when gamma-rays are scattered in air the scattered radiation is very heterogeneous, a considerable proportion having a penetrating power of the same order as that of the beta-rays of radium B+C. The softer scattered rays are absorbed to the same extent by equivalent thicknesses of aluminium and copper, as is the case with beta-rays. Moreover, they appear to differ in type from the harder constituents, which are more easily absorbed by copper than by aluminium.

In the case of radiations scattered from water evidence was obtained that some of the rays were completely absorbed in 3 to 4 millimetres of aluminium, indicating a radiation of similar penetrating power to the softer rays scattered in air. The harder constituents were more easily absorbed by copper than by aluminium.

Following a method suggested by Compton and by Ahmad, an estimate of the effective wave-length of the more penetrating scattered radiation from air and from water has been made from the apparent absorption values for these rays in aluminium and copper. It has been found that the effective wave-length of these rays lies between 0·08 and 0·10 Ångström units. For these rays the wave-length shift on scattering is then at least (0·08 − 0·017) = 0·063 Å.U., which exceeds the maximum predicted by Compton's theory, viz., 0·048 Å.U., for scattering at a single encounter with an electron. Our results suggest, therefore, that much of the radiation has undergone more than one scattering process. Moreover, the change in wave-length on scattering indicated by

our experiments is somewhat more than that suggested by Bruzau[5], who concluded that the effective wave-length of the scattered radiation from water was three times that of the primary rays.

We are indebted to the Medical Research Council for the powerful radon sources used, and wish to record our thanks to Professor Russ for his valuable advice and interest in the investigation.

References.

(1) Florance, Phil. Mag. xx. p. 921 (1910).
(2) Gray, Phil. Mag. xxvi. p. 611 (1913).
(3) Compton, A. H., Phil. Mag. xli. p. 749 (1921).
(4) Compton, A. H., Phil. Mag. xlvi. p. 897 (1923).
(5) Bruzau, M., *Ann. de Phys.* xi. p. 1 (1929).
(6) Rees & Clark, B. J. R. vol. v. new series, no. 53, p. 432 (1932).
(7) Compton, A. H., 'X-Rays and Electrons,' Chap. vi, pp. 185–190 (1927).
(8) Ahmad, N., Proc. Roy. Soc. cv. p. 507 (1924); cix. p. 206 (1925).
(9) Soddy & Russell, Phil. Mag. xviii. p. 646 (1909).
(10) Compton, A. H., 'X-Rays and Electrons,' p. 390 (1927).

LX. *A Rapid Method of Determining the Crystal Axes of Single Crystal Wires of certain Metals.* *By* R. Roscoe *and* P. J. Hutchings, *Carey Foster Research Laboratory, University College, London* *.

[Plate XVII.]

IN the course of some work on metal single crystals which we are carrying out under Professor E. N. da C. Andrade it is necessary to make frequent determinations of the crystal axes of wires which are stretched during the investigation, particularly wires of the hexagonal metal cadmium.

The elliptical slip-bands which appear on the surface of stretched single-crystal wires afford a means of determining the orientation of the crystal axes in the wire both as they were before stretch and as they are after stretch, provided :

(1) That the deformation of the wire takes place solely by glide and that only one set of parallel planes

* Communicated by Professor E. N. da C. Andrade.

is involved, in which case well-marked elliptical slip-bands develop. If the characteristic markings of double glide or twinning bands are frequent the method is not applicable.

(2) That the glide plane and the glide direction are already known in terms of the crystal axes. Thus for cadmium glide occurs on the basal hexagonal plane and in the direction of a digonal axis.

Let χ represent the angle between the axis of the wire and the glide plane, λ that between the axis of the wire and the glide direction, l the length of the wire, and let the suffix 0 denote values before the wire was stretched. Then

$$l_0 \sin \chi_0 = l \sin \chi, \quad . \quad . \quad . \quad . \quad . \quad (1)$$

$$l_0 \sin \lambda_0 = l \sin \lambda, \quad . \quad . \quad . \quad . \quad . \quad (2)$$

$$\cos \lambda_0 = \cos \chi_0 \cos \alpha, \quad . \quad . \quad . \quad . \quad (3)$$

where α is used to denote the angle between the major axis of the glide ellipse (the projection of the initial position of the axis of the wire upon the glide plane) and the direction of glide.

The angle χ can be measured directly under the microscope by turning the wire about its own axis, maintained perpendicular to the optic axis of the microscope and horizontal, until the slip-bands appear as straight lines, and measuring the angle between these lines and the axis of the wire. Although the method is useful for such metals as lead, which has a large mean separation between adjacent slip-bands ($4{\cdot}2\,\mu$), and which gives consequently very sharp ellipses for quite small extensions (10–20 per cent.), it is unsuitable for such metals as cadmium, which have a much smaller mean separation ($1{\cdot}0\,\mu$). In such cases much larger extensions are necessary, so that the wire is in the form of a thin ribbon before the slip-bands become well developed, and, while they are clearly visible when viewed perpendicularly to the ribbon surface, they do not show up when edge-on. This renders the above method of measuring the angle difficult, and, in addition, the angle is so small that large percentage errors are inevitable.

A method which enables χ_0 to be measured independently as well as calculated from equation (1), and which enables α and hence λ to be also determined, has

been described by Chalmers *, but his method requires the careful measurement of the coordinates of a glide ellipse on the graticule of the microscope eye-piece and subsequent plotting of the ellipse on squared paper. The time required is almost as long as that taken by an X-ray examination of the wire, and the accuracy obtainable is not greater than about one degree.

We have constructed an apparatus which enables the angles χ_0 and χ to be read off directly and the angle α to be calculated quickly with the accuracy usually necessary. The extended and ribbon-like wire is mounted flat on a stand, which enables it to be rotated about

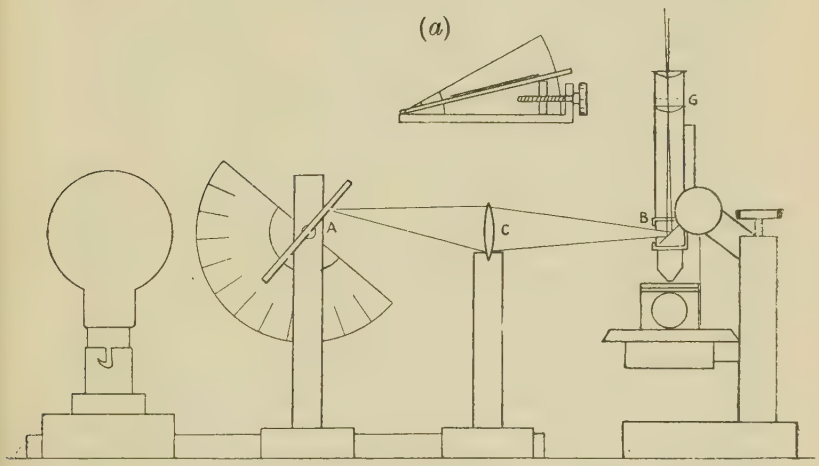

a horizontal axis perpendicular to its own (see fig., (*a*)), and this stand is mounted on the microscope stage. By altering the adjusting screw the whole of a semi-ellipse may be brought into focus at once in the field of view of the microscope. The angle between the horizontal and the axis of the wire then gives χ, which may be read off on the vertical protractor scale attached to the stand.

To avoid measuring up and plotting the elliptical traces of the slip-bands an ellipse of variable size and eccentricity is superposed upon the image of the wire in the field of view of the microscope. This ellipse is the pro-

* Phil. Mag. ser. 7, vol. xiv. p. 612 (1932).

jection of a fixed circular aperture, the plane and magnification of which can be adjusted. The glass plate A, prepared by photography, carries a black film on which is a series of concentric circles transmitting the light of a frosted electric lamp. A sharp image of the circles is formed in the focal plane of the microscope eye-piece by way of the lens C and vertical illuminator B. On the plate A there is, in addition to the transparent circles, a transparent horizontal diameter, and the plate is so mounted that it can be rotated about this line. The inclination of the plate to the horizontal is read off on a vertical scale graduated in degrees. In order that the circles may remain in focus when the plate is tilted the aperture of the vertical illuminator is kept small. It is necessary to arrange that the major axis of the glide ellipse shall be parallel to the transparent horizontal diameter. This is effected by rotating the microscope stage about its vertical axis.

To determine the required axes the image of one of the circular apertures is fitted to the glide ellipse by alternately adjusting its size and eccentricity. The appearance of the fitted elliptical image is shown in the photograph (Pl. XVII.), where S, S, S are slip-bands and F, E are images of two circular apertures, of which the latter is fitted. When this is complete the angle is read directly on the vertical scale attached to the plate A. The remaining observation consists in measuring the angle through which the stage must be rotated in order to bring the axis of the wire into alignment with the image of the horizontal diameter (the major axis of the fitting ellipse).

The relation between this measured angle β and the required angle α is indicated in fig. 1 of Dr. Chalmers's paper *, which shows a section of the wire by two glide planes DEF and LMN both before and after stretch. In (*b*) the glide planes are viewed perpendicularly as in the method described above, the plane LMN occupying the position RST after glide and BC representing the glide direction. Thus α = angle LBC, and the measured angle β is DAU, hence

$$\sin(\alpha-\beta) = \sin\alpha \cdot \frac{\tan\chi}{\tan\chi_0}.$$

But for greatly extended wires, such as those of cadmium,

* *Loc. cit.*

β differs from α by only a small correcting term, given by the equation

$$\alpha = \beta + \sin\beta \frac{\tan\chi}{\tan\chi_0} \quad . \quad . \quad . \quad . \quad . \quad . \quad (4)$$

Thus the method allows the angles χ and χ_0 (which are most usually required) to be read directly, and the determination of the remaining angle α requires only a small additive correction to be applied to a third reading. A check on the accuracy of the method is given by the ratio of the lengths of the wire before and after stretch, which enables a second value of χ to be calculated from χ_0. A series of readings for different single crystal wires of cadmium is given in the appended table, where the values of χ are compared in the last two columns.

Table of Measurements made on Cadmium Wires.

(Each value is the mean of three readings on different ellipses.)

l_0/l.	β.	χ_0.	χ (calculated from χ_0).	χ (observed directly).
·371	4·8°	18·6°	6·7°	8·0°
·200	6·7	57·9	9·7	9·0
·517	8·0	38·2	18·7	18·6

LXI. *On the Interpretation of Einstein's Unified Field Theory.* *By* W. H. McCrea, *M.A., Ph.D., Assistant Professor of Mathematics, Imperial College of Science* *.

1. *Introduction.*

DURING recent years Einstein has put forward a number of suggestions for a unified field theory of gravitation and electromagnetism. They are given in the first place by sets of field equations to be satisfied in space void of matter. In the complete unification it is of course impossible to separate out certain properties as

* Communicated by the Author.

electrical and certain as gravitational—at any rate when any electromagnetic effects whatever are present. But it turns out in some cases that *to a first approximation* certain features can be separated out and labelled *gravitational* and others *electromagnetic*.

Several attempts[1-4] have been made to study such interpretations in particular examples, but the results have been somewhat inconclusive. It is the object of the present note to go into the matter a little more closely, and to find the degree of definiteness of the interpretation in this method of first approximations. It is found that some of the difficulties previously encountered may be overcome, but the method is not completely satisfactory, at least without some complementary discussion of trajectories.

Some apology is needed for devoting this discussion to a form of the theory which its author would evidently now regard as superseded by his later suggestions; but it happens to be the form for which most particular cases have been investigated, and an exploration of any one form of the theory should provide an indication of how to proceed in interpreting any other form. The desire to be in a position to interpret any given form certainly requires no apology.

2. *Einstein's Interpretation.*

Einstein's theory [5] is formulated in terms of an orthogonal ennuple h_{sv} $(s, v=1, 2, 3, 4)$ defined at each point of a Riemannian space. It is not necessary here to recapitulate his general theory, but merely to consider his first approximation, in which he takes the case of nearly euclidean space, and writes

$$h_{sv}=\delta_{sv}+k_{sv}, \quad . \quad . \quad . \quad . \quad . \quad . \quad . \quad (1)$$

where $\delta_{sv}=1$, $s=v$; $\delta_{sv}=0$, $s\neq v$; $k_{sv} << 1$. His field equations then become, to the first order in k_{sv},

$$k_{\alpha\mu,\,\nu,\,\nu}-k_{\alpha\nu,\,\nu,\,\mu}=0, \quad . \quad . \quad . \quad . \quad . \quad . \quad (2)$$

$$k_{\alpha\mu,\,\alpha,\,\nu}-k_{\alpha\nu,\,\alpha,\,\mu}=0, \quad . \quad . \quad . \quad . \quad . \quad . \quad (3)$$

where $k_{\alpha\mu,\,\nu}\equiv \partial k_{\alpha\mu}/\partial x^{\nu}$; $k_{\alpha\nu,\,\nu,\,\mu}\equiv \partial^2 k_{\alpha\nu}/\partial x^{\nu}\partial x^{\mu}$, etc., with summation over repeated suffixes. He states further that it can be shown possible, in virtue of (3), to

make a change of coordinates, such that in the new system we have

$$k_{\mu\alpha,\,\alpha}=0; \quad k_{\alpha\mu,\,\alpha}=0. \quad . \quad . \quad . \quad . \quad . \quad (4)$$

It is helpful to give a proof of this result, for the sake of the subsequent discussion. We can write everything in terms of derivatives of the $h_{s\nu}$. We suppose that in some range of the variables the $h_{s\mu,\,\nu}$ and $h_{s\mu,\,\nu,\,\sigma}$ are of the order of magnitude of the $k_{s\mu}$. Working then to this order, the field equations $F_{\mu\alpha}=0$ (*loc. cit.*), following Einstein, reduce to (3), which is

$$h_{\sigma\mu,\,\alpha,\,\sigma}=h_{\sigma\alpha,\,\mu,\,\sigma}, \quad . \quad . \quad . \quad . \quad . \quad (5)$$

or
$$\partial(h_{\sigma\mu,\,\sigma})/\partial x^{\alpha}=\partial(h_{\sigma\alpha,\,\sigma})/\partial x^{\mu},$$

giving
$$h_{\sigma\mu,\,\sigma}=\partial f/\partial x^{\mu}, \quad . \quad . \quad . \quad . \quad . \quad (6)$$

where f is some function of x^1, x^2, x^3, x^4.

Let $h_{\sigma\mu}$ denote the vector obtained by transforming $h_{\sigma\mu}$ under the transformation of x^{α} to $\bar{x}^{\alpha}$. Then

$$h_{\sigma\mu,\,\sigma}=\frac{\partial^2 x^{\sigma}}{\partial\bar{x}^{\tau}\partial\bar{x}^{\mu}}+\frac{\partial^2 x^{\nu}}{\partial\bar{x}^{\sigma}\partial\bar{x}^{\rho}}k \;+\frac{\partial x^{\nu}}{\partial\bar{x}^{\mu}}\cdot\frac{\partial x^{\tau}}{\partial x^{\sigma}}h_{\sigma\nu,\,\tau}. \quad . \quad (7)$$

Suppose now the transformation is given by

$$x^{\mu}=\bar{x}^{\mu}+\bar{X}^{\mu}, \quad . \quad . \quad . \quad . \quad . \quad . \quad (8)$$

where X^{μ} is a function of the $\bar{x}^{\alpha}$, and is supposed of the same order of magnitude as the $k_{s\nu}$. Then, retaining only terms of this order, we have from (7)

$$\bar{h}_{\sigma\mu,\,\sigma}=\frac{\partial^2\bar{X}^{\sigma}}{\partial\bar{x}^{\tau}\,\partial\bar{x}^{\mu}}+h_{\sigma\mu,\,\sigma}, \quad . \quad . \quad . \quad . \quad (9)$$

and in $h_{\sigma\mu,\,\sigma}$ we can write x^{α} for x^{α}. So we have the required result

$$\bar{h}_{\sigma\mu,\,\sigma}=0, \quad . \quad . \quad . \quad . \quad . \quad . \quad (10)$$

if, dropping the bar and using (6),

$$\frac{\partial^2 X^{\sigma}}{\partial x^{\sigma}\partial x^{\mu}}+\frac{\partial f}{\partial x^{\mu}}=0,$$

that is, since any constant of integration can be included in f, if

$$\partial X^{\sigma}/\partial x^{\sigma}+f=0. \quad . \quad . \quad . \quad . \quad . \quad (11)$$

Further, we have in a similar manner to the same order

$$\bar{h}_{\mu\sigma,\,\sigma}=\frac{\partial^2\bar{X}^\mu}{\partial x^{\sigma^2}}+h_{\mu\sigma,\,\sigma}. \quad . \quad . \quad . \quad . \quad (12)$$

Hence we have the required result

$$\bar{h}_{\mu\sigma,\,\sigma}=0, \quad . \quad . \quad . \quad . \quad . \quad . \quad (13)$$

if $$\partial^2 X^\mu/\partial x^{\sigma^2}+h_{\mu\sigma,\,\sigma}=0 \qquad (\mu=1,\,2,\,3,\,4). \quad . \quad . \quad (14)$$

We must now show that the equations (11), (14) for the functions X^μ are compatible. It must be recalled that in each case there is summation over the suffix σ.

Let $X^\sigma=X_0^\sigma$ be any solution of (11). Then the general solution is, say, $X^\sigma=X_0^\sigma+X_1^\sigma$, where

$$\partial X_1^\sigma/\partial x^\tau=0. \quad . \quad . \quad . \quad . \quad . \quad (15)$$

Then (14) becomes

$$\partial^2 X_1^\mu/\partial x^{\sigma^2}=J^\mu, \quad . \quad . \quad . \quad . \quad . \quad (16)$$

where $$J^\mu=-h_{\mu\sigma,\,\sigma}-\partial^2 X_0^\mu/\partial x^{\sigma^2}.$$

Also we see that J^μ is such a function that

$$\frac{\partial J^\mu}{\partial x^\mu}=-h_{\mu\sigma,\,\mu,\,\sigma}-\frac{\partial^2}{\partial x^{\sigma^2}}\left(\frac{\partial X_0^\mu}{\partial x^\mu}\right)$$

$$=-\partial^2 f/\partial x^{\sigma^2}+\partial^2 f\partial x^{\sigma^2}, \text{ using (11)},$$

$$=0. \quad . \quad . \quad . \quad . \quad . \quad . \quad . \quad . \quad . \quad . \quad (17)$$

Therefore the functions X_1^μ satisfy equations of precisely the same form as those satisfied by the components of a vector potential in a field of given charge and current J^μ, the result (17) corresponding to the equation of continuity of charge. Hence from the known properties of these equations X_1^μ exists, and is completely determined when suitable boundary conditions are given. *Consequently functions* X^μ *exist determining by an infinitesimal transformation a coordinate system in which equations* (10), (13) *are satisfied to the required order.* This is Einstein's result [6]. (The analogy with the vector potential is here introduced solely to recall a property of differential equations of familiar type, and no physical significance is intended.)

Einstein's remaining field equations $G''^{\alpha}=0$ (*loc. cit.*) reduce, to the first order, to (2) or

$$h_{\alpha\mu,\,\nu,\,\nu}-h_{\alpha\nu,\,\mu,\,\nu}=0. \quad . \quad . \quad . \quad . \quad . \quad (18)$$

But in the new coordinates, dropping now the bars, we have $h_{\alpha\nu.\,\mu,\,\nu}=0$, so that (18) becomes

$$h_{\alpha\mu,\,\nu,\,\nu}=0. \quad . \quad . \quad . \quad . \quad . \quad . \quad (19)$$

Following Einstein we now write

$$\gamma_{\mu\nu}=k_{\mu\nu}+k_{\nu\mu}\,; \quad a_{\mu\nu}=k_{\mu\nu}-k_{\nu\mu}. \quad . \quad . \quad (20)$$

Then we have from the field equations from (10), (19) in the first place

$$\gamma_{\alpha\mu,\,\nu,\,\nu}=0, \quad . \quad . \quad . \quad . \quad . \quad . \quad (21)$$

$$\gamma_{\alpha\mu,\,\alpha}=0. \quad . \quad . \quad . \quad . \quad . \quad . \quad (22)$$

Now Einstein identifies these equations as expressing to this order the laws governing *the gravitational part of the field*, so that the $\gamma_{\mu\nu}$ can be regarded as gravitational potentials. The reason he does this is presumably that he has previously shown[7] that the gravitational field equations of general relativity for empty space can be written to the same order in precisely the form of (21), (22) in terms of a symmetric quantity like $\gamma_{\mu\nu}$; and one presumes that these latter correctly describe gravitational phenomena to this order.

It is important to notice that it is correct to treat the field as applying to *empty* space; for the energy and stress densities in the electromagnetic field which would normally appear on the right-hand side of equations (21) are quadratic in the field intensities, identified below with the $a_{\mu\nu}$, and therefore do not appear in the first approximation to the gravitational field.

In the second place we have from the field equations

$$a_{\alpha\mu,\,\nu,\,\nu}=0, \quad . \quad . \quad . \quad . \quad . \quad . \quad (23)$$

$$a_{\alpha\mu,\,\alpha}=0. \quad . \quad . \quad . \quad . \quad . \quad . \quad (24)$$

These Einstein interprets by taking $a_{\mu\nu}$ *to represent the electromagnetic force tensor* in the present coordinates, for it is antisymmetric, and equations (24) are of the form

$$\frac{\partial a_{21}}{\partial x^2}+\frac{\partial a_{31}}{\partial x^3}+\frac{\partial a_{41}}{\partial x^4}=0, \quad \text{since } a_{11}=0,$$

which, with this interpretation of $a_{\mu\nu}$, and writing x, y, z, ict for x^1, x^2, x^3, x^4, gives

$$\frac{\partial \gamma}{\partial y} - \frac{\partial \beta}{\partial z} - \frac{1}{c}\frac{\partial X}{\partial t} = 0,$$

or the familiar Maxwell equation $\operatorname{curl} H = \dot{E}/c$, where

$H = (\alpha, \beta, \gamma) = (a_{32}, a_{13}, a_{21})$ is the magnetic intensity,

and $E = (X, Y, Z) = i(a_{41}, a_{42}, a_{43})$ is the electric intensity.

Further, equations (23) express just the ordinary law of propagation of electromagnetic force in free space. The introduction of a dimensional factor is, of course, required to express the $a_{\mu\nu}$ as intensities in ordinary units.

3. *Transformation Theory.*

Consider now any infinitesimal *linear* transformation of the variables, *i. e.*, one of the form (8) but with $\bar{X}^\mu$ linear in $\bar{x}^\mu$. Then, from (9), (12) it follows that $h_{\sigma\mu,\,\sigma}$, $h_{\mu\sigma,\,\sigma}$ are unchanged to the first order, since here

$$\partial^2 \bar{X}^\sigma / \partial x^\sigma \partial x^\mu = 0, \quad . \quad . \quad . \quad . \quad . \quad (25)$$

$$\partial^2 X^\mu / \partial x^{\sigma 2} = 0. \quad . \quad . \quad . \quad . \quad . \quad (26)$$

We can therefore choose coordinates which are Galilean at any given point without altering the form of equations (21) *to* (24). It is this circumstance which in fact makes possible the above interpretation, for it is only in Galilean coordinates that the electromagnetic field equations take the stated form.

Degree of Arbitrariness.—It is necessary as well as sufficient for the preservation of the form of (21) to (24) that equations (25), (26) should be satisfied—that is to say, if the coordinates have been so chosen that (21) to (24) are satisfied, then they are indeterminate to the extent of functions X^μ satisfying (25), (26). It follows that we can set $X^\mu = X_0^\mu + \bar{X}_1^\mu$, where now $\bar{X}_0^\mu$ are linear functions, and X_1^μ satisfy

$$\partial \bar{X}_1^\sigma / \partial \bar{x}^\sigma = 0, \quad \partial^2 X_1^\mu / \partial x^{\sigma 2} = 0. \quad . \quad . \quad . \quad (27)$$

If, then, we continue to assume that the $\bar{X}^\mu$ and their first and second derivatives are of the same order of

magnitude as the $k_{s\alpha}$, we shall have to the first order, under the present transformation,

$$\bar{h}_{s\alpha}=\frac{\partial x^{\mu}}{\partial x^{\alpha}}h_{s\mu}=\frac{\partial \bar{X}^{s}}{\partial \bar{x}^{\alpha}}+h_{s\alpha}. \quad . \quad . \quad . \quad . \quad . \quad (28)$$

Hence
$$\gamma_{s\alpha}=\gamma_{s\alpha}+\partial X^{s}/\partial \bar{x}^{\alpha}+\partial \bar{X}^{\alpha}/\partial x^{s}, \quad . \quad . \quad . \quad (29)$$

$$a_{s\alpha}=a_{s\alpha}+\partial X^{s}/\partial \bar{x}^{\alpha}-\partial \bar{X}^{\alpha}/\partial \bar{x}^{s}, \quad . \quad . \quad . \quad (30)$$

giving *the law of transformation of* $\gamma_{s\alpha}$, $a_{s\alpha}$.

Suppose now that in addition the x^{μ}, $\bar{x}^{\mu}$ coordinates are Galilean at the origin. Then, since

$$\Sigma\, dx^{\mu 2}=\Sigma\, d\bar{x}^{\mu 2}+2\partial \bar{X}^{\mu}/\partial x^{\nu}\,.\,dx^{\mu}\,dx^{\nu}$$

to the first order, we must have

$$(\partial \bar{X}^{\mu}/\partial \bar{x}^{\nu})_{0}+(\partial X^{\nu}/\partial \bar{x}^{\mu})_{0}=0, \quad . \quad . \quad . \quad (31)$$

where the suffix denotes quantities evaluated at the origin.

Lorentz Transformation.—We shall now restrict ourselves to *linear* infinitesimal transformations, which corresponds to a particular choice of $\bar{X}^{\mu}$, or to *the general case in a sufficiently small neighbourhood* in which a linear approximation to $\bar{X}^{\mu}$ is valid to the first order.

If the coordinates are Galilean at the origin the linear transformation which preserves the Galilean form is orthogonal, *i. e.*, apart from a mere change of origin,

$$x^{\mu}=x^{\mu}+c^{\mu}_{\nu}\bar{x}^{\nu}, \quad . \quad . \quad . \quad . \quad . \quad . \quad . \quad (32)$$

where c^{μ}_{ν} is a small constant of the first order, such that

$$c^{\mu}_{\nu}+c^{\nu}_{\mu}=0. \quad . \quad . \quad . \quad . \quad . \quad . \quad . \quad (33)$$

Then from (29), (30) we have

$$\bar{\gamma}_{s\alpha}=\gamma_{s\alpha}, \quad . \quad . \quad . \quad . \quad . \quad . \quad . \quad . \quad . \quad (34)$$

$$\bar{a}_{s\alpha}=a_{s\alpha}+c^{s}_{\alpha}-c^{\alpha}_{s}. \quad . \quad . \quad . \quad . \quad . \quad . \quad (35)$$

There are six different $a_{s\alpha}$, and on account of (33) there are six independent c^{μ}_{ν}. Hence (35) is equivalent to the addition of an arbitrary constant to each $a_{s\alpha}$.

Now the transformation under consideration is precisely the general infinitesimal *Lorentz transformation.* Such a transformation does not affect gravitational phenomena,

which is consistent with (34), and does not affect the electromagnetic intensities *to the first order*. (The changes in the intensities are terms in the relative velocity, proportional to the c_μ^ν, multiplied by intensities, proportional to $a_{\mu\nu}$, and so of the second order in the present approximation [8]). Hence we must conclude that *the quantities a_{st} can represent the electromagnetic intensities in any sufficiently small neighbourhood only to within an arbitrary constant*, or alternatively that *they can be made to represent the field completely in that neighbourhood for any particular choice of coordinates*, but that a transformation will introduce additional constants.

Rotational Invariance.—Einstein introduces the notion of rotational invariance into his theory [9]. We here confine ourselves to *infinitesimal* orthogonal rotations, in order to preserve the form (1) of the h_{sv}. They are then given by

$$h^*_{sv}=h_{sv}+\beta_{st}h_{tv}, \quad . \quad . \quad . \quad . \quad . \quad (36)$$

where β_{st} are of the same order as the k_{sv}, and are constant, and the orthogonality is given by

$$(\delta_{st}+\beta_{st})(\delta_{su}+\beta_{su})=\delta_{tu}, \quad \text{or} \quad \beta_{tu}+\beta_{ut}=0, \quad . \quad (37)$$

to the first order. Then (36) becomes to this order

$$h^*_{sv}=h_{sv}+\beta_{st}, \quad . \quad . \quad . \quad . \quad . \quad . \quad (38)$$

or, using (37), the $\gamma_{\mu\nu}$, $a_{\mu\nu}$ transform according to

$$\gamma^*_{\mu\nu}=\gamma_{\mu\nu}, \quad a^*_{\mu\nu}=a_{\mu\nu}+\beta_{\mu\nu}-\beta_{\nu\mu}. \quad . \quad . \quad . \quad (39)$$

This, again, *is precisely equivalent to adding an orbitrary constant on to each of the $a_{\mu\nu}$*, and has, as might have been expected, precisely the same effect to this order as a rotation of the axes of the form (32). Thus Einstein's interpretation of the $a_{\mu\nu}$ is rotationally invariant only to within arbitrary additive constants. A special case of this was noted by Parsons [3].

This arbitrariness in the $a_{\mu\nu}$ corresponds to the fact that Einstein's interpretation is based on the circumstance of their satisfying (23), (24), and that these equations are still satisfied if an arbitrary constant is added to each $a_{\mu\nu}$. We shall not stop here to discuss the functional indeterminacy of $a_{\mu\nu}$ satisfying (23), (24).

This represents the unsatisfactory feature of the interpretation. In the light of what has been said about the Lorentz transformation it means that *the same ennuple field cannot completely represent the same electric field for all observers.*

4. *Applications.*

The simplest ennuple field illustrating most of the foregoing points is given by

$$h_{11}=h_{22}=h_{33}=h_{44}=1\,;\ h_{14}=k,$$

with the remaining components zero, where k is a constant such that $k \ll 1$. Then to the first order

$$ds^2=dx^{1^2}+dx^{2^2}+dx^{3^2}+dx^{4^2}+2k\,dx^1\,dx^4.$$

If, now, we make the transformation

$$x^1=\bar{x}^1+a\bar{x}^4,\quad x^2=\bar{x}^2,\quad x^3=\bar{x}^3,\quad x^4=bx^1+\bar{x}^4,$$

where a, b are any constants of order k, such that

$$a+b=-k,$$

we have, to the first order,

$$ds^2=d\bar{x}^{1^2}+dx^{2^2}+dx^{3^2}+dx^{4^2}\,;$$

so that the new coordinates are Galilean. Also

$$\bar{h}_{11}=h_{22}=\bar{h}_{33}=\bar{h}_{44}=1,\quad \bar{h}_{14}=k+a,\quad \bar{h}_{41}=b,$$

and

$$\bar{\gamma}_{\mu\nu}=0,\quad \bar{a}_{14}=k+a-b,$$

and all other components of $a_{\mu\nu}$ are zero. Therefore the $h_{\mu\nu}$ are to be interpreted as representing *an arbitrary uniform electric field parallel to the x^1 axis.* Incidentally this suffices to show that Parson's solution represents something more than a uniform field.

Einstein and Mayer's Solution [10].—This is a strict solution with radial symmetry of Einstein's equations, and is given by

$$h_{11}=h_{22}=h_{33}=\lambda=(1-e^2/r^4)^{1/4},\quad h_{44}=1/\mu,$$

$$h_{14}=-ex^1/r^3\mu,\quad h_{24}=-ex^2/r^3\mu,\quad h_{34}=-ex^3/r^3\mu,\quad (40)$$

and all other components vanish. Here

$$\mu = 1 + m \int \left(1 - \frac{e^2}{r^4}\right)^{1/4} \frac{dr}{r^2}, \quad r^2 = x^{1^2} + x^{2^2} + x^{3^2}, \qquad (41)$$

and m, e are constants. To the first order in e/r^2, m/r we have

$$a_{14} = -ex^1/r^3, \quad a_{24} = -ex^2/r^3, \quad a_{34} = -ex^3/r^3,$$
$$\gamma_{44} = 2m/r, \quad . \quad . \quad . \quad . \quad . \quad . \quad . \qquad (42)$$

and all other components are zero. It is easy to verify that the coordinates have been taken so that equations (4), and consequently (21) to (24), are satisfied to this order. From (42) Einstein and Mayer interpret the field as being due to a particle of charge e and mass m (but *cf.* § 5 below with regard to m) situated at the origin.

It is instructive, however, to study also the field as experienced by an observer at a particular point, say (X, 0, 0, T). Then at this point $h_{s\nu}$ reduces in the first order to

$$h_{11} = h_{22} = h_{33} = 1, \quad h_{44} = 1 + m/\mathrm{X}, \quad h_{14} = k = -e/\mathrm{X}^2,$$

with other components zero. As before, Galilean coordinates at the point are given by

$$x^1 = \bar{x}^1 + a\bar{x}^4, \quad x^2 = \bar{x}^2, \quad x^3 = \bar{x}^3, \quad x^4 = b\bar{x}^1 + (1 - m/\mathrm{X})\bar{x}^4,$$

with $a + b = -k$. Under this transformation the $h_{s\nu}$ given by (40) become *exactly*

$$h_{11} = h_{11} + bh_{14}, \quad h_{41} = (1 - m/\mathrm{X})h_{44}, \quad h_{14} = ah_{11} + h_{14},$$
$$h_{41} = +bh_{44},$$

with other components unchanged; whence

$$\bar{a}_{14} = -ex^1/r^3\mu + a\lambda - b/\mu, \quad \bar{a}_{24} = a_{24}, \quad a_{34} = a_{34}.$$

Hence if we now impose the condition that the electric field tends to zero at infinity, *i. e.*, a_{14}, $\bar{a}_{24}$, $a_{34} \to 0$, as $r \to \infty$, then we must take

$$a = b = -k/2.$$

This illustrates how the arbitrary constants may in some cases be fixed by boundary conditions.

Relation to Parson's Solution.—If the solution discussed by McVittie [2] and Parsons [3] were to represent a uniform

field it should be similar to that of Einstein and Mayer in any small region. We shall therefore again consider the latter field near the point (X, 0, 0, T) in a neighbourhood represented by $x^1=X+x$, $x^2=y$, $x^3=z$, where now, instead of taking e/X^2, m/X small, we take x, y, z to be small. Expanding to the first order in these variables we now obtain from (40)

$$h_{11}=h_{22}=h_{33}=a+bx, \quad h_{44}=g+kx, \quad h_{14}=c+ex,$$
$$h_{24}=fy, \quad h_{34}=fz, \quad . \quad . \quad . \quad . \quad . \quad (43)$$

and other components zero, where a, b, c, e, f, g, k are constants expressible in terms of e, m, X. These to the same order give a metric of the form

$$ds^2=(l+mx)(dx^2+dy^2+dz^2)+(n+px)\,dx^4$$
$$+2(q+rx)dx\,dx^4+2sy\,dy\,dx^4+2sz\,dz\,dx^4, \quad . \quad (44)$$

where $l, m, \ldots s$ are constants depending on $a, b, \ldots k$. Making now a transformation of the form

$$x=Dx+Ex^2, \quad \bar{y}=Fy, \quad \bar{z}=Fz,$$
$$\bar{x}^4=Ax^4+Bx+C_1x^2+C_2y^2+C_3z^2,$$

where A, ... F are constants, we can put (44) to the same order into the form

$$ds^2=d\bar{x}^2+(1-2\beta\bar{x})(d\bar{y}^2+dz^2)+(1-2\alpha x)\,d\bar{x}^4,$$

where α, β are constants, which agrees with Parson's metric (*loc. cit.*, equation (23)) to this order. But the transformation of the $h_{s\alpha}$ given by (43) gives a form of which Parsons' is only a particular case. A closer examination of the dependance of α, β on the other constants shows that α depends on m/X^2, and so can be said to depend on the intensity of the gravitational field, but β depends on (e/X^2) *and on* X, and so must be taken to depend on the departure of the electric field from uniformity.

5. *Trajectories.*

If we write $\gamma'_{\mu\nu}$ in place of what we have previously called $\gamma_{\mu\nu}$, then these quantities satisfy exactly the same equations as the quantities $\gamma'_{\mu\nu}$ used in the discussion

of the first approximation to the field equations of general relativity (see Pauli, *loc. cit.*). We have seen that their interpretation depends on this circumstance.

Consider, then, Einstein and Mayer's solution with $e=0$. We have, as before,

$$\gamma'_{11}=\gamma'_{22}=\gamma'_{33}=0, \quad \gamma'_{44}=2m/r=\gamma',$$

to the order m/r, where $\gamma'=\Sigma_\mu \gamma'_{\mu\mu}$. We compare with this Schwarzschild's solution for a particle of mass m^* in general relativity, with a metric given to the first order in m^* by

$$ds^2=(1+2m^*/r)(dx^2+dy^2+dz^2)+(1-2m^*/r)\,dx^{4^2},$$

$$(x^4=ict);$$

we find for the quantities $\gamma_{\mu\nu}$ of Pauli's discussion, defined by $g_{\mu\nu}=\delta_{\nu\nu}+\gamma_{\mu\nu}$,

$$\gamma_{11}=\gamma_{22}=\gamma_{33}=2m^*/r, \quad \gamma_{44}=-2m^*/r, \quad \gamma=\Sigma\gamma_{\mu\mu}=4m^*/r.$$

Hence the corresponding $\gamma'_{\mu\nu}$, defined by $\gamma'_{\mu\nu}=\gamma_{\mu\nu}-\frac{1}{2}\delta_{\mu\nu}\gamma$, are

$$\gamma'_{11}=\gamma'_{22}=\gamma'_{33}=0, \quad \gamma'_{44}=-4m^*/r=\gamma'.$$

Therefore the $\gamma'_{\mu\nu}$ are identical in the two theories to the first order if $m=-2m^*$.

We should take it that the identification of the gravitational potentials $\gamma'_{\mu\nu}$ must be ultimately based on the equations of motion of a test body, and that therefore comparison with known results for the $\gamma'_{\mu\nu}$ of general relativity is fruitful only if we assume these quantities to be related in a known way to the equations of motion of such a body—that is to say, we expect to find its orbit to the first order by substituting the new $\gamma'_{\mu\nu}$ in the equations of motion of general relativity.

As a consequence, since in the special case of the field of a single massive particle the two theories give the same $\gamma'_{\mu\nu}$, we expect them to give the *same* orbit to the first order in m^*. In particular *the advance of the perihelion*, which depends on m^* in the first order, *would be the same on the two theories*, in contradistinction to the result of Blackwell [4].

This leaves us in a dilemma, for if this reasoning is correct, the orbits in the new theory are *not* geodesics, but if it is at fault then it is difficult to see on what grounds the identification of the $\gamma^{i}_{\mu\nu}$ of the new theory is based. A full discussion of trajectories in unified field theories is demanded, since only this can give a definitive method of deriving physical interpretations.

References.

(1) G. C. McVittie, Proc. Roy. Soc. A, cxxiv. pp. 366–374 (1929).
(2) G. C. McVittie, Proc. Edinb. Math. Soc. (2) ii. pp. 140–150 (1930).
(3) J. D. Parsons, *ibid.* (2) iii. pp. 37–45 (1932).
(4) A. Blackwell, Proc. Roy. Soc. Edinb. lii. pp. 327–330 (1932).
(5) A. Einstein, *Berlin. Sitz.* pp. 18–23 (1930); the field equations are (11), (12), p. 21, and the interpretation is given on p. 23.
(6) A somewhat analogous result is proved by D. Hilbert, *Göttingen Nachr.* pp. 53–76 (1917), where a single set of equations $h_{\mu\sigma,\ \sigma}=0$ has to be satisfied, and both suffixes of $h_{\sigma\mu}$ behave like tensor suffixes.
(7) A. Einstein, *Berlin. Sitz.* p. 688 (1916). See also D. Hilbert, *loc. cit.* and W. Pauli, *Math. Encykl.* v. 2, p. 736 (1920).
(8) See, for example, A. S. Eddington, 'Mathematical Theory of Relativity,' Chap. vi. (1924).
(9) A. Einstein, *Berlin. Sitz.* pp. 217–221 (1928).
(10) A. Einstein and W. Mayer, *Berlin. Sitz.* pp. 110–120 (1930),

June 1933.

LXII. *Lattice Distortion in Nitrided Steels and Theory of Hardness.* *By* W. A. Wood, *M.Sc., Physics Department, National Physical Laboratory, Teddington, Middlesex* *.

[Plate XVIII.]

Introduction.

WORK on tungsten magnet steels has shown experimentally that there exists a relation between the distortion of the lattice as disclosed by the diffusion of the X-ray spectra and the hardness of the material. The conclusion was based on experiments which, as described in previous papers[1] precluded the complication of fine-grained structure. This factor also causes a spreading of the spectrum lines, and its presence would confuse any interpretation of the broadening[2]. But it was found that steels softened by annealing at 900° C.

* Communicated by Dr. G. W. C. Kaye, O.B.E.

recovered their hardness by further heating at 1250° C., and the X-ray spectra, which were sharp after the first heating, became very diffuse after the second. The point was made that the second heating produced a growth in grain-size, so that the broadening of the lines and the increase in hardness could only be due in this case to the alternative cause, that of lattice distortion.

The same point is relevant to the present work. This deals with steels case-hardened by the recently developed process of nitriding. An essential step in the method is the heating of the steels in a stream of ammonia for several hours at about 500° C. The tempering should tend to oppose the formation of a structure sufficiently fine in grain to cause spreading of the X-ray lines. Any broadening observed might reasonably be attributed solely to the lattice distortion effect. The surface layers of the steels absorb nitrogen and attain hardness values of 1000 to 1200 Brinell, values higher than the 700 to 800 Brinell of case-carburized steels. They provide appropriate material therefore for investigation of lattice distortion and hardness. Particular attention is paid below to the influence of nitriding on the nature of the X-ray lines. Extreme hardness is found to be associated with a remarkably diffuse form of spectrum, the interpretation of which raises points of interest in connexion with theories of hardness.

Procedure.

The work was carried out in the following stages :—

1. X-ray analysis was made of steels of the chromium-aluminium type used for nitriding, first in the state immediately preceding the treatment with ammonia, and second in the state immediately subsequent.

2. Further examination was made in the case of a typical specimen, nitrided at 500° C. for 100 hours, of the way in which the X-ray spectra changed across the section of the hard surface layer.

3. The X-ray results were compared at each stage with the measured hardness of the material.

Experimental Data.

In the X-ray work the Debye method of analysis was used. Each specimen was mounted similarly at the centre of a cylindrical camera of radius 5·50 cm. A

specially designed holder ensured the accurate registration of the face of the specimen with a diameter of the camera. A tubular slit, 4 cm. in length and 1 mm. in diameter, directed the incident beam on to the steel. Iron Kα radiation was employed. The specimens were in the form of blocks, approximately $1'' \times 1'' \times \frac{1}{2}''$. They were photographed first, set at 30° to the incident beam, and then at 60°. The first setting gave in focus diffraction lines produced by reflexions at angles less than $\theta \sim 45°$; the second gave those corresponding to glancing angles greater than $\theta \sim 45°$. Fig. 1 *a* (Pl. XVIII.) reproduces a photograph showing the small-angle reflexions. The remaining figures 1 *b* to 7 all cover the larger angle range $2\theta \sim 90°$ to $2\theta \sim 160°$.

The condition of the steel below the surface was investigated by gradually etching away the surface electrolytically in dilute hydrochloric acid. In this process the whole specimen was first coated with paraffin wax. A zone which extended over about one-sixth of one face was then cleared of wax. The specimen was placed in the electrolyte. After a measured interval of time a second neighbouring zone was bared, and the specimen again immersed. The procedure was repeated until the hardened case in the first zone had been dissolved away, the time necessary for this being known from preliminary work. The succeeding zones then formed a stepped surface which ranged from the first, in which the core of the steel was exposed, to the sixth, in which the original surface was untouched. From each step X-ray photographs and hardness measurements were taken. They were taken to indicate the way in which the nature of the spectrum and the hardness varied through a section of the hard surface layer.

The hardness measurements were made in the Engineering Department of the National Physical Laboratory. The static indentation method in a Vickers hardness testing machine was used, the indenting tool being a 136° diamond pyramid and the load 10 kgm. The hardness values given below were obtained from the measured diagonal width of the impressions, in connexion with the tables of diamond pyramid hardness numbers set out in the British Standards Institution Specification No. 427, 1931. A somewhat pitted surface was usually produced as a result of prolonged etching. Over such an area the

hardness might not be perfectly uniform. This difficulty could be obviated by arranging for the incident beam to fall on the particular spot, indicated by the indenting tool, at which the hardness was measured.

Observations.

1. The spectra of the steel before nitriding comprise only the iron lines. As shown in fig. 7 (Pl. XVIII.), which reproduces the (220), (211), and (200), they are in a sharply resolved state. The side of the unit cell is 2·86 Å.

2. The spectra of the steels after nitriding contain a number of other lines. They are characterized by the

Table I.

Spacings (Å.U.).		Intensities.
	4·20	α_1 strong.
	(3·72)	α_1 very weak.
	2·98	α_1 weak.
	2·52	α_1 medium.
2·32	..	α_1 strong.
2·19	..	α_1 strong.
2·08	(2·08)	α_1 strong.
	1·90	α_1 strong.
1·60	..	α_1 weak.
1·35	..	α_1 medium.
1·23	..	α_1 weak.

curious feature that, whereas in the earlier part of the spectrum they are sharp, in the later part they are extraordinarily diffuse. We consider first the reflexions from the surface. The spacings of the planes corresponding to the lines observed are given in columns 1 and 2, Table I.; those in the first column agree with lines to be expected from a production of the *e*-phase of the iron-nitrogen system, investigated by G. Haag[3]. Those in the second column belong to a compound, at present unidentified, which approximates to a body-centred cubic type. All these lines, as shown in fig. 1 *a* (Pl. XVIII.), are sharp.

A comparison of the intensity of the above lines with reflexions occurring at angles greater than $\theta \sim 45°$ presents

the following point: whereas small-angle lines are normally strong and sharp, the large-angle lines diffuse and rapidly fade into the background (fig. 1 *b*, Pl. XVIII.). This they do despite the fact that normally, according to Haag's observations on the chemically prepared compound, they should persist strongly, showing resolution of the iron $K\alpha_1$ and α_2 wave-lengths for values of θ up to 80°. But fig. 1 *b* (Pl. XVIII.) is devoid of lines; it is taken under the same conditions as fig. 7, which includes the (220), (211), and (200) iron lines. This abnormally rapid falling off in the intensity of the lines with increasing diffraction angle is considered to be a fundamental point in the relation of distortion to hardness. It is discussed later.

3. Examination of the spectra from beneath the surface shows that the first change is the disappearance of the surface layer of nitrides; the thickness of the layer is quite small. Next the iron lines begin to materialize from the background as the case is penetrated. This is illustrated by the succession of figs. 1 *b* to 6 (Pl. XVIII). These high-angle iron lines at first are in a very diffuse state, and, even after allowing for apparent loss in intensity due to spreading, they are abnormally weak. The remarks in the preceding paragraph on the abnormal falling away in intensity therefore apply equally here. This type of spectrum appears to hold over the greater part of the hardened case. The transition to the sharp state at the core (fig. 6, Pl. XVIII.) occurs in a small fraction of the thickness. Table II. gives the depths below the surface to which the photographs correspond. It will be seen that fig. 6 (Pl. XVIII.) is very similar to fig. 7, which represents the state of the steel before the nitriding treatment. The effect of the treatment is therefore first to produce a thin nitride layer on the surface in a very distorted form, and second, the main effect, to produce a case of steel characterized by an extremely diffuse and weakened spectrum.

4. In Table II. the hardness measurements are summarized and related to the typical X-ray photographs reproduced. The different values in the last column refer to hardness measurements made at different places in the same zone. Comparison with the photographs shows that the highly diffuse spectra correspond with high values of hardness. The sharp spectra are

associated with the soft state before nitriding, and with the core alone after the treatment. Removal of the nitride layer, which is complete in the steel of fig. 2 (Pl. XVIII.) does not affect the case hardness adversely. The nitride skin by itself has therefore little to do with the extreme case hardness; it consists of material which, judged by the variability of the surface values, is comparatively soft. It is seen that the hardness persists through the major portion of the case, and that the degree of hardness follows closely the degree of diffusion in the spectra.

TABLE II.

Depth below surface.	X-ray photograph.	Hardness numbers.
mm.		
0·00	Fig. 1 *a* ($\theta<45°$)	1206, 974, 1064
	Fig. 1 *b* ($\theta>45°$)	
0·03	Fig. 2 ($\theta>45°$)	1168, 1150, 1168
0·06	Fig. 3 ($\theta>45°$)	1187, 1132, 1187
0·18	Fig. 4 ($\theta>45°$)	1168, 1132, 1132
0·23	Fig. 5 ($\theta>45°$)	895, 642, 920, 743
Core 0·30	Fig. 6 ($\theta>45°$)	289, 290, 297
Before Nitriding	Fig. 7 ($\theta>45°$)	278, 280, 282

Discussion and Theory of Hardening.

Extreme hardness is seen to accompany a state of the steel which is characterized by a highly diffuse type of spectrum. Light on the source of the hardness should be thrown by knowledge of the cause of this diffusion.

At first sight the presence of an extremely fine-grained structure might be considered responsible for the effects observed. This explanation would be based on the knowledge that if the grains were less than 10^{-4} or 10^{-5} cm. they would not contain sufficient cooperating planes for perfect resolution of the diffraction spectra[4]. To the existence of this factor in the present case the following objections arise:—In the first place the average grain-size required to produce a line-broadening of the magnitude observed in figs. 1 *b* and 2 (Pl. XVIII.) would be, according to the accepted formulæ[5], of an order less than 10^{-7} cm. It does not appear reasonable that a grain-size of colloidal dimensions should be produced in the steel by prolonged heating at 500° C. In the

second place the rate at which the line-breadth is observed to vary with diffraction angle differs greatly from that required by the theoretical relationships. To satisfy these a line-breadth of 5 mm., which, as shown by the photographs, is of the order observed at an angle of 70°, should be associated with line-breadths of about 2 mm. at 35°. This is contrary to the experimental result. The lines in the latter region, as in fig. 1 *a* (Pl. XVIII.) are much narrower. Further, photographs of the steel at the core show signs of discontinuities in the lines; they afford in that way direct evidence of a grain-size exceeding about 10^{-3} cm.

One is led to the alternative factor of distortion. Here certain conclusions are indicated. First, the distortion is not of the simple type, where broadening of the lines is produced by irregularities in the lattice spacings[6]. The variation in the line-breadths at different angles is still too large, though not as discrepant as in the case of the small crystal theory, to be explained by a deviation of spacings from a mean value. Also, the equivalent change in spacing necessary to cause diffusion of the degree observed in fig. 2 (Pl. XVIII.) would be of the order of 1 to 2 per cent. Such an amount extending over the grain would produce instability in the lattice.

It is desired to draw particular attention to the abnormal falling away of the intensity of the lines diffracted at large angles. This suggests one of the following alternatives: either (i.) the power of the iron atoms to scatter the X-radiation through large angles of diffraction is abnormally diminished, or (ii.) the absolute intensity of the lines might be lost in an enhanced background formed by irregular scattering from amorphous material. The second suggestion is less feasible, for if the rays scattered from the amorphous proportion present were strong enough to submerge the high-angle lines, then they should be equally able to submerge the small-angle reflexions. This as shown by the first figure, they do not.

There remains the suggestion that the effective scattering power of the atoms is abnormally decreased at high angles as a result of the production of a hard state. A change in scattering power at different angles means, according to the theory of X-ray diffraction, a derangement of the electron distribution about the atoms. The normal distribution across a series of simple lattice planes may

be considered to involve statistically a peak intensity of electrons on the planes themselves and a minimum of intensity halfway between the planes. Now a permanent disturbance which increased the minimum at the expense of the peak would explain the type of result observed. The disturbance might be pictured broadly as one which caused, on the average, a diffusion of electrons from the atomic planes to the more rarefied space between them. The effect would accentuate the decrease in intensity, of high order spectra, since the scattering by the outer electrons would interfere more appreciably with that from the planes.

An electron disturbance of this type would be a reasonable consequence of the processes which produce hardening. It might well be expected to result from the stresses set up in the lattice by the interpenetration of nitrogen atoms; it would also tend to follow from a random superposition of nitrogen in the interstices between the iron atoms upon the lattice. The disturbances would be large for the following reason: the amount of nitrogen present is of the order of 8 to 11 per cent. by weight, since it forms on the surface the close-packed hexagonal *e*-phase FeN_3. Consequently the lattice at the boundary of the grains, where the nitrogen concentration will be greatest, will be on the point of swinging over from the body-centred cubic form of iron to a hexagonal arrangement; it will therefore tend to be unstable. The instability will be evinced locally by capacity for particularly high distortion of spacings and by high electron disturbance of the type described.

The electronic derangement could affect the hardness of the material. The disturbed distribution would tend to obliterate, especially at the surface of the grains, that distinctive electron arrangement which normally bestows on a particular plane the property of facilitating "slip." Each grain would be surrounded by a layer (or contain points) which would not possess marked slip planes. The layer would, by a binding action, oppose tendencies to slip within the grain.

The suggestion differs from the hypothesis of an amorphous layer surrounding the grains, in that it postulates a periodicity of the lattice right to the boundary. It differs also from the idea that hardness should be due merely to the atomic displacements accompanying pure

lattice distortion. This theory does not explain the observation that aluminium, which hardens on cold working, does not show signs of ordinary lattice distortion. Aluminium does, on the other hand, show the enhanced fading away of high-order spectra after cold working, of which the case of nitrided steel is an extreme example. The presence of lattice distortion in a material, as shown by line-broadening, would of course necessarily indicate a large electron disturbance effect, and therefore a degree of hardness. On the other hand, the latter effect may be present, as shown by X-ray intensities, and therefore produce hardening even when no lattice distortion occurred. This would hold in the case of a structure which would not stand much lattice distortion before disruption.

Summing up, the X-ray results appear to require the postulation of the electron disturbance effect. It appears possible that the nature of this effect, which tends to diffuse the electron distribution, should diminish the distinctive arrangements conducive to slipping and cause hardness. Also the effect would be a reasonable consequence of strains in metals developed by cold work, or by the dispersion of a foreign atom in the lattice. It also fits in with variations in electrical and magnetic properties often produced by these processes.

Summary.

An X-ray investigation has been made of the changes brought about in the case-hardening of steels by the nitriding process. It is shown that the method produces a surface layer of nitrides and a case of steel characterized by an abnormally diffused and weakened spectrum. Extreme hardness values are associated with this type of spectrum. The interpretation of the X-ray results require the postulation of a distorted atomic lattice and a disturbance of the electron distribution. On the basis of the latter effect a tentative theory of hardness is developed.

References.

(1) W. A. Wood, Phil. Mag. xiii. (Suppl.) p. 355 (1932).
(2) W. A. Wood, Phil. Mag. xv. p. 553 (1933).
(3) G. Haag, *Z. f. Phys. Chem.* 8 B, p. 455 (1930).
(4) V. Laue, *Z. f. Krist.* lxiv. p. 115 (1926).
(5) R. Brill, *Z. f. Krist.* lxviii. p. 387 (1928).
(6) W. A. Wood, Phil. Mag. xiv. p. 656 (1932).

May 1933.

LXIII. *Notices respecting New Books.*

Functions of a Complex Variable. By T. M. Macrobert. 2nd Edition. (Macmillan & Co. Price 14*s.*)

THE first edition of this work has long occupied a unique position, in that it stands alone as a successful text-book suited admirably to those who require a knowledge of Complex Variable work but who are not primarily interested in the theory as such. As is well known, the book contains an account of the elementary general theory of the Complex Variable, and proceeds to set out the theory of the more frequently occurring non-elementary functions of pure mathematics and of the functions arising from the differential equations of applied mathematics. Throughout no undue stress is laid on points of logical rigour.

The second edition embodies its predecessor and differs little from it. Addition has been made in the form of four short appendices, the first three of which amplify material already in the text. The fourth appendix gives a short and simple account of one aspect of the Fourier Integral.

The type and manner of setting out of the first edition have been maintained, and the second edition needs no recommendation after the undoubted success of its predecessor. This book is of great value to all who require an intimate and practical acquaintance with the methods of the Complex Variable.

Mémoires sur la Mécanique Ondulatoire. By E. Schrödinger. Translated by Al. Proca. (Librairie Félix Alcan, Paris, 1933. Price 50 fr.)

This book consists of French translations of nine of Schrödinger's papers, originally published in 1926–27, in which the theory of wave-mechanics was first developed. Its interest to-day is mainly historical, since Schrödinger's original method of obtaining the wave-equation by means of the Hamilton-Jacobi equation and the motion of "action surfaces" in the configuration space has been largely abandoned. A number of critical notes, however, which he has prepared for this edition throw an interesting light on the change in his ideas brought about by the developments of the last six years. Indeed, it is not too much to say that this book will be of value rather as a revelation of an original mind at work than as a text-book on wave-mechanics.

[*The Editors do not hold themselves responsible for the views expressed by their correspondents.*]

Fig. 1.

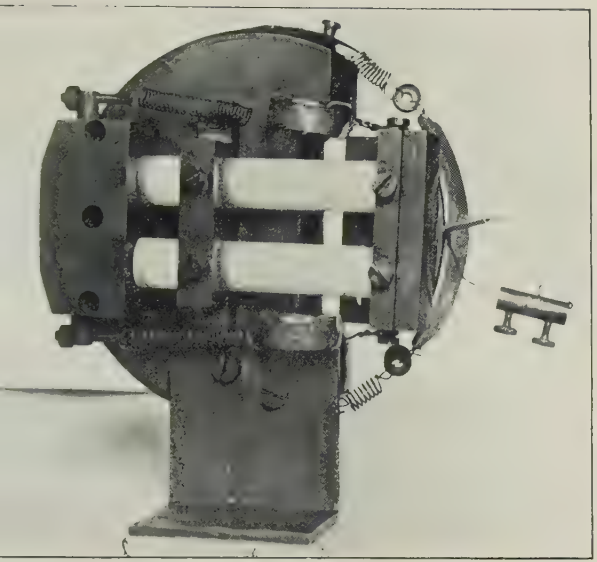

(*a*)

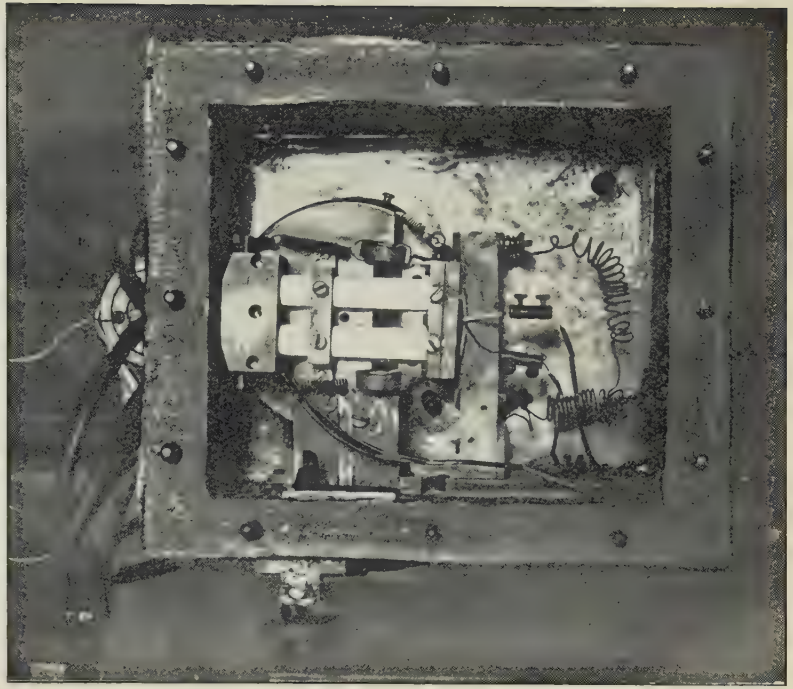

(*b*)

Precision camera designed for high temperature X-ray spectroscopy.

Fig. 2.

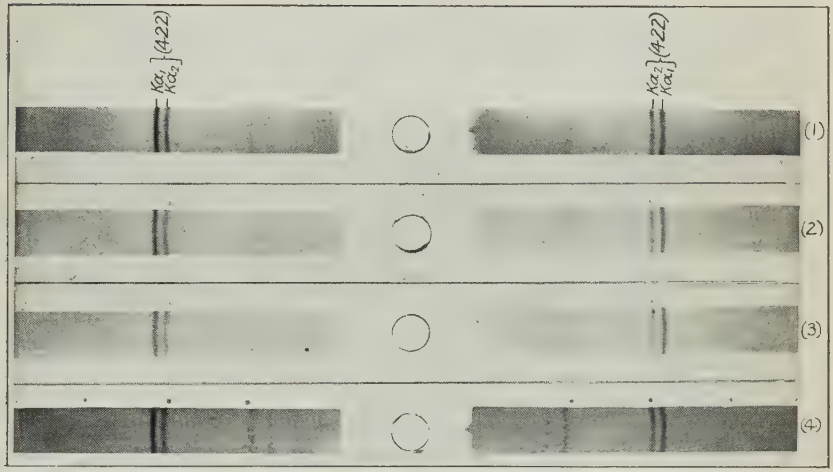

Palladium: (1) No heat treatment; exposure made in air.
(2) No heat treatment: exposure made *in vacuo*.
(3) Heated at 100° C. for 1 hour, cooled and exposed *in vacuo*.
(4) Heated at 300° C. for 4 hours, cooled and exposed *in vacuo*.

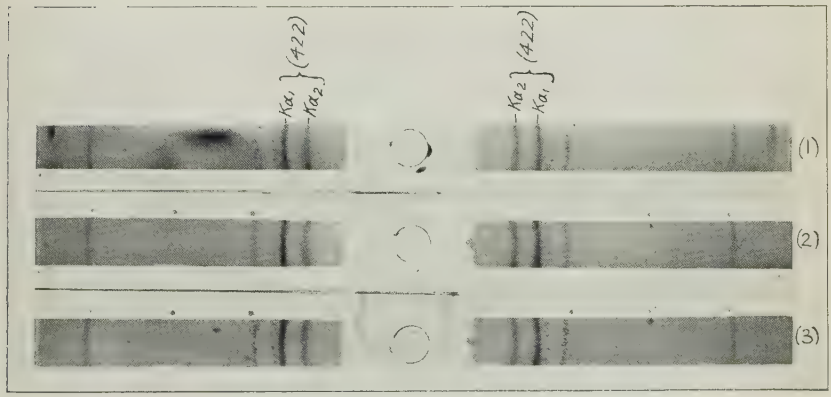

Rhodium: (1) No heat treatment; exposure made in air.
(2) No heat treatment; exposure made *in vacuo*.
(3) Heated at 400° C. for 1½ hours, cooled and exposed *in vacuo*.

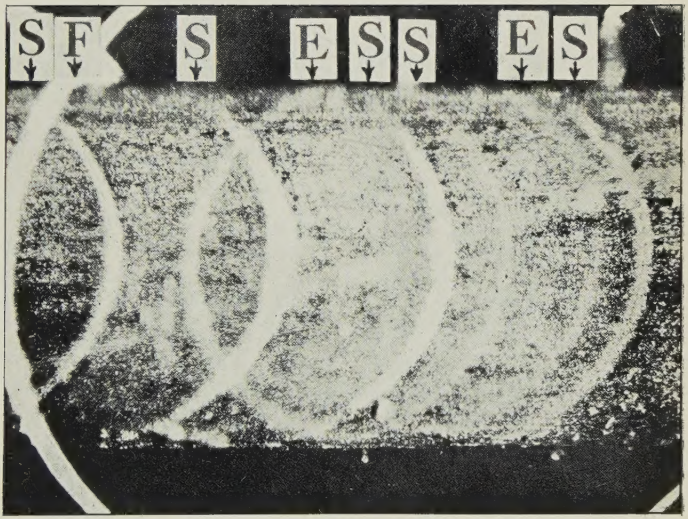

Photograph of stretched single-crystal wire of cadmium.

S, S, S, slip-bands; E, E, fitted ellipse; F, second projected ellipse for fitting larger eccentricities.

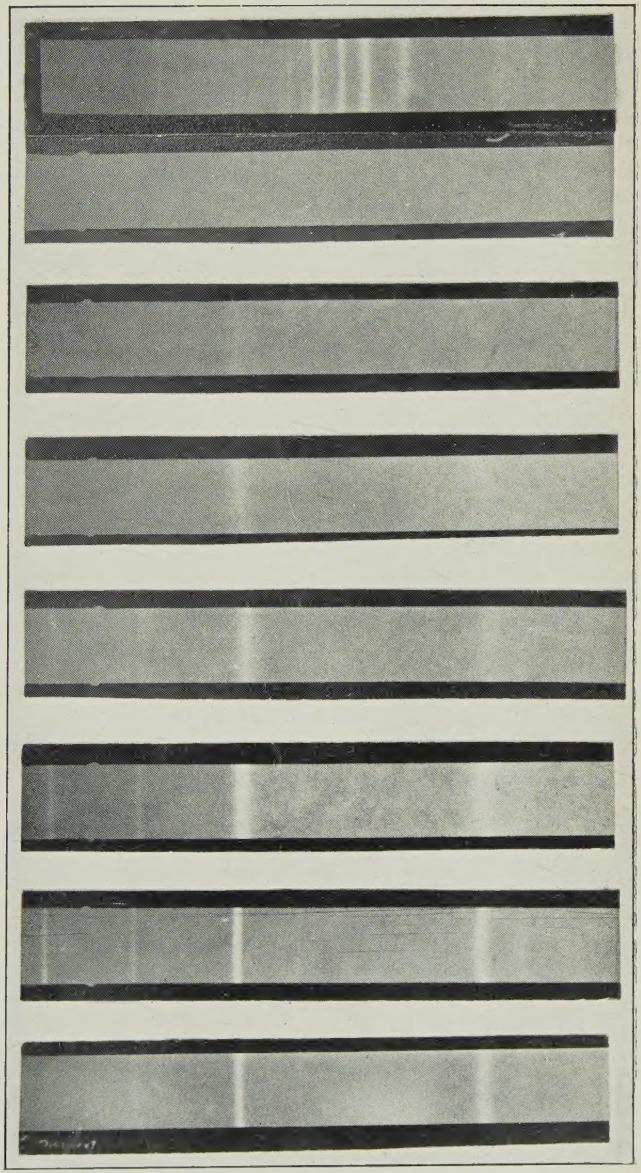
1 a.
1 b.
2.
3.
4.
5.
6.
7.